NWP SAF

RTTOV v12 beta test reports and responses

Version 1.1

19th December 2016

RTTOV v12 beta test reports and responses

This documentation was developed within the context of the EUMETSAT Satellite Application Facility on Numerical Weather Prediction (NWP SAF), under the Cooperation Agreement dated 29 June 2011, between EUMETSAT and the Met Office, UK, by one or more partners within the NWP SAF. The partners in the NWP SAF are the Met Office, ECMWF, KNMI and Météo France.

Copyright 2016, Met Office, All Rights Reserved.

Change record				
Version	**Date**	**Author**	**Approved**	**Remarks**
1.0	24/11/16	JH		Initial version.
1.1	19/12/16	JH		Updated after comments by S. Keogh.

Table of Contents

1. INTRODUCTION 4

2. ISSUES RAISED DURING BETA TEST PHASE 5

3. SPECIFIC ISSUES RAISED BY BETA TESTERS 8

1. INTRODUCTION

This document lists the issues raised during the RTTOV v12 beta test phase. Section 2 documents ad-hoc comments and bug reports made by developers and testers and the resolution of these issues. Section 3 summarises the specific issues raised by the three official beta testers and the NWP SAF responses to these issues. These tables do not include general comments made by beta testers which did not require any particular action or response from the developers. The full beta test reports and NWP SAF responses are appended for reference.

Issues which were fixed are highlighted in green in the tables. Issues for which no action was taken are in grey. Issues/suggestions which may be investigated for a future update are in blue.

2. ISSUES RAISED DURING BETA TEST PHASE

Date reported	Reported by	Description	Response	Date resolved	FCM rev
12/08/16	Sylvain Heilliette	Typo in readme.txt for beta coefficients web page	Minor issue since all coefs, atlas data and information are on the same page whose link I sent out. This is specific to the beta. I updated the readme.txt on the beta web page.	15/08/16	-
15/08/16	Sylvain Heilliette	Compilation failure in src/coef_io_11/rttov11_write_hdf5.F90 with gfortran 4.6.3 (minor bug related to INTENT of one argument).	This also highlighted some issues (memory leaks) in the v11/v12 coef conversion subroutines: all fixed.	16/08/16	2062
15/08/16	Sylvain Heilliette	Missing coefficient files in some tests	Documentation has been updated to say that not all individual tests are expected to run (some remain defined for coefficients not currently in the package, but which might be regenerated in the future, for example).	11/11/16	-
17/08/16	Sylvain Heilliette	Problems reading HDF5 coef files on IBM (AIX v7.1, xlf 13.1, HDF5 v1.8.17). Worked OK with ifort on Linux.	Sylvain managed to fix this by recompiling the HDF5 library for static linking only (no dynamic libs).	-	-
15/08/16	Robin Faulwetter/ Simon Proud	Coef download script does not work	Fixed (permission issue on server)	15/08/16	-
16/08/16	Robin Faulwetter	Description of test scripts is not clear: should state which scripts are called by test_core.sh.	Documentation updated to clarify which scripts are run by test_core.sh; test_cpu.sh has been removed from the user package and documentation.	11/11/16	-
15/08/16	Simon Proud	Failures in test_cpu.sh related to converting v9 predictor 101L AIRS files to binary format.	This was a problem with a couple of coefficient files: during development a bug was fixed in the code which converts v11 format files to v12 format, but I must have forgotten to re-convert these two files (AIRS and IASI-NG) after the code was updated. Converting them again fixed the failures.	15/08/16	-
22/09/16	Simon Proud	Sensor name field in example scripts is too short	Fixed	23/09/16	2081

06/10/16	Simon Proud	It is possible to supply cloud/aerosol coefficient files to the scaer/sccld arguments of the rttov_read_coefs subroutine (i.e. to get them the wrong way around) without any warnings, although the simulations are then wrong.	For ASCII files it is true that the file reading will work if cloud/aerosol files are accidentally swapped. I have added checks in the ASCII reading subroutines which catch the case when the wrong file has been supplied based on the section names. For binary files I have added an string at the top of the files to differentiate cloud/aerosol files (minor change in file format). This is not an issue for HDF5 format files as the cloud/aerosol files have different stuctures.	11/11/16	2128
04/10/16	Louis-Francois Meunier	Comment on Fortran atlas interface: the atlas setup calls do not need both coef and single_inst arguments: add an argument to select IR or MW emissivity atlases and the single_inst argument can be of type rttov_coefs. For CNRM atlas single_inst is mandatory; for IR atlases it's presence triggers single_inst initialisation; single_inst is ignored for TELSEM2. Similar for BRDF atlas.	Good idea, this has been implemented.	05/10/16	2090
10/10/16	Louis-Francois Meunier	Performance comparisons showed v12 slightly slower than v11.3 for clear-sky direct model MW simulations.	Simple modifications made in rttov_transmit.F90 to reduce cache misses.	11/10/16	2094
09/10/16	Philippe Chambon	Bugs in Mietable generation code: one affects calculation of backscatter coefficient which is not currently used in RTTOV and the other affects optical properties for non-recommended combinations of PSD and snow particle (the official snow properties are unaffected).	Fixes implemented.	11/10/16	2095
16/08/16	James Hocking	Memory leaks in visible/IR cloud coef I/O	Fixed	16/08/16	2064
17/08/16	James Hocking	A couple of additional memory leaks related to internal visible/IR scattering variables and MW simulations with CLW (the latter is a long-standing bug, fix for v11 posted on website)	Fixed	17/08/16	2068
16/09/16	James Hocking	Issue in sunglint calculation which can result in NaNs for extremely low wind speeds	Fixed	16/09/16	2078

11/10/16	James Hocking	The method of using different BRDFs for the direct solar source term and the diffuse radiation in the DOM algorithm is not appropriate: the current implementation requires a strictly Lambertian surface.	The code has been changed accordingly: this only affects solar DOM simulations which use the sunglint BRDF model.	11/10/16	2096
25/10/16	Jerome Vidot	Bug when initialising coefficients for solar scattering simulations if all channels are read from HDF5 coefficient file.	Fixed.	25/10/16	2110

3. SPECIFIC ISSUES RAISED BY BETA TESTERS

BJ Sohn (Seoul National University) beta test report

Description	Response	Date resolved	FCM rev
User guide typos	Fixed	11/11/16	-
TELSEM2 frequency extrapolation	This is doing no worse than the original TELSEM (more details in the full response below). User guide gives information about frequency extrapolation.	-	-
TELSEM2 missing values over Arctic sea ice	TELSEM2 developers were contacted and they provided updated atlas data with gaps filled by interpolation	12/10/16	-

Simon Proud (University of Oxford) beta test report

Description	Response	Date resolved	FCM rev
Compilation problems with gfortran and f2py	Makefiles were modified to fix this	01/11/16	2115
Suggestion to use gap-filled MODIS BRDF dataset	We will investigate this for a future update to the BRDF atlas	-	-
Some tests defined in tests.0/ do not work	Added comment on this in user guide	11/11/16	-
Comments on documentation	Most comments addressed. A few were not for the reasons given in the responses below.	11/11/16	-
Compile script treats "non-y" input as "n"	Compilation and coef download scripts modified to require explicitly "y" or "n"	27/10/16	2113
Option to input water vapour profiles as relative humidity	We will consider this for a future update	-	-

Robin Faulwetter (DWD) beta test report

Description	Response	Date resolved	FCM rev
Compile script said f2py was installed, but compilation with f2py failed	Updated script to try simple f2py compilation as a test of a functional f2py installation	15/11/16	2133
Linking statically on Cray/ifort does not work with -fPIC flag	Removed this from the cray-mo-ifort compiler flags (only required for f2py which is unlikely to be required in supercomputer environments)	14/01/16	2098

Coef download script fails silently on wget errors	The script now reports any non-zero wget error codes	27/10/16	2113
Suggestion to enable parallel compilations with different compilers	The build system is flexible enough to allow this (as described fully in the repsonses below). This is an advanced feature not required by typical users so it is not documented in the user guide.	-	-
Mismatches in subroutine argument order and declaration order	Aside from the cases where this is required this is something we will remedy as we update the code in the future.	-	-
Wrongly set executable bits on some source files	Fixed	14/01/16	2098
Suggestion to modify rttov_test.pl to make it easier to work with work-load schedulers	Added argument to rttov_test.pl which allows a scheduler command to be inserted before each executable is run from the script.	23/11/16	2145
Suggestion to improve reporting of test suite issues in the shell scripts	As noted below this is not very easy, but is something we can consider in the future	-	-
Help for syntax of RTTOV executables	I have modified the code so that for all RTTOV executables the full syntax is printed out if no arguments are supplied.	14/01/16	2098
OpenMP performance	As we discussed there were probably hardware issues which explain this	-	-
Suggestion for improved coef reading on MPI systems	This is something we can look at in the future	-	-
Removal of interface files, use modules instead	We do not plan to do this for the reasons given below in the responses	-	-
Specifying a directory for rttov_read_coefs	Added an optional path argument as discussed (and did the same for rttov_read_scattcoeffs for RTTOV-SCATT).	23/11/16	2143
Allow rttov_user_profile_checkinput to modify the input profile using regression limits	For the reasons given below in the responses I do not plan to implement this	-	-
Profile names in the GUI	I have added labels to the test suite profiles which are displayed in the GUI	26/10/16	2112
Cfraction/CTP for simple cloud not displayed in GUI	The GUI now shows the CFRACTION value	26/10/16	2111
Jacobians for other surface variables in GUI	This is something we can look at in the future	-	-
Channel selection for 1DVAR retrievals in the GUI	This is already possible	-	-
Documentation comments	All comments addressed in the documentation	11/11/16	-

RTTOV-12 Evaluation Report

B.J. Sohn

School of Earth and Environmental Sciences
Seoul National University
Seoul, 151-747, Korea
Tel. +82-2-880-8166 E-mail: sohn@snu.ac.kr

(05 October 2016)

Contents

1. Compilation of the RTTOV-12 and execution of the test script

1.1. Unpacking the RTTOV code

1.2. Compiling and installing the RTTOV code

1.3. Running the test script

2. Evaluation of RTTOV-12 *Users Guide*

3. Clear-sky simulations

3.1. New extrapolation method

3.2. IR surface emissivities

3.3. Sea ice emissivities from new TELSEM2 atlas

4. Cloudy-sky simulations (IASI hyperspectral channel simulations)

4.1. Simulations of cloud-affected radiances using a 'simple cloud approach'

4.2. Simulations of cloud-affected radiances using a 'cloud profile approach'

4.3. Impact of new parametrization for ice particle on cloud retrieval

(Minimum residual method)

5. Aerosol simulations

5.1. New aerosol scattering model for various aerosol types

5.2. Impact of dust loadings

5.3. Impact of DOM streams on the simulation

References

List of Table

List of Figures

1. Compilation of the RTTOV-12 and execution of the test script

1.1. Unpacking the RTTOV code

Following command was used to unpack the code

tar –xvf rttov120.tar.gz

Total 16086 files were successfully unpacked in subdirectories; source code, coefficient files, and test scripts are successfully stored in *src, rtcoef_rottov12*, and *rttov_test* directories respectively.
BRDF coefficient files and emissivity files were downloaded from website (http://nwpsaf.eu/downloads/rttov12_files/rttov12_beta.html) and stored in *brdf_data*, *emis_data* respectively.

1.2. Installing and compiling the RTTOV code

PGI Fortran compiler has been used to build the RTTOV model from 485 source codes in *src* directory. The compiling time took about 747 seconds, which is considered to be fast enough to handle with a moderate computing power. Used procedures are following:

make ARCH=pgf90

1.3. Running the test script

Problems were not found.

2. Evaluation of RTTOV-12 *Users Guide*

User's Guides are found to be well-documented and informative. Some typos are found and we suggest them changed.

- Page 5: gives gives → gives
- Page 14: mmr_claer → mmr_cldaer
- Page 14: g/cm^3 for clouds→ g/m^3 for clouds
- Page 20: demonstratation → demonstration
- Page 24: depedent → dependent
- Page 32: the the MW → the MW
- Page 35: Alterntively → Alternatively
- Page 39: non-consective → non-consecutive

- Page 46: atmsosphere → atmosphere (4th row in table 17)
- Page 46: atmsosphere → atmosphere (5th row in table 17)
- Page 50: simuilations → simulations
- Page 55: mutiplied → multiplied
- Page 55: the the albedo → the albedo
- Page 63: coefficent → coefficient
- Page 65: *forPC → for PC*
- Page 93: kg/m2/s→kg/m^2/s
- Page 124: R e al→Real
- Page 124: kg/m2/s→kg/m^2/s

3. Clear-sky simulations

3.1. New extrapolation method

In this section, simulated clear-sky brightness temperatures (TBs) for Moderate Resolution Imaging Spectroradiometer (MODIS) infrared (IR) channels from both RTTOV v11.3 (henceforth referred to as v11) and RTTOV v12-beta (henceforth referred to as v12) are presented, to examine how the new extrapolation method in v12 affects results in comparison with v11. In these simulations, Thermodynamic Initial Guess Retrieval (TIGR) profiles (#1–1614) over the tropics (#1–872) and mid-latitudes (#873–1614) are used as inputs to the model. Surface emissivity is assumed to be 1.0, and surface pressure, temperature, and water vapor are given by the values at the lowest-level. Ready-made shell script (i.e. *example_fwd.sh*) and associated routines (i.e. *example_fwd.F90*) are modified to simulate multi-cases.

TBs of sixteen MODIS IR channels (20–36, except 26) are simulated using both v11 and v12, and differences between two versions are given in Figure 1. As expected, most of channels show well-matched TBs between v11 and v12 since the coefficients for MODIS IR channels were not changed during the version update. However, small biases are found in three MODIS IR channels (i.e., 24: 4.466 μm, 35: 13.935 μm, 36: 13.935 μm) at two profiles (#1251, #1582 given in x-axis). Simulated TBs at the three channels using v11 and v12 and their differences with v12 simulations are given in Table 1. The maximum TB difference between v11 and v12 is about 0.07 K at channel 36 for the profile #1582 though the same coefficients are used for both simulations.

Because of the biases found over the strong CO_2 channels, we examine TIGR temperature profiles in conjunction with model-provided upper/lower limits describing the valid range for the simulation (Figure 2). It is shown that most of TIGR temperature profiles are in the range provided

for v11. Although some profiles are located between the upper limits for v11 and for v12, those cases did not cause the TB biases. Only two temperature profiles (#1251 and #1582) appear outlying the valid range for both v12 and v11 above the 0.1 hPa level. In v11, the constant-value extrapolation was performed to fill the values between the top of the input profile and the top of the coefficient profiles. Considering that the upper limits for the simulation have a decreasing tendency from 0.3 hPa to 0.005 hPa, all the extrapolated values may be outside the valid range for both profiles. However, in v12, any profile values obtained by the extrapolation that exceed the limit are clipped to the limits. We expect that this difference could make the biases between the two versions. Nonetheless, such limitation should be very minor since it occurs in the rarefied air situation above 0.1 hPa, with a much smaller magnitude of the TB difference.

In v11 and v12, users are allowed to choose the *apply_reg_limits* option. When *apply_reg_limits* option is set *true*, profiles exceeding the imposed limits are clipped to the upper (or lower) limit of the input for the simulation. Here, *apply_reg_limits* option is set *true* for the v11 simulation. The resultant TBs of v11 become much closer to those of v12 (see Table 1). This indicates again that interpolation method is linked to the TB differences. It is noted that there are remaining TB differences around −0.03 K. TB differences between v12 and v12 with the *apply_reg_limits* simulation also show the same values (see Table 1). That is, when *apply_reg_limits* option is set *true* for both v11 and v12, TB differences between two versions become zero (Figure 3). Because v12 *apply_reg_limits* option only changes exceeded values over 0.1 hPa – 0.05 hPa into the limit values, the remaining TB differences around −0.03 K are caused by exceeding input values.

In summary, two versions show small TB differences in strong CO_2 channels because of the new extrapolation method for v12. When the *apply_reg_limits* option is chosen, two versions yield same TBs for all MODS IR channels. We cannot conclude that simulated TBs from modified profiles with an aid of the *apply_reg_limits* option are realistic because the original profile is altered. But, at least we conclude that the new extrapolation scheme used for v12 looks reasonable.

3.2. IR surface emissivities

New IR surface emissivity model and atlas were updated in v12, and so we are much interested in examining how these changes make impact on the TOA radiance simulation. For ocean, previous IREM model parameterizes the emissivity from satellite viewing angle (Sherlock, 1999), while the new IREMIS model uses the zenith angle, 10 m wind speed, and skin temperature for emissivity parameterization. The new land emissivity atlas named CAMEL is also introduced, in addition to the previous emissivity atlas (UWIR) by Borbas et al. (2010).

In this section, Suomi-NPP Cross-track Infrared Sounder (CrIS) TBs are simulated with clear-sky conditions, using both v11 and v12. Since coefficients for the CrIS sensor for v12 are not much different except for trace gas absorption lines, the difference between v11 and v12 may be attributed largely to the difference in surface emissivity model or different emissivity atlas. By comparing two simulated TBs against CrIS measurements over both ocean and land areas, the impact of emissivity update on the TB simulation is evaluated. In these simulations, the Korea Meteorological Administration (KMA) United Model (UM) forecast fields (i.e., surface temperature, surface pressure, wind speed at 10 m altitude, temperature and water vapor profiles) at 25-km resolution and 70 vertical levels are used as inputs, along with the location and zenith angle of the collocated CrIS observations.

In this test, we selected the 17UTC 13 October 2013 case, which is characterized by the clear area over the East China Sea and adjacent land regions. Figure 4a shows the geographical distribution of the CrIS zenith angle in this case. In Figures 4b–c, emissivities at 900 cm^{-1} from v11 and v12 are given. Both emissivities are very similar to each other, especially over the ocean. Since the ocean emissivity from IREM in v11 is parameterized only with the satellite zenith angle, the emissivity and satellite zenith angle are nearly parallel to each other. In contrast, the emissivity from IREMIS and satellite viewing angle are not parallel since the IREMIS emissivity is parameterized with 10 m wind speed and skin temperature as well as satellite zenith angle. For land, the new CAMEL atlas represents the emissivity relatively lower than that from the UWIR atlas, especially over the eastern China, Korea, and Japan regions.

The distribution of CrIS TB at 900 cm^{-1} is given in Figure 4d. In the clear area, TBs warmer than 280 K are found. Meanwhile, cloud areas are found in the northwest, southwest, and southeast edges of the scene. Several small areas over the East China Sea are also contaminated by low level clouds. Over the clear areas, v11 and v12 simulate reasonably well the distribution of TB at 900 cm^{-1} (Figures 4e–f). Because the 900 cm^{-1} is a window channel, TB at 900 cm^{-1} is mostly determined by surface temperature and emissivity. When comparing the variability in surface temperature and emissivity within the scene, TB distributions in Figures 4e–f appear to be mostly reflecting the horizontal distribution of UM surface temperature.

For selected clear regions, described as black squares in Figure 4d, the emissivity spectra from v11 (with ISEM model and UWIR atlas) and v12 (with IREMIS model and CAMEL atlas) are compared (Figure 5). Corresponding CrIS observations are also given. Over the ocean, surface emissivity differences and TB differences between v11 and v12 are not significant (Figures 5a–b). The emissivities from IREMIS model tend to be slightly lower than those from ISEM model, except

for the wavenumber range less than 800 cm^{-1} (Figure 5a). Because of that, TBs from v12 generally show the values lower than those from v11. Mean TB biases from all 1305 channels against CrIS observation are very small for both simulations (0.135K vs. 0.111K for v11 vs. v12). Over the land, the emissivity differences between UWIR atlas and CAMEL atlas are relatively larger than those over the ocean (Figure 5c). The CAMEL emissivity is higher over the midwave-infrared (MWIR) band (1210–1750 cm^{-1}) and lower over the shortwave-infrared (SWIR) band (2155–2550 cm^{-1}) than the UWIR emissivity. The emissivity differences are associated with the reduced mean TB bias against observation from v11 (0.016 K) to v12 (–0.007 K) (Figure 5d). Overall, both ocean and land cases show the reduced mean TB biases against the CrIS observations when new emissivities are used.

Here, we further examine the impact of angular correction, which was developed by Borbas (2014), on the TB simulation over the land. When the angular correction is applied for both UWIR and CAMEL, emissivities over the longwave-infrared (LWIR) band (650–1095 cm^{-1}) and over the SWIR band become slightly smaller and larger, respectively (Figure 5e). Over the MWIR band, the impact of angular correction appears to be neutral. For v11, the angular correction gives rise to the change in the mean TB bias from 0.016 K to 0.004 K (Figure 5f), while the mean TB bias is changed from –0.007 K to –0.019 K for v12. The reasons of the increased bias in v12 are not clear to us.

3.3. Sea ice emissivities from new TELSEM2 atlas

In v12, a land surface emissivity atlas within the microwave frequencies (so called TELSEM2: Tool to Estimate Land-Surface Emissivities at Microwave frequencies version 2) was introduced. Emissivity data produced at frequencies between 19 and 85 GHz (i.e. Special Sensor for Microwave Imager (SSMI) frequencies) provide emissivities down to 6 GHz and up to 200 GHz using the interpolation as well as the extrapolation scheme. In this section, newly-included emissivities for the sea ice in TELSEM2 are compared with the emissivity data over the Arctic sea ice, which were based upon a new approach so-called “combined Fresnel equation” approach. One paper describing the emissivity retrieval method over the sea ice and obtained results is prepared for the journal submission, and scientific outcomes can be shared (via personal communication at this moment). The retrieved emissivities are produced by solving the radiative transfer equation for microwave transmission. In order to obtain the surface emissivities, surface temperature retrieved from AMSR-measured 6.9 GHz polarized brightness temperature, RTTOV-simulated brightness temperature with the use of European Centre for Medium Range Forecast Reanalysis – Interim (ERA-interim) atmospheric profiles are used.

There are no problems to download the TELSEM2 codes from the NWP SAF RTTOV-12 beta test homepage, following the user's manual, and unpack and compile the codes. It took about 5 minutes from the download to the test running. Unpacking and compiling of TELSEM2 were similar with RTTOV codes.

In order to generate the sea ice emissivities at the frequencies of Advanced Microwave Scanning Radiometer – EOS (AMSR-E), the ready-made Fortran code (i.e. *test_telsem2.F90*) was used along with inputs of the 25 km × 25 km EASE (Equal-Area Scalable Earth) grid geolocation data downloaded from NSIDC (National Snow Ice Data Center), AMSR-E frequencies (i.e. 6.925, 10.65, 18.7, 23.8, 36.5, and 89.0 GHz), and zenith angle information (here 55°). The sea ice emissivities at both polarizations were generated for all AMSR-E channels.

Figures 6 and 7 show the geographical distributions of the obtained TELSEM2 sea ice emissivities over the Arctic regions. The obtained outputs seem to be fairly reasonable in physical perspective, in comparison to the well-known optical characteristics of the polar sea ice. The emissivities of multiyear sea ice are smaller than those of first-year sea ice over the whole microwave frequencies. Vertically polarized emissivities tend to be larger than horizontally polarized emissivities. However, it is shown that the emissivities at frequencies lower than 18 GHz appear to be the same values as for 18 GHz, and the emissivities at frequencies higher than 85 GHz appear to be fixed as the values at 85 GHz. The manual indicates the extrapolation to produce emissivites down to 6 GHz and up to 200 GHz. We are not sure about the cause of producing such same data. It may be due to the error in the extrapolation modules. Further examination is needed. Also, there found to be some erroneous values depicted by purple dots over the Central Arctic Ocean. It was not possible to track down the problem.

We gave an effort of how reasonable TELSEM2 sea ice emissivity might be. This assessment should be important when considering the fact that the current status of the data assimilation over the polar region is extremely poor. A little amount of satellite radiance measurements is directly assimilated because of the lack of sea ice surface information such as sea ice emissivity. In this effort, we compare the v12 TELSEM2 emissivities with products from the “combined Fresnel equation” method (Lee and Sohn, 2015). In this emissivity retrieval, 6.9 GHz sea ice temperatures are assumed to be the same at other frequencies (here lower than 36.5 GHz). Then, emissivities are obtained by running RTTOV with inputs of atmospheric T/q profiles from ERA-interim analysis.

Figure 8 shows the AMSR-E derived horizontally polarized emissivities at 6.9, 10.6, 18.7, 23.8, and 36.5 GHz. General features are quite similar to the TEMSEM2-generated emissivities, but details are significantly different. Note that our products are emissivities directly retrieved from

instantaneous satellite-measured TBs (here from TBs for 1 January 2010). With higher frequencies, the contrast between the multiyear sea ice and first-year sea ice becomes more visible (green vs. yellow). As pointed out, the same distributions of TELSEM2 emissivities at the frequencies lower than 18 GHz should be erroneous, probably related to the extrapolation scheme.

Figure 9 shows the corresponding vertically polarized emssivities on 1 January 2010. The 6.9 GHz emissivity distributions nicely capture the feature that would be expected for emissivities at the Brewster angle. Since emissivity is given at 55º, we expect a near unity value at the lower frequency, such as shown in 6.9 GHz. With higher frequencies, more distinct patterns reflecting the contrast between multiyear sea ice and fresh-year sea ice -- see the contrast between green and reddish color in 36.5 GHz.

It is also noted that the horizontal component has larger differences between TELSEM2 and the instantaneous retrievals. This is true because the horizontal polarization is more sensitive to the surface conditions (e.g. surface roughness, salinity, and snow depth over the sea ice), in comparison to the vertical component, and TELSEM2 may not reflect such variations causing the changes in the emissivity.

In summary, the TELSEM2 atlas in v12 seems to provide the general features that might be expected from the distribution of sea ice concentration. However, those values may not be accurate enough to use for the radiance simulation, which is required for the data assimilation. In addition, further examination is required to examine why the extrapolation did not work.

4. Cloudy-sky simulations (IASI hyperspectral channel simulations)

4.1. Simulations of cloud-affected radiances using a 'simple cloud approach'

IASI hyperspectral radiances under overcast cloud condition (cloud fraction = 1.0) were simulated by using cloud schemes in v11 and v12. In doing so, fifty atmospheric profiles over the ocean were randomly selected from the ECMWF 137-level short-range forecasts. Each profile contains temperature, water vapor, and other trace gases profiles. In both v11 and v12 simulations, cloud tops are specified at 7 different pressures (200, 300, 400, 500, 600, 700, and 800 hPa). The cloud scheme used for the simulations is so-called a 'simple cloud scheme' which requires cloud top pressure and fraction as inputs, but excludes the full scattering calculation. Solar effect was excluded, thus the radiative processes considered in this simulation are pure thermal absorption and emission by the atmospheric gases and cloud. IASI 8461 channel TBs were simulated using v11 and v12, and their mean TBs are given in Figure 10. Also given is the TB difference (v12 minus v11) -- Figure 10c. The differences over the whole IASI wavenumbers are hundredths of a Kelvin regardless of cloud

top pressure. Results suggests that the 'simple cloud' simulation in v12 produces nearly the same results as shown in v11.

4.2. Simulations of cloud-affected radiances using a 'cloud profile approach'

Different from the 'simple cloud scheme approach' we tested the 'cloud profile approach' which uses cloud hydrometeor profiles as inputs. It has been noted that ice cloud simulations for IASI channels using v11 appear to have problems in the range of 800-1000 cm^{-1} (see the online RTTOV 11 General Discussion), when the cloud profile approach is used. Here we attempt to examine whether simulations are improved with the new cloud parameterization in v12. In doing so, we used 4219 atmospheric profiles and associated cloud profiles (i.e.: cloud fraction, cloud liquid water content, and cloud ice water content) from ECMWF short-range forecasts. Cases showing the maximum cloud fraction greater than 0.99 over the ocean were selected and simulated. Simulation results are given with cloud top pressures. Here the cloud top pressure is defined by the lowest pressure at which the cloud fraction exceeds 10% of its maximum (so-called effective cloud top pressure) -- Pavelin et al. (2008).

For the ice cloud simulation, the effective size of ice particles should be determined before calculating the optical property of ice cloud. In determining the effective diameter, the McFarquar et al. (2003) scheme generates a relatively larger effective diameter than that generated by the Boudala et al. (2002) scheme, even if the ice water content is same. Henceforth, the McFarquar et al. (2003) and Boudala et al. (2002) schemes are referred to as M scheme and B scheme respectively. Along with the diameter specification from two cloud schemes, ice optical properties are determined from the cloud parameterization (i.e. hexagonal or aggregates). Note that v11 uses hexagonal or aggregates type for the parameterization while v12 replaced those types with the empirical data base (i.e. SSEC database)

In the results, the erroneous curved shape over the 800-1000 cm^{-1} band is found in the simulations from v11 aggregates type with M scheme as well as with B scheme. The curved shape is also found in the simulation from v11 hexagonal type with B scheme. On the other hand, the v11 hexagonal with M scheme does not show such curved shape. The simulation results indicate that v12 which uses the SSEC database did not produce such curved pattern regardless of the cloud size scheme.

In order to examine how TB distributions are changed in v12 simulations, in comparison to v11 simulation, v11 simulated TBs were subtracted from the v12 simulations. In the v11 simulations, two ice diameter schemes (M and B schemes) were combined with ice crystal types (aggregates and

hexagonal), yielding 4 combinations (i.e. aggregates + B, hexagonal +B, aggregates + M, and hexagonal + M). TB simulations from v12 with the two different ice diameter schemes were obtained, and subtracted from the corresponding B or M simulation of v11. In Figure 12, the differences appear to be large for B scheme, and as in Figure 12a-c, the differences indicate that the curved features over the 800-1000 cm^{-1} band were removed in v12. It is also noted that larger changes are made for clouds with higher cloud tops. It is probably due to the fact that in the version update, major changes were made for ice clouds (not for water clouds), more influencal in high clouds where ice crystals are prevalent.

Besides those parameterization methods, the Baran scheme option is available. Thus, it is quite interesting to examine how the Baran scheme gives different results with the version upgrade. In this comparison, v11 and v12 used Baran 2013 and Baran 2014 ice cloud parameterization schemes, respectively. Simulated IASI TBs for cloudy cases using Baran 2014 scheme (v12) show a flat shape over the window region while Baran 2013 (v11) have an erroneous slant line shape. Hence, we conclude that the Baran scheme generates features more agreeable to observations under cloudy condition. The TB differences are positive in this case and changes seem to be made more for higher clouds (Figure 13c).

4.3. Impact of new parametrization for ice particle on the cloud retrieval (Minimum residual method)

In the previous section, substantial differences in TBs are noted between v11 and v12, and between cloud schemes. If we use these simulations for developing the retrieval algorithm of cloud properties, the dependence on the RTM version and cloud scheme should imply different training data needed for the algorithm development. Here we examine the impact of the different cloud scheme on the cloud retrieval. In doing so, the minimum residual method described by Eyre and Menzel (1989) was used. The method simultaneously retrieves cloud top pressure and cloud fraction by minimizing the difference between observed and forward-model calculated radiances. A ‘simple cloud approach’ option in v11 was chosen for the minimization procedures. For true IASI-observed radiances under the cloud condition, simulated TBs with parameterizations of the hexagonal type and with the use of SSEC database were selected for v11 and v12, respectively, in conjunction with M scheme for the diameter parameterization. Those parameterizations were chosen because they are the combinations not showing the curved pattern in the window region. The corresponding background, which are needed for running the forward model, was obtained by adding the United Model 3-hour forecast error to the same ECMWF atmospheric states used for the previous cloudy radiance

simulation.

In order to assess retrieved cloud top height, the previously defined effective cloud top pressure is taken. For the assessment of cloud fraction, we define the effective cloud fraction as the maximum value amongst all level values. Correlation between the effective cloud top pressure and the retrieved cloud top pressure from v12 cloudy radiances is higher than that from the use of v11 (Figure 14). Both results show that retrieved cloud top pressures seem to have larger biases when the retrieved cloud fractions are small. Since we only used cases having an effective cloud fraction larger than 0.99, small values of retrieved cloud fraction reflect a bad retrieval. Correlation coefficient between the retrieved cloud top from v11 and v12 simulation is 0.96 (Figure 15). However, some cases having lower limited value of cloud top pressure in v11 (i.e. 200 hPa) show much higher values when retrieved using v12. As those cases have a large effective cloud top, we conclude that the cloud top retrieval is improved with the use of v12 for the simulation. Since the minimum residual method adjusts the cloudy radiances to the simple cloud simulation, it is suggested that v12 radiances are more representative of level of cloud top.

5. Aerosol simulations

A new scattering algorithm for aerosols, which is called as Discrete Ordinates Method (DOM), is introduced in v12. Since the previous 'Chou-scaling' scheme has been used only for considering the thermal emission in the aerosol-affected TB simulation, better aerosol-affected TB simulations may be expected from the v12 with DOM. In this section, we intend to simulate the aerosol influences on IASI radiances, and to examine how TBs from v12 differ from those from v11, with respect to the aerosol types and aerosol amounts. Considering that regression coefficients for the IASI channels are not much changed in v12 except for the trace gas absorption lines, TB differences in this aerosol simulations between v11 and v12 simulations can be largely attributed to aerosol influences. In the v12 simulations with the DOM, the number of DOM streams should be from 2 to 128, in order to determine the accuracy of DOM. Here, the sensitivity of TB to the used number of DOM streams is also examined.

5.1. New aerosol scattering model for various aerosol types

The RTTOV contains climatological profiles for various aerosols, which are defined as the mixture of thirteen aerosol particle types. The aerosol compositions for pre-defined climatological aerosol profiles in v12 are given in Figure 16. Once an aerosol profile is selected, its optical property at given wavelength is calculated from pre-defined optical properties of aerosol particles which are

contained in the aerosol profile. Here, all climatological aerosol profiles given in v12 are employed for the test. Atmospheric condition is fixed with the US 1976 standard atmosphere profile. For the aerosol simulation the sample script (*/src/test/ example_aer_file_fwd.F90*) was modified. The TB differences between v11 and v12 are plotted for various aerosol types in Figure 17. Positive differences smaller than 0.2 K in magnitude are found for the continental and maritime type aerosols over the IR spectra range of 750–1300 cm^{-1}, 2000–2200 cm^{-1}, and 2400–2800 cm^{-1}, except for the *desert* type aerosol. In particular, large positive biases are found over the CO_2 absorption band (800–850 cm^{-1}) and the window region. For the *desert* aerosol profile, negative biases are shown over the O_3 absorption band (1030 cm^{-1}) and around the window channels, which are likely due to optical properties of 'mineral (nuclei mode)' as one of compositions for the *desert* type aerosol profile.

5.2. Impact of dust loadings

In this section, we examine the impact of the DOM used in v12 on the simulation of IASI TBs for various aerosol amounts. For this comparison, the *desert* aerosol profile is chosen, and its aerosol concentration at each pressure level is modified by multiplying weights of 0.25, 0.50, 1.0, 2.0, and 4.0. As done before, atmospheric condition is fixed with the US 1976 standard atmosphere profile. The differences in IASI TBs between v11 and v12 are shown in Figure 18. The biases over the 750–1300 cm^{-1}, 2000–2200 cm^{-1}, and 2400–2800 cm^{-1} tend to change from the positive to the negative as the aerosol amount increases. In particular, large differences up to −0.8 K are found in the split-window channel over 900 cm^{-1} and 1100 cm^{-1}.

5.3. Impact of DOM streams on the simulation

In order to use DOM in v12, the number of DOM streams should be defined as an even integer. The default value is 8 and the maximum value can be set 128. When the number of DOM streams increases, the accuracy of DOM increases but at the expense of increased computational time. Here we examine the influence of the number of DOM streams on the accuracy of the IR TB simulation so that we may have an idea of what might be the optimized number. In doing that, IASI TBs are simulated from v12 with 8 (default), 12, 16, 20, and 24 DOM streams, respectively. The US 1976 standard atmosphere profiles with the climatological *desert* profile in v12 are used as inputs. The differences between IASI TBs simulated with various DOM streams are plotted in Figure 19. When we compare TBs from 8 and 12 DOM streams (Figure 19a), most of differences are presented over the IR spectra range of 750–1300 cm^{-1}, 2000–2200 cm^{-1}, and 2400–2800 cm^{-1}. The magnitudes of the biases are very small (±0.01 K). When the number of DOM streams is larger than 12, very little TB

differences are found. In Figures 19b and 19c, TB differences between 12 and 16 DOM streams, and between 16 and 20 DOM streams are presented, respectively. When the number of DOM streams exceeds 20, there seems to be no practical change in simulated IASI TBs. Therefore, we conclude that the default value (i.e. 8) for the number of DOM streams may be changed to 12 for more accurate simulation. But the stream numbers greater than 12 might not be necessary. Overall, the default value of 8 should be a reasonable choice.

References

Borbas, E. E., and B. C. Ruston, 2010: The RTTOV UWiremis IR land surface emissivity module. *NWP SAF report.* http://nwpsaf.eu/vs_reports/nwpsaf-mo-vs-042.pdf.

Borbas, E, 2014: The RTTOV UWiremis module Investigation into the angular dependence of IR surface emissivity. *NWP SAF report.* http://nwpsaf.eu/vs_reports/nwpsaf-mo-vs-050.pdf.

Eyre J. R., and W. P. Menzel, 1989: Retrieval of cloud parameters from satellite sounder data: a simulation study. *J. Appl. Meteorol.*, **28**, 267–275.

Lee, S.-M., and B. J. Sohn, 2015: Retrieving the refractive index, emissivity, and surface temperature of polar sea ice from 6.9 GHz microwave measurements: A theoretical development, *J. Geophys. Res. Atmos.,* **120**, 2293–2305.

Pavelin, E. G., S. J. English, and J. R. Eyre, 2008: The assimilation of cloud-affected infrared satellite radiances for numerical weather prediction. *Q. J. R. Meteorol. Soc.,* **134**, 737–749.

Sherlock, V., 1999, ISEM-6: Infrared Surface Emissivity Model for RTTOV-6. *NWP SAF report.* http://nwpsaf.eu/deliverables/rtm/papers/isem6.pdf.

List of Table

Table 1: Simulated MODIS TBs for three CO_2 channels using v11 and v12 with default and *apply_reg_limits* option. When *apply_reg_limits* option is set *true*, the profile values are clipped to the regression limits. The values in parentheses are TB differences against v12 default simulations. TBs are simulated for TIGR 1251th and 1582th profiles.

List of Figures

Figure 1: TB differences between v11 and v12 at sixteen MODIS IR channels. Simulation using v11 and v12 are done with TIGR profiles.

Figure 2: All TIGR temperature profiles (grey lines) are given with their mean profile (black line). Among the TIGR profiles, 1251th (purple line) and 1582th (orange line) profiles are highlighted since they show notable TB differences between v11 and v12 at three MODIS CO_2 channels. Red and blue lines indicate the upper and lower limits of the valid ranges for v11 and v12, respectively.

Figure 3: TB differences between v11 and v12 simulations at three MODIS CO_2 channels when *apply_reg_limits* option is set *false* (upper panels) and *true* (bottom panels). The profile values are clipped to the regression limits if *apply_reg_limits* option is set *true*.

Figure 4: (a) CrIS viewing angle, and surface emissivities at 900 cm^{-1} from (b)v11 (ISEM for ocean and UWIR for land), (c) from v12 (IREMIS for ocean and CAMEL for land). TBs at 900 cm^{-1} from (d) CrIS, (e) from v11, (f) from v12 for the case of 17UTC 13 October 2013. Clear areas for further analysis are outlined by black squares in (d).

Figure 5: Mean CrIS emissivity spectrum from (a) ISEM and IREMIS models, (c) UWIR and CAMEL atlases, and (e) angular corrected UWIR and CAMEL atlases. Corresponding simulated TBs are given in (b), (d), and (f) with CrIS observation. Black, red, and blue lines indicate the CrIS observation, v11, and v12, respectively.

Figure 6: The TELSEM2-generated horizontally polarized emissivities over the Arctic sea ice at six AMSR-E frequencies.

Figure 7: Same as Figure 6 but for vertically polarized emissivities.

Figure 8: Retrieved horizontally polarized emissivites over the Arctic Ocean on 1st January 2010, for AMSR-E 6.925, 10.65, 18.7, 23.8, and 36.5 GHz.

Figure 9: Same as in Figure 8 except for vertically polarized emissivities.

Figure 10: IASI simulated TBs using a simple cloud scheme with given seven different cloud top pressures. Spectral distributions are for (a) v11 and (b) v12, and for (c) the difference between (a) and (b).

Figure 11: IASI simulated TBs with given seven different cloud top pressures; (a) for aggregates type with B scheme, (c) for hexagonal type with B scheme using RTTOV v11, (e) for SSEC database properties with B scheme in RTTOV v12. (b), (d) and (f) are same as in (a), (c) and (e) except with M scheme.

Figure 12: Differences in simulated TBs between v11 and v12 (v12 minus v11). For the v11 simulations, M scheme is used with (a) aggregates type and (c) hexagonal; B scheme is used with (b) aggregates type and (d) hexagonal type. For the v12 simulations, the SSEC database is used with M scheme (a, c), and with B scheme (b, d).

Figure 13: IASI simulated TBs from the Baran scheme with respect to seven different cloud top pressures (a) using v11, (b) using v12, and (c) the difference between (a) and (b).

Figure 14: Scatter plots of effective cloud top pressures and retrieved cloud top pressures from the minimum residual method using simulated IASI radiances from (a) v11 and (b) v12. Individual colors indicate the cloud fraction retrieved from minimum residual method.

Figure 15: Scatter plot of retrieved cloud top pressures using v11 and v12 simulated cloudy radiances. Individual colors indicate the corresponding effective cloud top pressure.

Figure 16: Aerosol compositions of climatological aerosol profiles included in v12.

Figure 17: Difference of IASI TBs between v11 and v12 for (a) continental clean, continental average, continental polluted, urban, and desert, and (b) maritime clear, maritime polluted, maritime tropical, Arctic, and Antarctic aerosol profiles.

Figure 18: Difference of IASI TBs between v11 and v12 with *desert* aerosol profiles for various aerosol amount. Aerosol amount is modified by multiplying weight values of 0.25 (black), 0.50 (blue), 1.0 (cyan), 2.0 (yellow), and 4.0 (red) to climatological *desert* aerosol profile in v12.

Figure 19: Differences of IASI TBs simulated from v12 with various number of DOM streams. For calculating TB differences, the number of DOM streams are defined as (a) eight and twelve, (b) twelve and sixteen, and (c) sixteen and twenty.

Table 1: Simulated MODIS TBs for three CO_2 channels using v11 and v12 with default and *apply_reg_limits* option. When *apply_reg_limits* option is set *true*, the profile values are clipped to the regression limits. The values in parentheses are TB differences against v12 default simulations. TBs are simulated for TIGR 1251th and 1582th profiles.

Profile number	Channel number (wavelength)	TB (ΔTB)			
		v12	v11	v11 *apply_reg_limits*	v12 *apply_reg_limits*
1251	26 (4.466 μm)	241.20 (·)	241.22 (0.02)	241.20 (0.00)	241.20 (0.00)
	35 (13.935 μm)	237.35 (·)	237.37 (0.02)	237.34 (–0.01)	237.34 (–0.01)
	36 (14.235 μm)	221.74 (·)	221.78 (0.04)	221.74 (0.00)	221.74 (0.00)
1582	26 (4.466 μm)	238.87 (·)	238.93 (0.06)	238.84 (–0.03)	238.84 (–0.03)
	35 (13.935 μm)	238.07 (·)	238.12 (0.05)	238.05 (–0.02)	238.05 (–0.02)
	36 (14.235 μm)	229.29 (·)	229.36 (0.07)	229.28 (–0.01)	229.28 (–0.01)

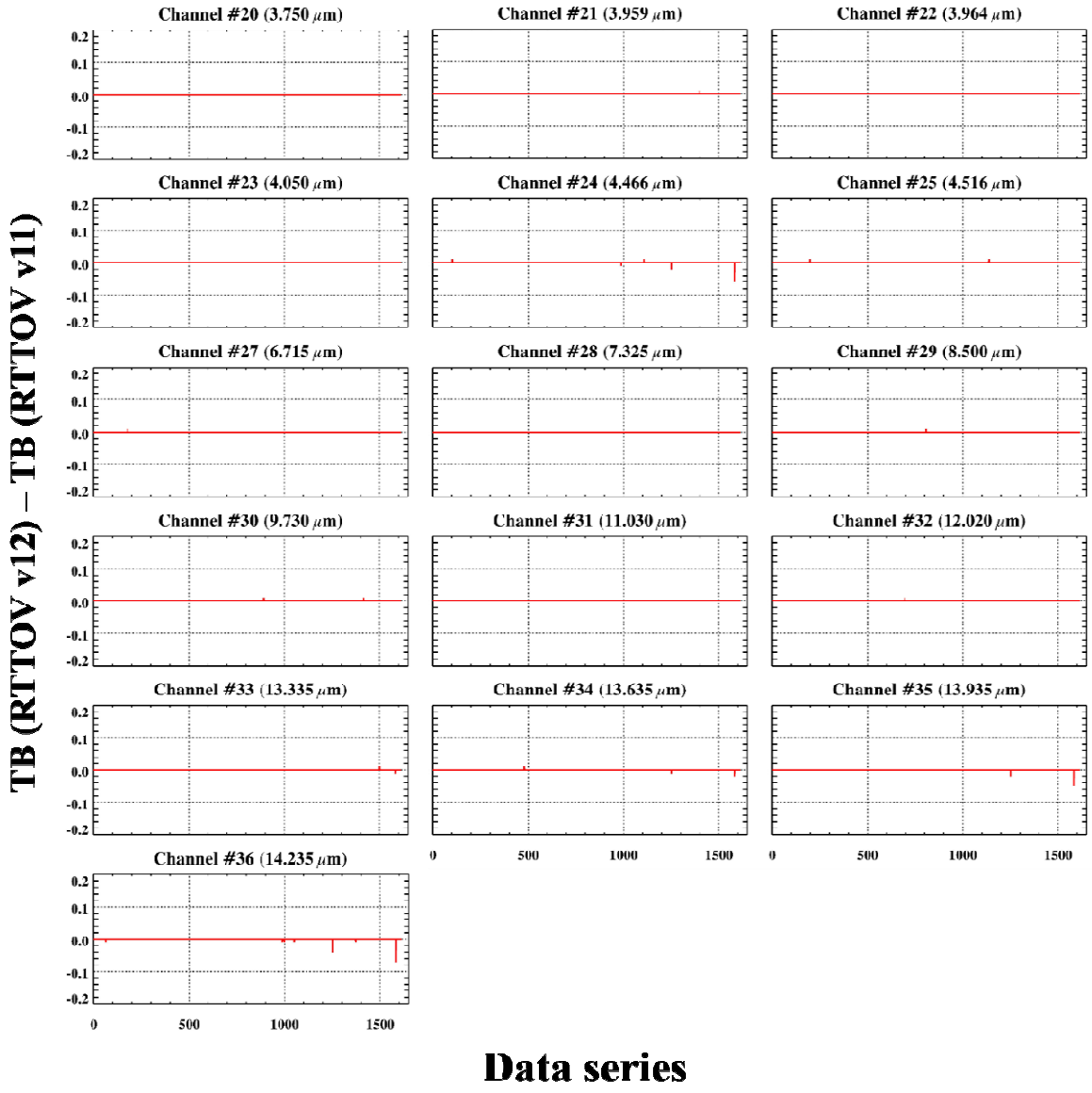

Figure 1: TB differences between v11 and v12 at sixteen MODIS IR channels. Simulation using v11 and v12 are done with TIGR profiles.

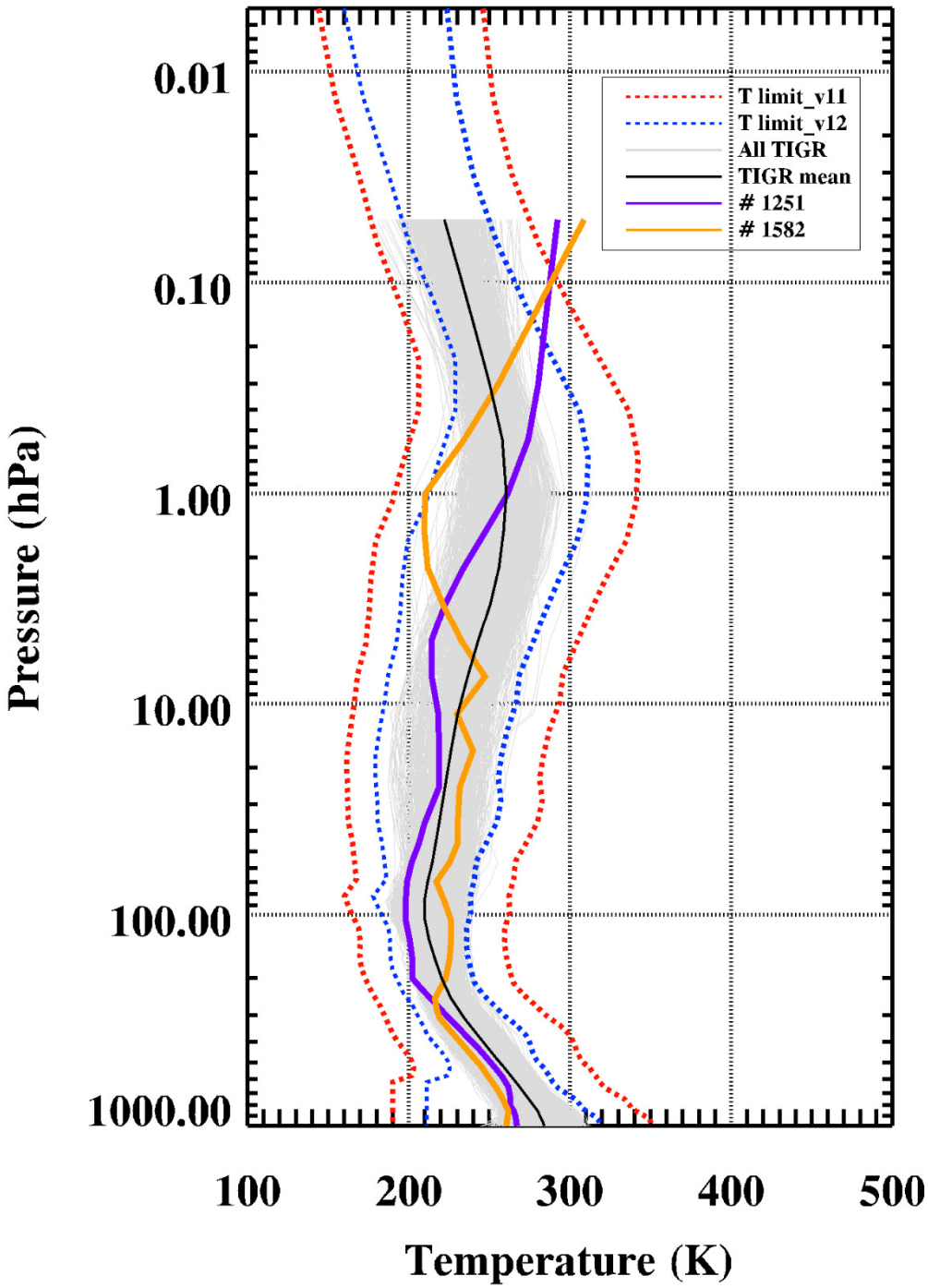

Figure 2: All TIGR temperature profiles (grey lines) are given with their mean profile (black line). Among the TIGR profiles, 1251th (purple line) and 1582th (orange line) profiles are highlighted since they show notable TB differences between v11 and v12 at three MODIS CO_2 channels. Red and blue lines indicate the upper and lower limits of the valid ranges for v11 and v12, respectively.

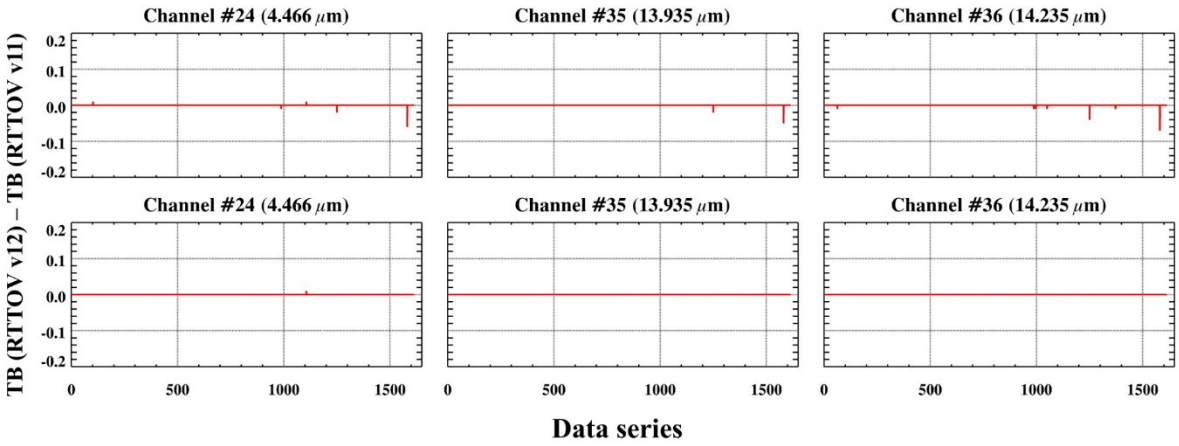

Figure 3: TB differences between v11 and v12 simulations at three MODIS CO_2 channels when *apply_reg_limits* option is set *false* (upper panels) and *true* (bottom panels). The profile values are clipped to the regression limits if *apply_reg_limits* option is set *true*.

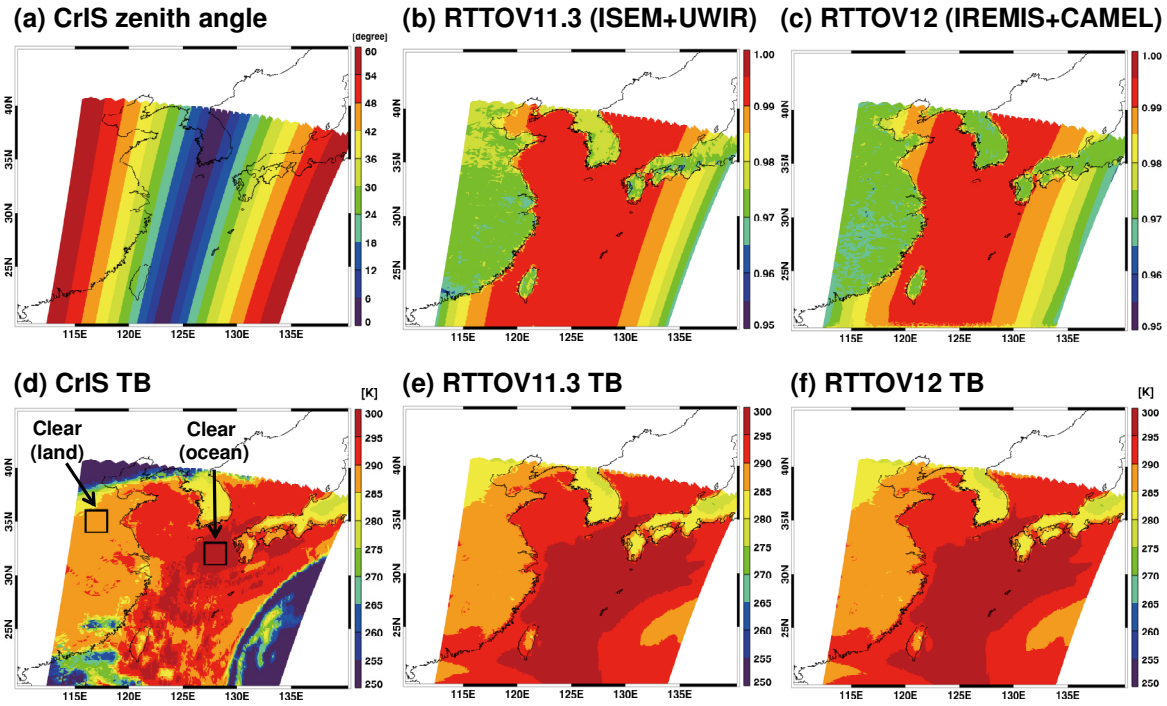

Figure 4**:** (a) CrIS viewing angle, and surface emissivities at 900 cm^{-1} from (b)v11 (ISEM for ocean and UWIR for land), (c) from v12 (IREMIS for ocean and CAMEL for land). TBs at 900 cm^{-1} from (d) CrIS, (e) from v11, (f) from v12 for the case of 17UTC 13 October 2013. Clear areas for further analysis are outlined by black squares in (d).

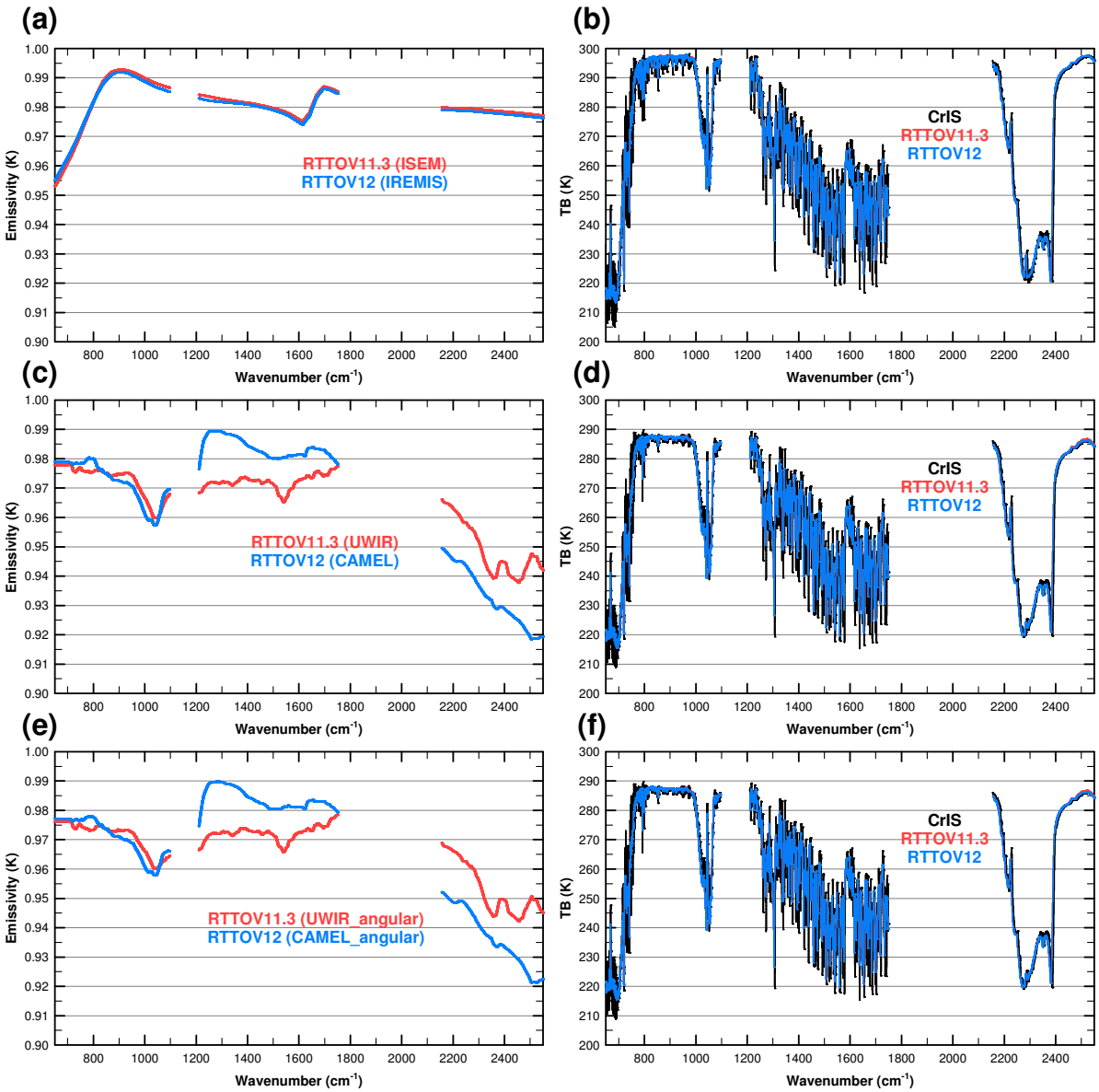

Figure 5**:** Mean CrIS emissivity spectrum from (a) ISEM and IREMIS models, (c) UWIR and CAMEL atlases, and (e) angular corrected UWIR and CAMEL atlases. Corresponding simulated TBs are given in (b), (d), and (f) with CrIS observation. Black, red, and blue lines indicate the CrIS observation, v11, and v12, respectively.

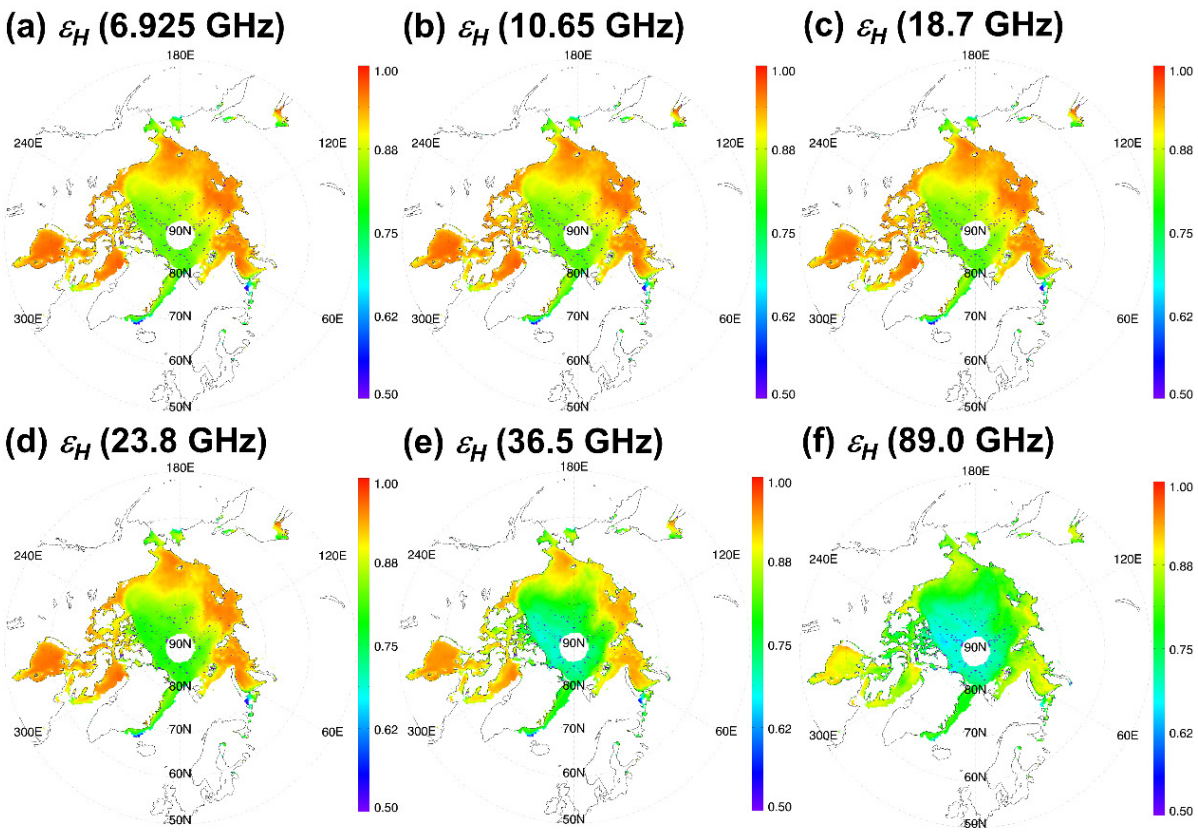

Figure 6: The TELSEM2-generated horizontally polarized emissivities over the Arctic sea ice at six AMSR-E frequencies.

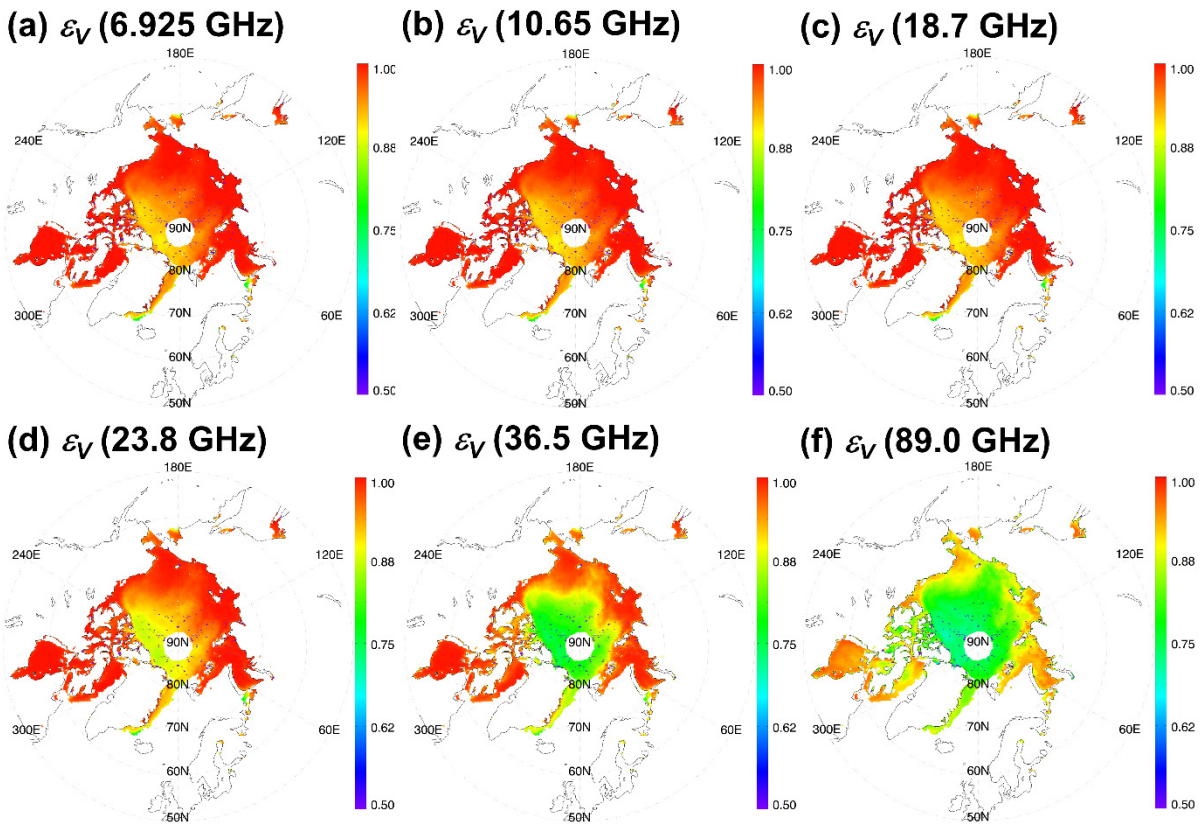

Figure 7: Same as Figure 6 but for vertically polarized emissivities.

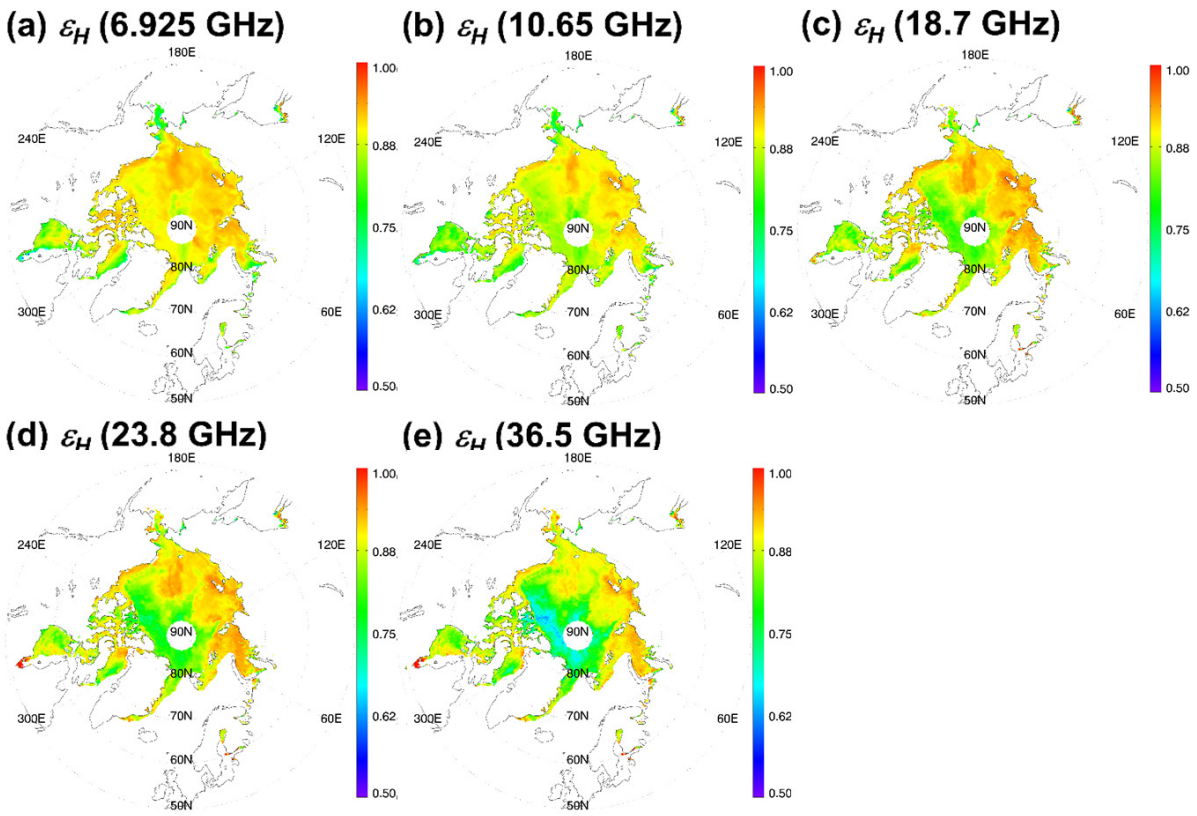

Figure 8: Retrieved horizontally polarized emissivites over the Arctic Ocean on 1st January 2010, for AMSR-E 6.925, 10.65, 18.7, 23.8, and 36.5 GHz.

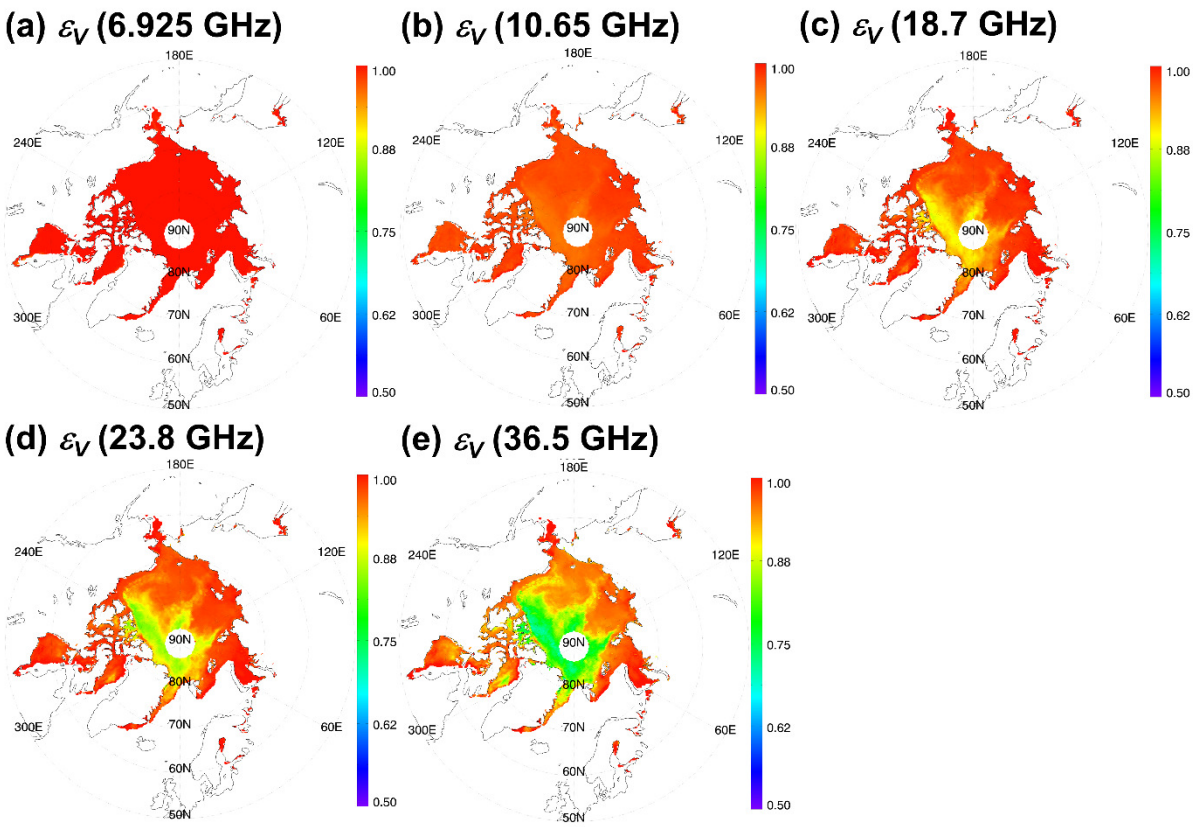

Figure 9: Same as in Figure 8 except for vertically polarized emissivities.

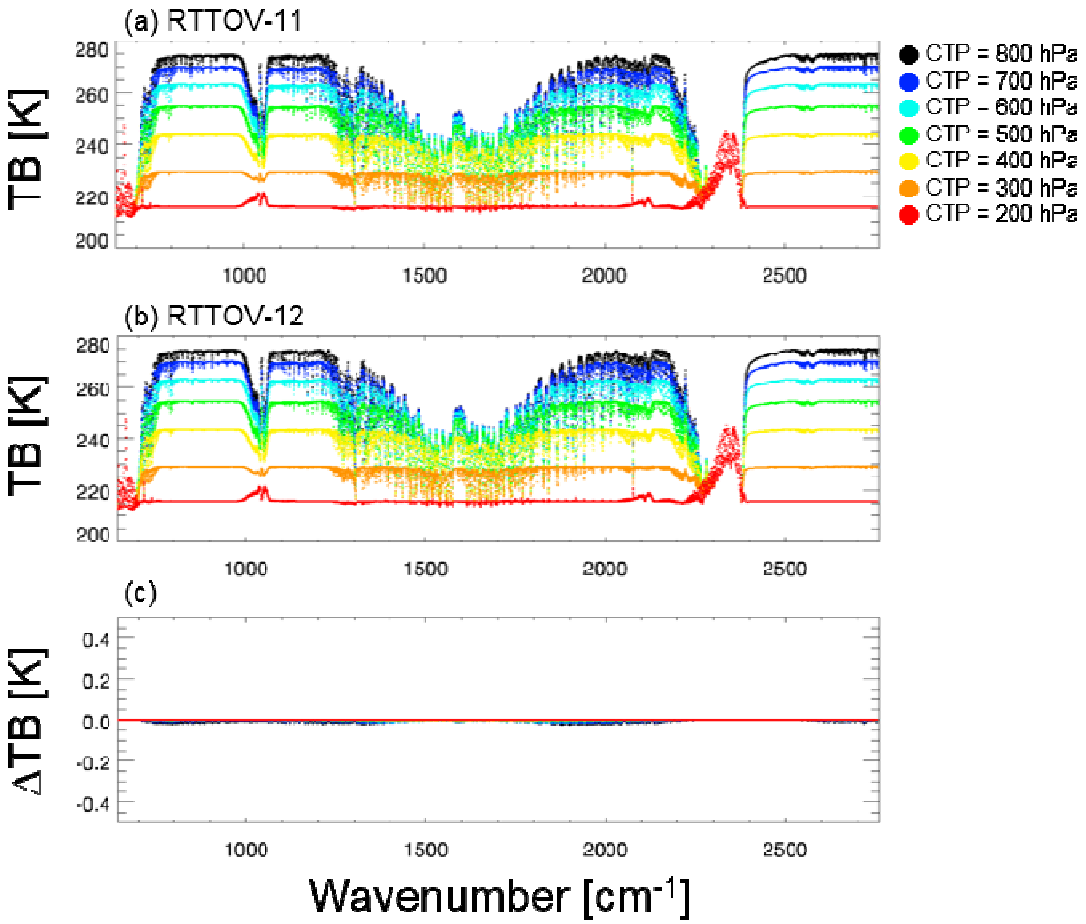

Figure 10**:** IASI simulated TBs using a simple cloud scheme with given seven different cloud top pressures. Spectral distributions are for (a) v11 and (b) v12, and for (c) the difference between (a) and (b).

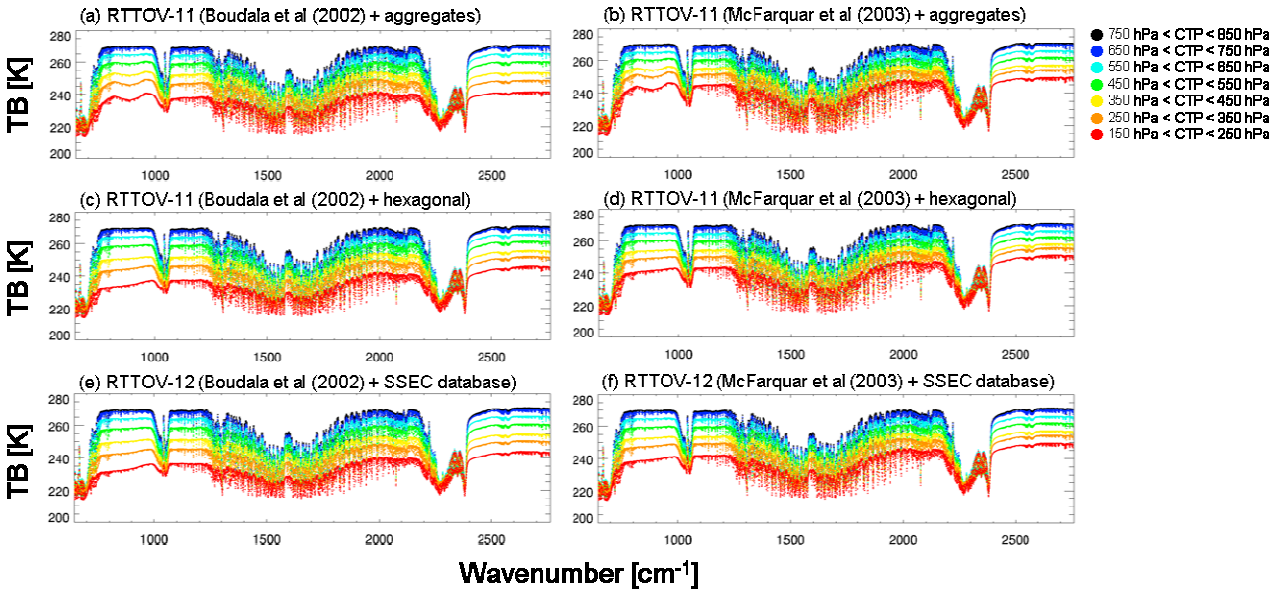

Figure 11: IASI simulated TBs with given seven different cloud top pressures; (a) for aggregates type with B scheme, (c) for hexagonal type with B scheme using RTTOV v11, (e) for SSEC database properties with B scheme in RTTOV v12. (b), (d) and (f) are same as in (a), (c) and (e) except with M scheme.

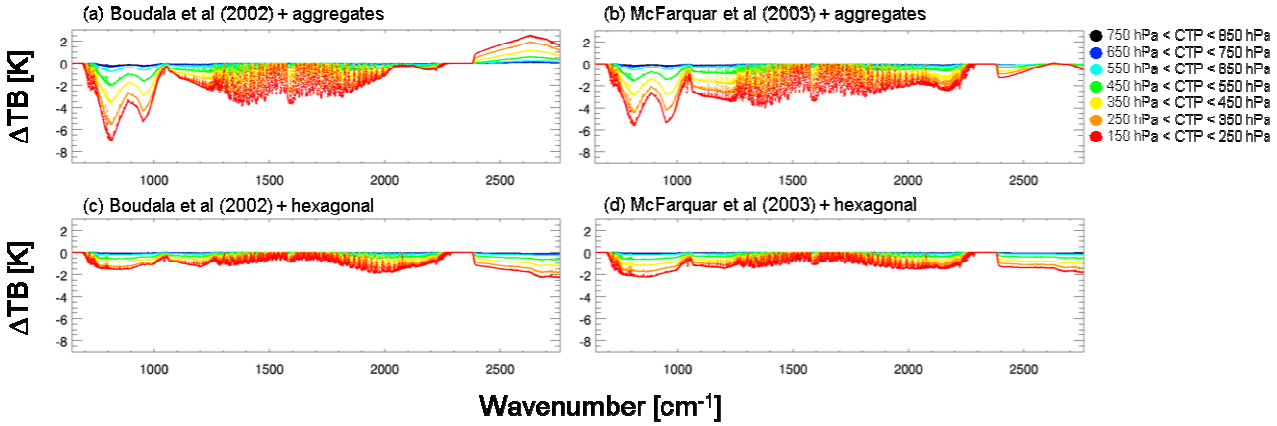

Figure 12: Differences in simulated TBs between v11 and v12 (v12 minus v11). For the v11 simulations, M scheme is used with (a) aggregates type and (c) hexagonal; B scheme is used with (b) aggregates type and (d) hexagonal type. For the v12 simulations, the SSEC database is used with M scheme (a, c), and with B scheme (b, d).

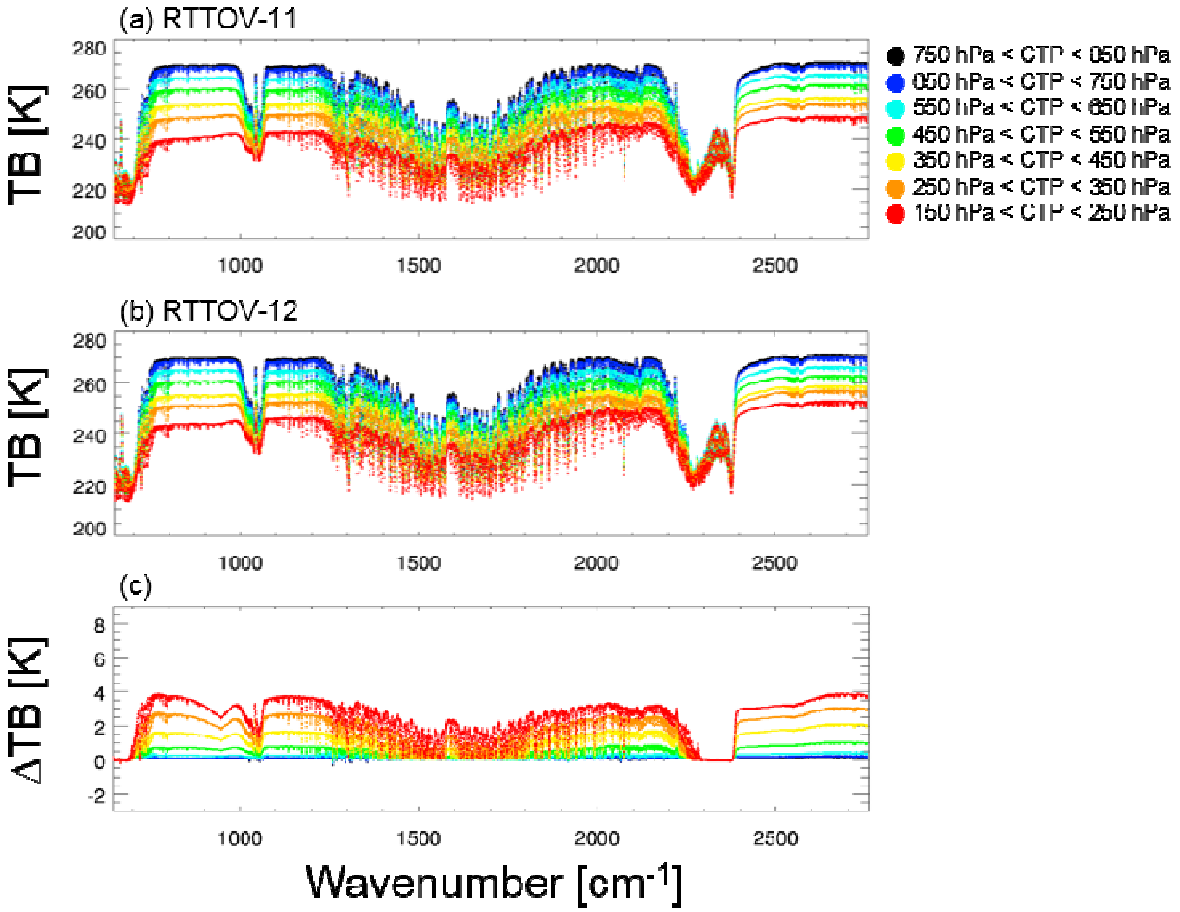

Figure 13**:** IASI simulated TBs from the Baran scheme with respect to seven different cloud top pressures (a) using v11, (b) using v12, and (c) the difference between (a) and (b).

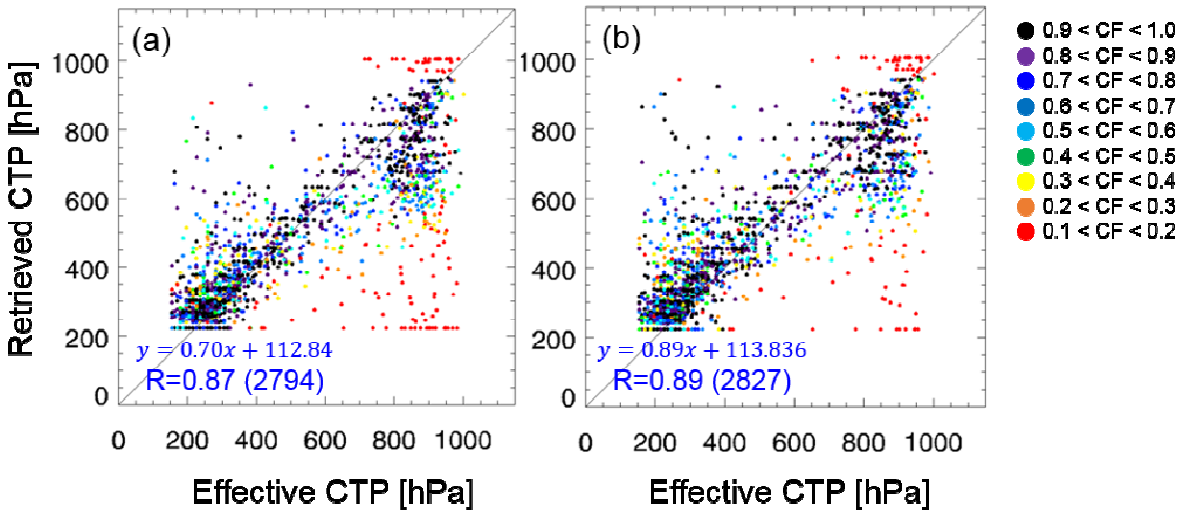

Figure 14: Scatter plots of effective cloud top pressures and retrieved cloud top pressures from the minimum residual method using simulated IASI radiances from (a) v11 and (b) v12. Individual colors indicate the cloud fraction retrieved from minimum residual method.

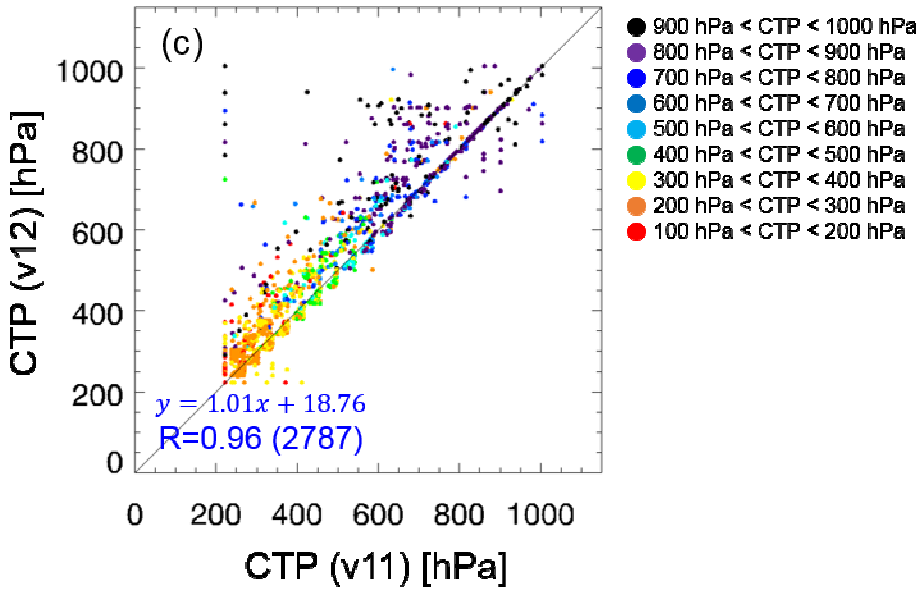

Figure 15: Scatter plot of retrieved cloud top pressures using v11 and v12 simulated cloudy radiances.

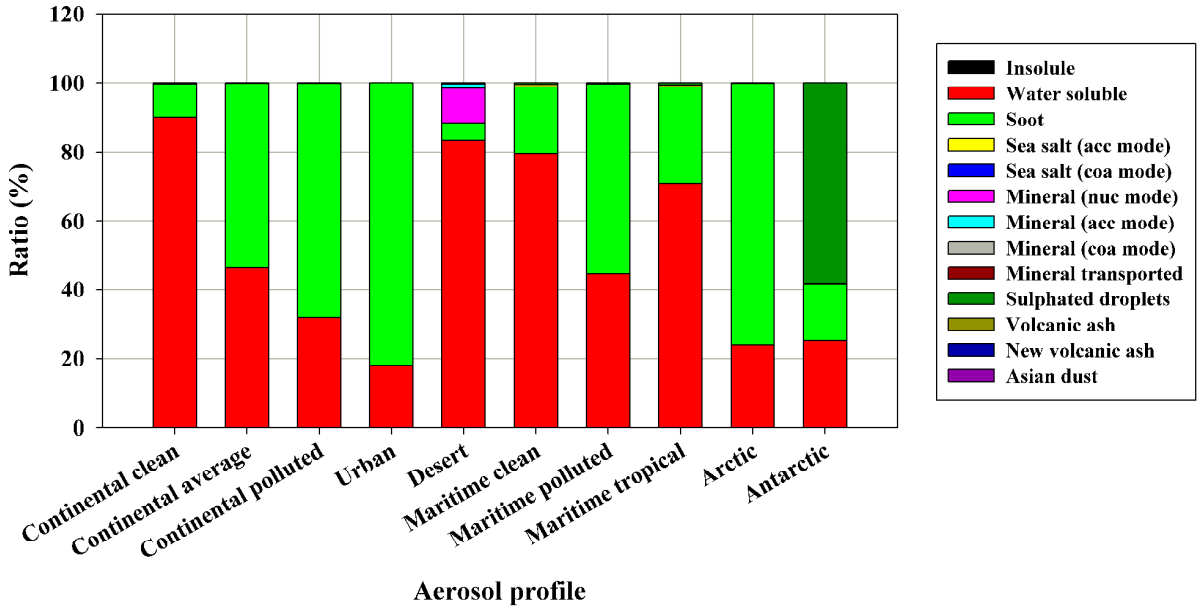

Figure 16: Aerosol compositions of climatological aerosol profiles included in v12.

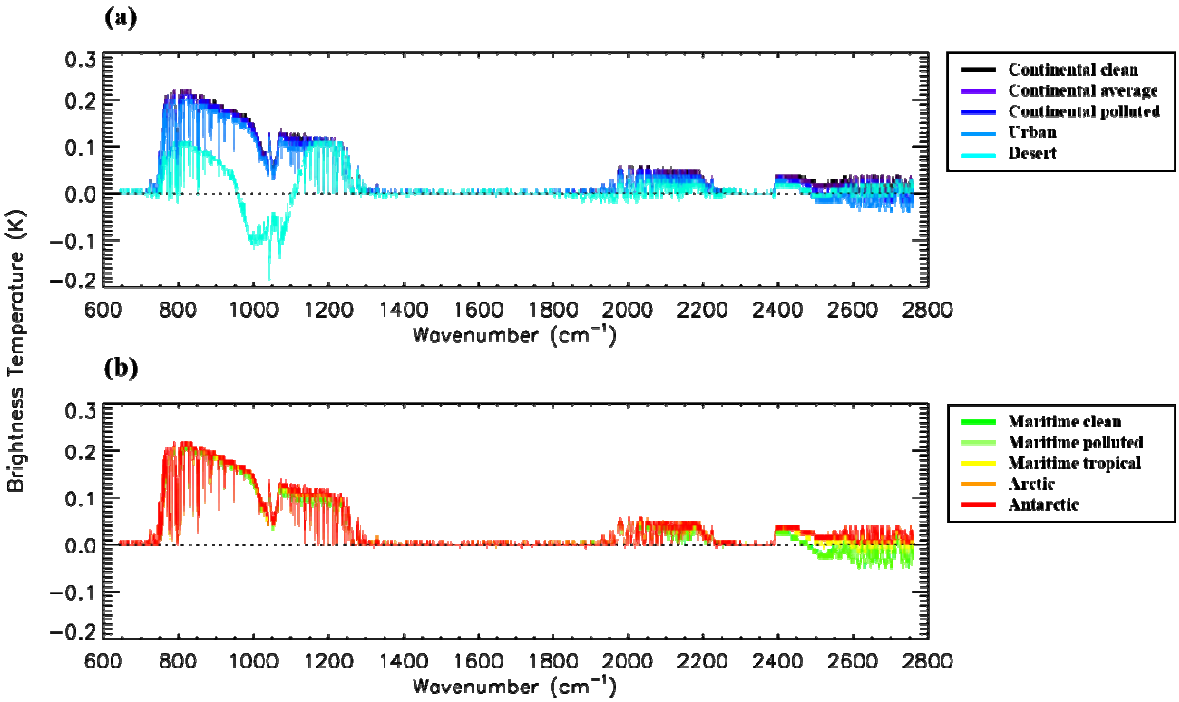

Figure 17: Difference of IASI TBs between v11 and v12 for (a) continental clean, continental average, continental polluted, urban, and desert, and (b) maritime clear, maritime polluted, maritime tropical, Arctic, and Antarctic aerosol profiles.

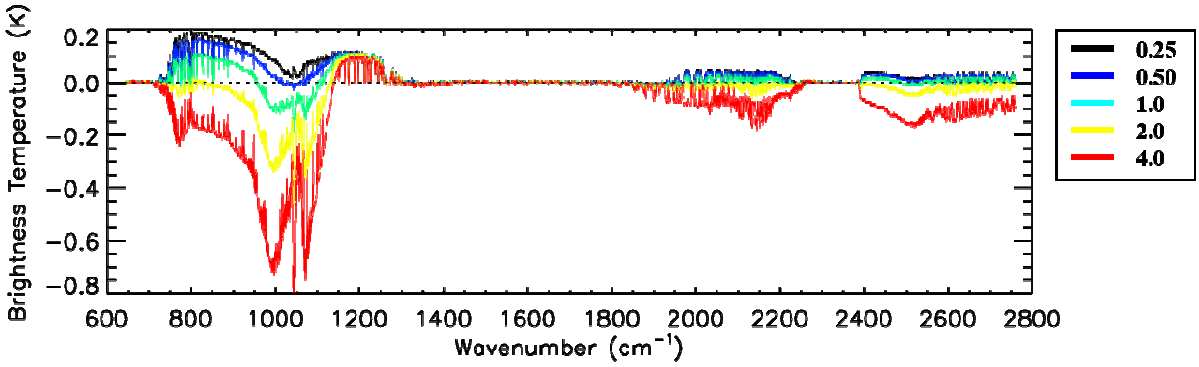

Figure 18: Difference of IASI TBs between v11 and v12 with *desert* aerosol profiles for various aerosol amount. Aerosol amount is modified by multiplying weight values of 0.25 (black), 0.50 (blue), 1.0 (cyan), 2.0 (yellow), and 4.0 (red) to climatological *desert* aerosol profile in v12.

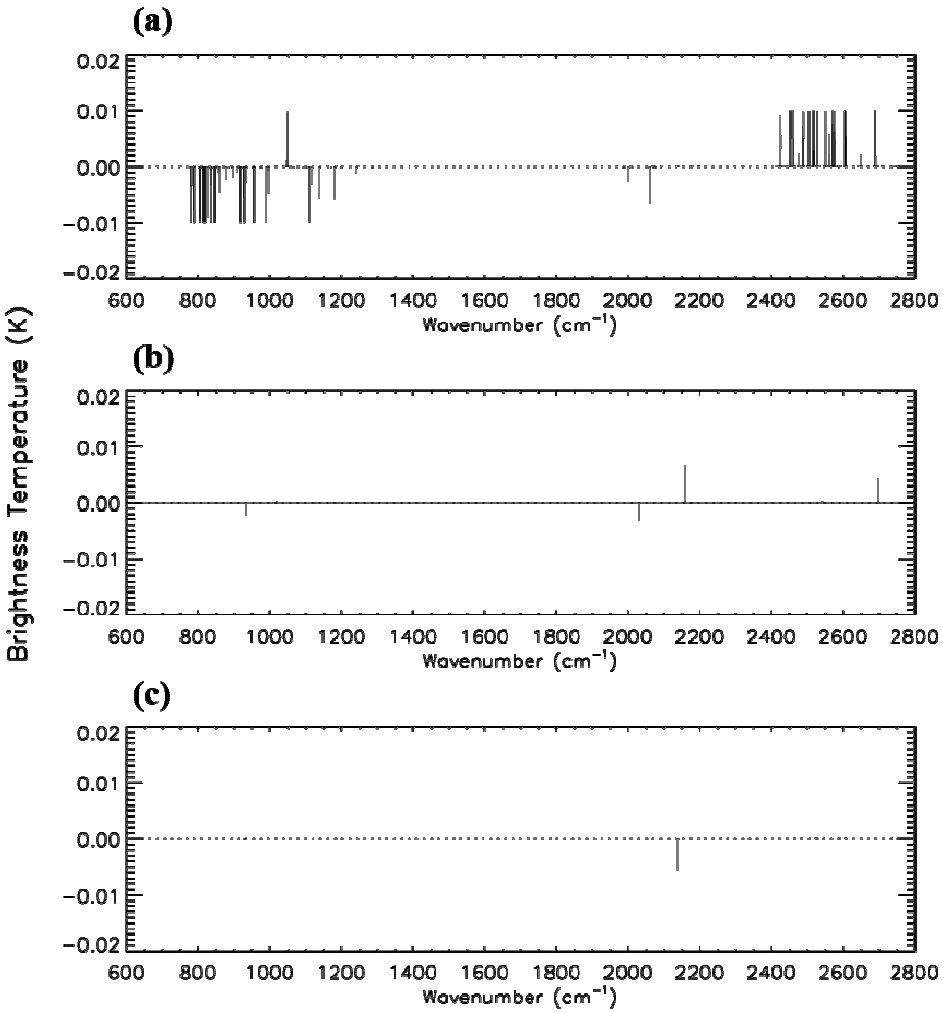

Figure 19: Differences of IASI TBs simulated from v12 with various number of DOM streams. For calculating TB differences, the number of DOM streams are defined as (a) eight and twelve, (b) twelve and sixteen, and (c) sixteen and twenty.

Responses to SNU beta test report

Section 1

N/A

Section 2 - user guide

These typos have been fixed in user guide.

Section 3 - clear-sky simulations

Section 3.1 - new extrapolation method

These are among highest-peaking MODIS channels where the tails of the weighting functions can reach above 0.1hPa and as such the extrapolation method employed near the top-of-atmosphere can have a small impact on radiances as observed here. These results are expected and it is right that with *apply_reg_limits* set to true the differences between v11 and v12 are eliminated (at the precision shown in Table 1). By clipping all extrapolated profile data at the regression limits in v12 it is believed that we should do *no worse* than allowing the regression limits to be exceeded since the regression limits follow the trends in the training profiles whereas constant-value extrapolation will not. In addition, by applying this clipping RTTOV no longer generates extrapolated values that result in warnings to the user.

Note that Figure 2 suggests the v11 and v12 coefficient regression limits are different: this is not the case. In both models the max/min envelopes of the training profile set are stretched by +/-10% for temperature and by +/-20% for each gas and these stretched max/min profiles are the profile limits applied within RTTOV. In RTTOV v11 (and earlier versions) the stretched limits were stored in the coefficient files. In RTTOV v12 we now store the strict max/min envelope in the coefficient file and we apply the stretching to create the regression limits when the coefficients are read in. This avoids ambiguity in what the limits in the coefficient files represent and makes it easier to test the impact of different stretching factors or even to enable users to apply their own factors (although this has not been included in the user documentation).

Section 3.2 - IR surface emissivities

Regarding differences between ISEM (v11) and IREMIS (v12) over sea, it is true that in many cases the models do give similar emissivity values. Based on testing carried out during development, the largest differences between the model emissivities is expected at wind speeds above ~12m/s, at zenith angles above ~65º (for GEO instruments only), and, in the 10-12µm window (where the T-skin-dependent refractive indices are used), for skin temperatures below ~300K (although in the case of skin temperature the differences were smaller for some instruments than for others).

Regarding the angular correction in the UW and CAMEL emissivity atlases: the same correction is currently applied to both atlases. This is implemented as a zenith-angle-dependent scale factor applied to the atlas emissivities. Therefore, given atlas emissivities of similar magnitude, the angular corrections will also be very similar in magnitude and so it is not surprising that a 0.012K decrease in mean TB difference with the UW atlas is mirrored by a 0.012K decrease in the same with the CAMEL atlas.

Section 3.3 - Sea ice emissivities from new TELSEM2 atlas

Regarding the frequency extrapolation: both TELSEM and TELSEM2 extrapolate at constant value below 19GHz (there is no difference between the two atlases). Above 89GHz TELSEM also extrapolates with constant value. However TELSEM2 has some improvements in the treatment of

higher frequencies such that the emissivities should be applicable above 200GHz. Therefore TELSEM2 should at the very least be no worse than TELSEM (over land there are only a very limited number of data points with different emissivity values between the atlases). The user guide has been updated to provide explicit information regarding the extrapolation applied by TELSEM2.

Regarding sea ice emissivities: since this is an atlas (not a dynamic model) it can only provide climatological emissivity values for sea ice. As observed here it may well be that they are not good enough for retrieval/emissivity applications. If users have better information regarding sea ice emissivities they can provide them as inputs to the model. Development of a dynamic sea ice emissivity model could be considered for future RTTOV development.

I contacted the TELSEM2 developers regarding the missing sea-ice values over Central Arctic Ocean and they have provided updated atlas datasets in which the missing data points have been filled by interpolation.

Section 4 - cloudy simulations

Section 4.1 - simple cloud

This is expected.

Section 4.2 - Chou-scaling

These results fall within expectations. It should be noted that the Baran 2014 ice scheme is available in v11 (selected as *profiles(:)%ish=4*) and this has not been modified in v12 for IR channels.

Section 4.3 - impact on cloud retrievals

This is good news that the SSEC ice properties are an improvement over the v11 properties.

Section 5 - aerosol simulations

Section 5.1 - DOM scattering solver

The aerosol optical properties have not changed between v11 and v12 so if everything else is consistent, the differences here are due only to the differences between Chou-scaling and DOM.

Section 5.2 - impact of dust loadings

It is reasonable that as the concentration of scattering material increases the BT differences between Chou-scaling and DOM also increase.

Section 5.3 - impact of DOM streams

This is an interesting analysis and confirms what was observed during development. The user guide has been updated to reflect this advice.

--END--

RTTOV-12 Beta Test Report

Simon Proud

0. Synopsis

In this document I lay out my thoughts on RTTOV-12, based upon running the test scripts and implementing the new version in two of University of Oxford's existing algorithms. I provide information on a comparison between the algorithm results between version 11.3 and version 12 (beta).

Overall I think that RTTOV-12 is an improvement over the previous version in terms of functionality and that the new version experiences no reduction in speed due to the changes that have been made. I only have some minor concerns, primarily to do with the documentation, to report. In my view RTTOV-12 is ready for release without significant modification.

In section 1 I give background information about compiling RTTOV on our systems. In section2 I describe the implementation of RTTOV-12 within our algorithms, including a comparison with the previous version. Section 3 gives details of the test script results on two of our systems. Section 4 examines the documentation.

1. Compiling RTTOV-12

I tested RTTOV compilation on 4 systems:

1) Desktop PC running Ubuntu 12.04, 16Gb RAM, Intel i7 processor. Does not have f2py, has HDF5 1.8.17, netCDF 4.4.1 and netCDF-fortran 4.4.4. Compiled using the Intel compilers (v2015) and the GNU compilers (v4.8.4).

2) Workstation PC running Ubuntu 16.04, 16Gb RAM, Intel i7 processor. Has f2py, has HDF5 1.8.17, netCDF 4.4.1 and netCDF-fortran 4.4.4. Compiled using the PGI compilers (v2016) and the GNU compilers (v5.3.1)

3) Virtual Machine, Ubuntu 14.04 running inside Windows VMWare, 7Gb RAM, Intel i7 processor. Has f2py, HDF5 1.8.11, netCDF 4.1.3. Compiled using the GNU compilers, (v4.8.4).

4) Server, Ubuntu 12.04, 32Gb RAM, AMD Opteron 6128. Does not have f2py, HDF5 1.8.15, netCDF 4.3.3, netCDF-fortran 4.4.2, GNU compilers (v4.6.3). Compiled with OpenMP.

I used the rttov_compile.sh script to build RTTOV on all systems, compiling with openmp on 1) and 4). I selected to compile against HDF5 but not against f2py (i.e: The wrapper) and compilation was successful on all 4 machines.

However, on the two machines with f2py I was not successful in compiling with the wrapper/GUI enabled when using the GNU compilers (it did work with PGI, though). Setting RTTOV_F2PY=1 caused

the compilation to fail in the GUI directory on both machines. This only seems to occur with gfortran, not with other compilers. I mailed the rttov-beta email address with details of this problem and am happy to help test any updates that may resolve the issue.

2. Implementation of RTTOV-12 in our algorithms

I tested RTTOV by implementing it within 2 algorithms used by Oxford University. Overall, there were no problems caused by replacing v11.3 with v12: The user guide section that explains the differences between versions is an adequate reference when converting the code – most of the changes are self-explanatory anyway. Below I describe some specific aspects of the implementation in each algorithm:

ORAC: Optimal Estimation of Aerosol and Cloud

The ORAC algorithm is designed to estimate cloud properties (optical depth, height, effective radius etc) and aerosol properties (optical depth at 550nm, angstrom exponent, etc) from a given satellite radiometer image. It can operate on a wide variety of instruments, most importantly the ATSR series of sensors, the SEVIRI and AHI geostationary sensors as well as MODIS and VIIRS. ORAC forms a central part of ESA's Cloud-CCI project, being used as the sole algorithm (known there as CC4CL) to produce long-term datasets of cloud properties from the ATSR series of instruments. Additionally, ORAC is one of several algorithms used in the Aerosol-CCI (although this component does not use RTTOV, we use our own radiative transfer scheme there).

Processing is divided into three stages:

1) Pre-processing, ingesting ECMWF atmospheric profiles, preparing the satellite data, extracting land/sea surface BRDFs and computing clear sky atmospheric transmission on multiple layers (using RTTOV v11.3 by default).
2) Main processing, performing recursive radiative transfer calculations in the presence of aerosol and/or cloud contamination until the clear sky transmissions are perturbed enough to match those expected from the actual satellite observations.
3) Post-processing, quality control etc.

Whilst RTTOV only runs in the first part of the processing chain, the results from the RTTOV calculations are essential for the main processor, and thus RTTOV forms a core part of the ORAC algorithm. I tested ORAC/RTTOV-12 with the Intel, GNU and PGI compilers using 15 days' worth of orbits (daylight only) of AATSR data equally spread across 2008.

The quality of an ORAC retrieval is determined by the retrieval 'cost' for a pixel, with lower cost signifying a higher probability of a good retrieval. The number of iterations required for the retrieval to converge is also a useful indicator of retrieval quality. In some cases the cost can be low yet the retrieval still poor, and in these cases the number of iterations is typically high (>20).

Integration with the new version

No problems were encountered upgrading to the new version of RTTOV. The user guide section that details the changes in the new version was sufficient to explain what I needed to change in the ORAC code (only the order of parameters in the rttov calls). Compilation against the RTTOV-12 was successful first time.

Runtimes

There seems to be little difference between the time taken to run RTTOV between versions 11.3 and 12 as part of the ORAC pre-processor. For the ~25,000x512 AATSR orbit the average RTTOV-11 runtime was 18min 23 sec and for RTTOV-12 it was 18 min 25 sec.

As expected, the server system was fastest due to the multithreading capabilities (ORAC automatically switches to parallel RTTOV in this case). The desktop (1) and workstation (2) PCs had similar runtimes (on identical hardware), indicating that OS and HDF/netCDF library versions do not greatly affect runtime.

In terms of compilers, on machine 1 the GNU compilers were an average of 10% faster than Intel. On machine 2 the PGI compilers were around 4% faster than GNU. Because RTTOV forms a central part of the pre-processor I can't determine how much of those speed differences is contained within the RTTOV calls.

Output data

The pre-processor output from both versions of RTTOV was broadly similar, but did show some differences for the solar and mixed channels on AATSR. Because many of the changes made in the latest version of RTTOV focus upon the solar channels this is not surprising. I did not see any appreciable difference in the output for thermal channels.

For the main processor, running with RTTOV-12 input data results in a small improvement in the output. When retrieving over water clouds the average cost is 0.4% lower and a successful retrieval is made on slightly more pixels (0.003% improvement). For ice clouds there is little improvement, with 50 (out of 3 million) extra pixels converging and a mean cost that is 0.0007% lower.

However, cloud retrievals rely mainly upon the thermal channels. The differences noted above are mostly due to slight improvements in the transmission calculations for the 1.6 micron channel that's used to retrieve cloud effective radius. Examining the data shows that the main improvements are for optically thin low-altitude clouds that are notoriously hard to retrieve. Therefore, although the statistics show only a slight improvement between RTTOV-11 and -12, this improvement is particularly important as it allows us to perform much better over thin cloud.

Conclusions

My overall impression in that RTTOV-12 represents an improvement over the previous version when implemented in ORAC. The results are slightly improved, significantly in the thin cloud case, and the run-time is no greater. I will be recommending to the Cloud-CCI that RTTOV-12 is used for our next reprocessing. I will also be recommending that Aerosol-CCI investigates using RTTOV-12 as the main radiative transfer algorithm, as I believe that the improvements in the solar spectrum mean that it is as accurate as our existing method but likely to be significantly faster.

Simulated Satellite Images

Aside from ORAC we also use RTTOV to produce simulated geostationary satellite images from climate model output and/or weather forecast data. These simulated scenes are compared to the actual data from the satellites, and are used by colleagues in the climate-modelling group as a rough benchmark of the performance of their models. Unlike ORAC, this simulation method makes use of both the clear-sky *and* cloudy capabilities of RTTOV. Previously we only made use of the thermal channels, but the ability of RTTOV-12 to simulate cloudy conditions in solar channels mean that as part of this test I expanded our method to work in the visible spectrum.

Processing steps:

1) Loading model data: Temperature, specific humidity, cloud cover, liquid/ice water content and air density on the model levels. If running with the 137 level ECMWF forecast only every other level is used.
2) Initialise RTTOV and compute surface emissivity + brdf. I use the UWIR atlas but have also tested with the new CAMEL IR atlas.
3) Set up RTTOV profile, set clouds(6,:) = Ice water content from model, water cloud is assumed to be polluted continental cumulus (this was found to work best) and is stored in clouds(4,:)
4) Compute solar and viewing geometry for the simulated scene.
5) Run RTTOV for each pixel in the image.

The choice of a fixed type for water cloud, and the, typically, low model resolution compared to satellite image resolution, will naturally introduce some errors in the resulting simulated image. However, images produced by this method were found to be accurate enough to help with some model analyses.

For this algorithm, I did not compare runtimes between the old and new versions of RTTOV as the introduction of the solar channels leads to a much longer runtime in RTTOV-12. As with ORAC I found it very easy to switch between v11 and v12, although as the emissivity and brdf atlases are used here the switch was a bit more time consuming due to the new types for the atlas. Overall, I had no major problems with the migration.

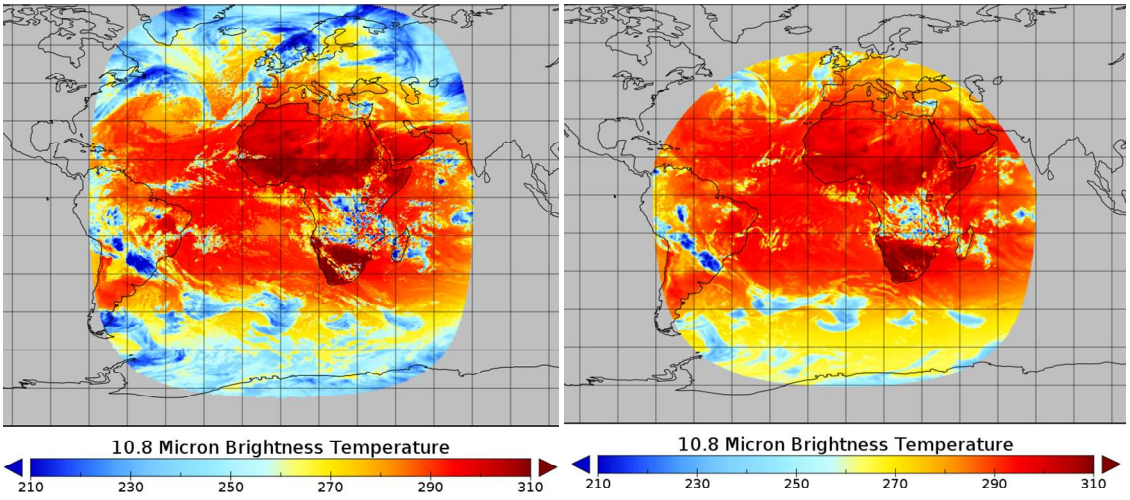

Actual (L) and simulated (R) SEVIRI images for 19th December 2015. A solar and viewing angle cut-off is applied, meaning the most Northern and Southern parts of the SEVIRI disk are not shown.

Results

For the thermal channels, there are small differences between v11 and v12. The majority of these differences are most likely due to the change in ice optical properties between v11 and v12 (I use the Baran properties). The remaining differences seem be due to RTTOV-12 taking cloud water content in kg/kg rather than g/m^3 – I use the default option in both RTTOV versions and hence for RTTOV v11 I converted the model output (kg/kg) into g/m^3, possibly introducing some error. The new option to allow units of kg/kg is very useful in RTTOV v12.

Compared to actual satellite data the RTTOV simulations show some bias (see above figure). Deep convective clouds often appear too warm in the simulated images (by up to 20K, see Central Africa) whilst low, semi-transparent, cloud often has too little thermal contrast with the surface (see the Southern Atlantic in the images). This may be due to the choice of water cloud model in the simulation. For clear-sky pixels RTTOV produces very good results, 90% of clear-sky pixels are within 1.2K of the measured brightness temperature. That said, many of the cloudy differences appear to be due to the ECMWF forecast used to generate the image and are not down to RTTOV itself. The forecast substantially underestimates cloud liquid water content in the Western Atlantic, for instance. Below is a histogram showing the brightness temperatures for the SEVIRI scene described above. The simulated data has a larger peak at around 290K than the actual data, most likely because of the missing low cloud described above. The actual data has substantially more pixels with a low (<240K) brightness temperature and somewhat more hot (>305K) pixels.

-	Actual	Sim UWIR	Sim CAMEL
Mean BT	279.5	285.3	285.4
Min BT	189.7	200.7	200.7
Max BT	330.4	329.3	329.9
BT Std Dev	20.87	15.66	15.71

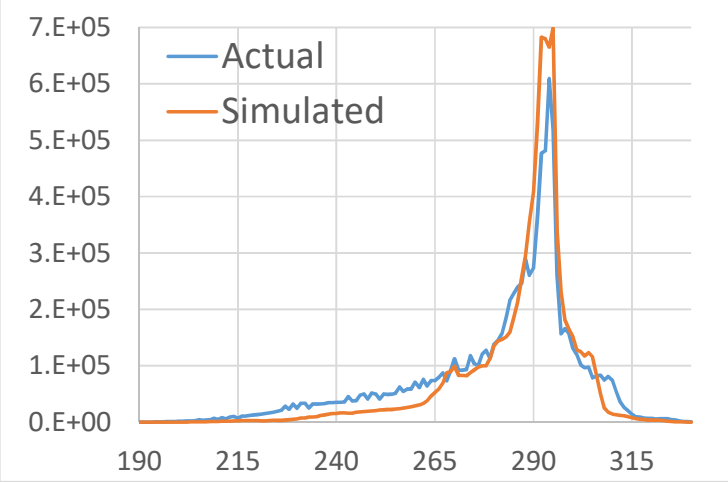

Histogram of actual and simulated 10.8 micron brightness temperatures across the SEVIRI disk.

When comparing the UWIR and CAMEL emissivity atlases there are, in terms of full+disk statistics, very few differences (see table above). However, the CAMEL atlas has an improved spatial resolution and this is noticable when looking at subsets of a scene, even at SEVIRI resolution. For higher resolution instruments, particularly polar orbiting ones, this improvement in atlas resolution is likely to have a significant effect upon results. I would therefore recommend that the CAMEL atlas is the default wherever this is possible.

Overall, the thermal results from RTTOV-12 are similar enough to those from v11.3 to give confidence in the data.

Visible Channel Simulations

The ability of RTTOV-12 to simulate cloudy visible channels is very welcome and is likely to be of particular use to us. To test RTTOV's solar capabilities I extended the above algorithm to include the solar channels for SEVIRI. Adding the solar channels was pleasantly straightforward, as the required BRDF database is very similar to the emissivity database so many of the calls can simply be duplicated. This commonality between database calls is appreciated and will make life easy for other users who also wish to extend their use of RTTOV into the solar channels.

As a first-step for including the solar channels I added the BRDF database and switched off the cloud processing (cfrac(:)=0) to produce clear-sky images. In most places, the BRDF database seems good.

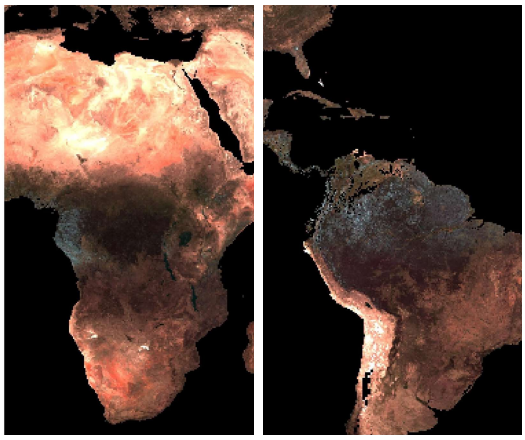

However, there are a number of locations with unphysical reflectances, probably due to cloud contamination. The inset images above show examples of this for the May BRDF database file (RGB composite, 1.6, 0.8 and 0.6 micron). The land surface is unexpectedly light in Cameroon and Gabon (left hand image) and in Colombia and Northern Brazil (right hand image). This is a known issue with the MODIS BRDF product, so I suspect it's been fed through into this BRDF database. A work-around may be to generate the BRDF database from the gap-filled BRDF library here: https://www.umb.edu/spectralmass/terra_aqua_modis/modis_brdf_albedo_cmg_gap_filled_snow_free_product_mcd43gf_v005

This still has some cloud contamination, but much less than the 'official' MODIS products, for future versions of the BRDF atlas it may be a good idea to use this data as input.

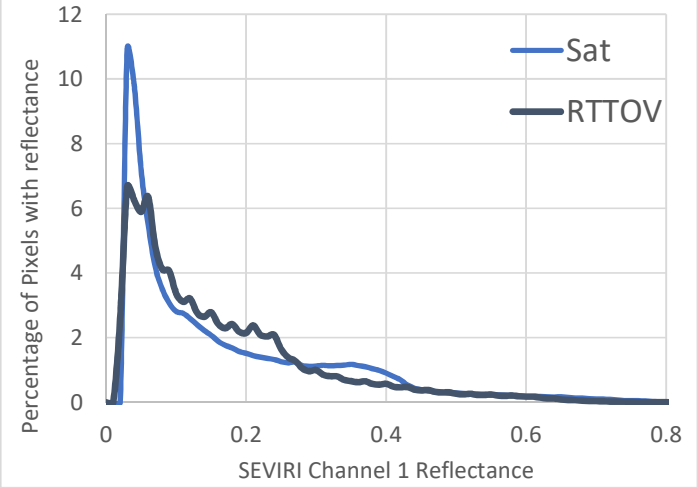

When comparing SEVIRI channels 1, 2 and 3 there are some significant differences between actual and simulated reflectances. The actual satellite data tends to have lower values, particularly in the 0.8 micron channel, and for all channels the variation in reflectance across the SEVIRI disk is lower in reality than is reflected in the RTTOV simulations. The graph to the left shows a histogram of pixel reflectances in the 0.6 micron channel – a much larger low-reflectance peak is visible for the actual (sat) data than for the RTTOV data. This corresponds to sea/ocean pixels. I suspect that part of this is due to RTTOV's selection of a sea surface reflectance, possibly the values chosen by RTTOV are somewhat too high. It's also possible that the ECMWF profile fed into RTTOV may be responsible for some of the bias.

-	Sim 0.6um	Actual 0.6um	Sim 0.8um	Actual 0.8um	Sim 1.6um	Actual 1.6um
Mean	0.179	0.17	0.225	0.193	0.196	0.18
Min	0.027	0.013	0.011	0.001	0.009	0.001
Max	1.164	0.942	1.385	1.027	1.695	0.691
Std Dev	0.154	0.136	0.198	0.154	0.195	0.14

The table above shows a comparison of statistics for the simulated and actual SEVIRI data for 12 images spread across the year (one for each month, but varying dates within the month). All images are 12:00 UTC. As well as the reflectance differences noted above it's also interesting to see that the

1.6 micron reflectances for RTTOV are significantly above 1, something that seems to happen for Antarctic (i.e: Ice) pixels.

This short analysis of RTTOVs visible-channel simulations shows that RTTOV v12 is broadly accurate but that some substantial differences do exist. These are most likely caused by incorrect surface reflectance terms and could also be due to errors in the atmospheric profiles used to generate the data. My study with the ORAC algorithm showed that, for AATSR, the visible wavelength transmission simulations in RTTOV are good (otherwise we would get poor quality results). That supports my conclusion that the problem most likely does not lie with RTTOV's simulation capabilities themselves, but with the input surface and atmosphere data.

3. RTTOV test results

I ran the test suite on all machines mentioned in the introduction, on machines with multiple compilers I compiled/ran the tests using each compiler and did not see any differences in output.

However, some issues were encountered when running rttov_test.pl, seemingly caused by missing coefficient files. Some of these were corrected by running the coefficient converter tool (as described in the test suite document) but others ones couldn't be fixed in this way. The same errors occur when running on all systems/compilers, so (apart from the errors) I'm confident that the RTTOV tests are successful and that there's no difference in behaviour between platforms or compilers.

I also ran the test_cpu.sh script to assess intra-compiler speed. On the machine with gfortran and ifort both compilers performed similarly with no clear speed differences, the overall average time taken for 40 runs of the test script was within 1% for the two compilers.

On the machine with gfortran and pgfortran, however, the pgi compilers were clearly faster. Gfortran took, in total, 20 hours to run the 40 iterations of the test script whilst pgi took only 13 hours.

A report was submitted to the RTTOV beta email address regarding the failure of some of the tests, I'm happy to provide more information and testing as-needed.

4. The documentation

Overall the documentation is well-written and easy to follow. It gives a good overview of the capabilities of RTTOV and, together with the example source code, gives users a detailed understanding of what is needed to incorporate RTTOV into their own applications. I think that the structure of the user guide is good and, as such, my only comments are related to areas where the documentation is not entirely clear or where I think that more information would be useful. I first give some general commends and then list specific comments in series, starting with page 5 of the user guide.

SO2 coefficients document

I have no comments regarding this document, it is easy to understand and nicely describes the new SO2 coefficient files.

The test suite document

I also have no comments about this document, it's clear and accurately describes the test suite.

The GUI guide

As the GUI guide relates to v11.3 of RTTOV I did not examine this document, once it's updated to v12 I'm happy to have a look through it.

The user guide

General comments

Subsection headings don't stand out, occasionally making it hard to navigate the document. For example, the heading for section 8.6 is, to me at least, less noticeable than the nearby "Emissivity atlases" and "Discrete Ordinates Method" headings. Could be improved by making the subsection fonts a bit bigger.

A better mention of what exactly defines a VIS or IR channel within RTTOV would be nice. I know the border is fuzzy and there are mixed channels but it'd be good to have clear mention somewhere in the introduction of this. Currently it's somewhat buried on page 50 at the start of section 8.2.

In quite a few places 'which' and 'that' have been mixed up.

Specific comments

In section 2, page 5 middle of paragraph: "radiances for satellite infrared or microwave"

> Would be good to mention that VIS radiances are now also supported.

Sec 2, P5: "Optionally ozone, carbon dioxide…"

> It seems that the addition of SO2 has been missed from this list.

Sec 2, P5: "Not all parameters have to be supplied as RTTOV can assume default values"

> Are these default values given anywhere? I can't see them. It'd be great to have the reference/default values listed somewhere for reference, maybe as an appendix?

Sec 2, P5: "RTTOV v12 is mainly based on the 91-level 83 diverse profile dataset…"

> Add a link to this dataset: http://nwpsaf.eu/site/software/atmospheric-profile-data/

Sec 2, P7: "for infrared cloud- and aerosol-affected radiances (sections 8.5 and 8.6)"

> This makes it sound like RTTOV is not capable of performing cloud/aerosol calculations in the visible spectrum, even though sections 8.5 and 8.6 explicitly mention visible calculations.

Table 1, P8: To avoid confusion it would be good to include a footnote stating that the ppmv values are for wet air.

Table 3, P10/11: Instrument convention is not always clear for channel numbering. For example, with VIIRS it's unclear what the order is. I can find some official documents that list all the M-bands, then all the I-bands then the DNB band. I find others with the DNB band before the I-bands and yet others that list the channels with increasing wavelength (i.e: I1 between M4 and M5). In most cases this can be figured out by examining the coefficient file, but scope for confusion still exists with, for example, the order of the M7/I2 and M10/I3 band combinations. For channels given in this way a link to the 'official' convention should be included to prevent confusion.

Above table 4 P13: "It is possible to pass multiple profiles…"

> Is there a hard-limit on the maximum number of profiles? i.e: Other than that imposed by the computer memory / operating system limits. Or, for a machine with unlimited resources, could an unlimited number of profiles be passed to RTTOV?

Sec 4, P14: Typo on first line of 'coefficient files' paragraph, "exectuables". There should also be a 'to' after 'available on the same line.

Sec 4, P14: In middle of page, section about FASTEM version is a bit confusing. States that the default version is 6 but then, at the end of the sentence, states that there's no default version.

Sec 4, P14: New IREMIS model, it's stated that 'Most IR coefficient files" support this model. Is that the IR only coefficients (v7) or also the VIR/IR coefficients (v9)?

(nothing to note, P15-32)

Sec 7.2, P32: "If the opts flag is set to false the RTTOV reference profile is used"

An appendix/link to the reference profile would be good.

Sec 7.3, P34: Is the interpolation of pressure levels done for each profile variable, or only those that change between profiles? i.e: If I have 2 profiles, identical aside from CO2 quantity, will the temperatures, humidity etc be interpolated once and stored in both profiles or interpolated twice, once for each profile? I presume the latter.

Sec 7.3, P35: Because there are variables for profiles%s2m%p and also profiles%elevation is not immediately clear how the surface is treated. It would be good to explicitly state that s2m%p is used to compute the lowest layer in the profile and that elevation is not used for this purpose. A few of my colleagues made this mistake with the previous version of RTTOV.

Table 12, P38: It's not clear that the wind fetch parameter actually is (not described elsewhere in user guide), just that it's used for the BRDF.

Sec 7.5, P40: Is there any guidance about which version of FASTEM should be used in a given situation? As in, why are FASTEM v1-5 included if v6 is recommended?

Sec 7.8, P45: The description of the overcast radiance array could be confusing: It states that 'black cloud' is assumed at the bottom of each layer. Makes sense for IR simulations but black cloud not appropriate for the visible channels.

Sec 7.9, P47: "For "solar" channels (those with wavelength <3um)…"

Should this be "solar only" channels? On P50 the user guide states that channels under 5micron will have a solar component, so the above should be changed to clarify if the radiance units apply only to solar-only channels or to all solar channels.

Sec 8.1, P50: This seems somewhat redundant as it repeats information from the previous sections.

Sec 8.2, P51: A lower date limit of 1/1/1950 is given, is there also an upper limit?

Sec 8.5, P57: "Set opts%rt_iraddclouds" should be "Set opts%rt_ir%addclouds"

Table 21, P58: For consistency with the new default unit for IWC/LWC it'd be better to have the IWC limits listed in this table shown as kg/kg rather than g/m3

Table 22, P58: Naming the ice clouds as 'cirrus' is confusing, the Baran and Baum optical properties can apply to other types of ice clouds too (such as deep convection) and I presume that's also true for their implementation within RTTOV.

Sec 8.6, P61: “Remember that the cloud coefficient file must match…”

Typo? Should be aerosol coefficient file.

Sec 8.9, P65: “that so-called ‘solar pumping’ has on observed TOA”

Typo: Should be something like “has been observed for TOA”.

Pages 83, 85 and 87: In the type column of these tables there are typos: rtov_emissivity and rtov_reflectance (missing a t in rttov_)

5. Minor Issues

The VIIRS coefficient file contains a typo: “Original spectral response functions are **extrated** from the following files:”

When the rttov_compile.sh script asks yes/no questions it does not error-check what the user enters. For example, when it asks ‘do you want to compile with the wrapper? y/n’ then typing something like ‘d’ results in no being selected. Could catch users out if they’re not paying attention.

6. Conclusions and general comments

Overall I find RTTOV v12 to be an improvement over the previous version. I encountered no difficulties installing/compiling this version and it was very simple to replace v11.3 with v12 in the existing algorithms that I tested with. The quality of data from my algorithms seems, at worst, equivalent to that produced with RTTOV v11.3 and in some cases there are substantial improvements in the results. The test suite runs successfully on a range of machines and compilers whilst the speed of RTTOV v12 is comparable to v11.3, despite the addition of extra features.

My only concerns are the compilation failure of the GUI with gfortran and the cloud contamination in the BRDF atlas. Additionally, the visible wavelength simulations show some large differences when compared to actual satellite images. It’s likely that this is due to the BRDF atlas and/or atmospheric profile errors although I cannot rule out a problem within RTTOVs radiative transfer model. It would be good if this is investigated before release, and I suspect this may already be included in the science and validation document.

Otherwise, I think that RTTOV v12 is in a suitable condition for release and I look forward to using it within my work.

Additional features

Whilst testing RTTOV there were a few things I thought of that would make ‘would be nice’ features. None of them are particularly important in terms of functionality (all could be done by the user) but could make the RTTOV experience a bit easier. This section can be regarded as something of a wish

list for things that could be included in later versions of RTTOV v12 (I presume it's too late for v12.0) or in v13, if it's deemed there's a need for these things.

Twlight simulations: Section 8.2 states that solar simulations are only possible for SZA<84 degrees. It would be good, if possible, to have this extended so that twilight simulations (ideally including those with the sun below the horizon) can also be included.

A useful feature would be the ability to enter water vapour profiles in terms of relative humidity, as this is often the quantity output by the non-ECMWF NWP models. Conversion of RH to ppmv within RTTOV would help improve consistency rather than having the user do this.

The inclusion of a land/sea mask that complements the BRDF/Emis atlas would be good. That way the user wouldn't need to manually set the land/sea flag themselves, but could leave it to the atlas if desired.

Very long term: Integration with GPU-based systems. Because the memory requirements for running a single RTTOV profile seems quite small I think RTTOV would be well-suited to a GPU environment (through CUDA, OpenACC or similar), and this would be something that'd create some very large reductions in runtime for users. This would be quite challenging as most GPU-based compilers are C rather than Fortran. A very long shot, so maybe something for RTTOV v14!

Responses to Simon Proud beta test report

Section 1 - Compilation

As discussed we found the solution to problems compiling with gfortran and f2py (modification of the Makefiles).

Section 2 - Implementation in algorithms

ORAC

It is good that RTTOV v12 improves the retrievals from the ORAC algorithm. In fact for clear-sky simulations there are only very small differences in the transmittances and brightness temperatures/reflectances in all channels between v11 and v12. The largest difference for clear-sky visible/near-IR simulations is in the calculation of sea surface BRDF: this has been improved (see below), at least away from sun glint, so perhaps this is the cause of the improvements in retrievals.

Simulated Imagery

It is good to know that the switch from v11 to v12 was relatively easy and that the new kg/kg option for cloud inputs is useful.

It is worth saying that the Baran 2014 ice properties for thermal channels are the same between v11 and v12 (these are selected as "*profiles(:)%ish=4*" in v11 and "*profiles(:)%ice_scheme=2*" in v12). The original Baran parameterisation in v11, referred to as Baran 2013 (*ish=3*), has been removed in v12. As we discussed off-line, the differences you saw were most likely to be due to the differences between Baran 2013 (in v11) and Baran 2014 (in v12).

The comparison against observations is interesting. As you note it can be hard to distinguish between errors due to the model fields used as input and those due to the RT modelling. We are currently engaged in an RT model intercomparison of cloudy simulations which hopefully will inform future improvements in the RTTOV scattering simulations.

It is good to see that the higher resolution of the CAMEL atlas is useful.

The cloud contamination in the BRDF atlas is a known issue and there is a quality flag available which provides some indication of this. Your suggestion of the gap-filled dataset is very interesting and we will investigate whether this can be used to update the BRDF atlas for a future version.

The sea surface BRDF model in RTTOV v11 is known to over-estimate the reflectance due to sun glint and to under-estimate the reflectance away from sun glint. Users have commented on the latter case in particular as the calculated BRDFs are practically zero. For v12 I modified the sea surface BRDFs to incorporate a fixed water reflectance spectrum. For the direct surface-reflected solar beam this spectrum is added to the calculated sun glint model BRDF. For the downward-scattered surface-reflected radiation the fixed spectrum is used on its own (because in this geometry the sun glint BRDF is not appropriate). I have carried out some clear-sky comparisons against SEVIRI observations which showed reduced bias away from sun glint, but increased bias in the presence of sun glint. I think this is a good trade-off as the non-glint condition is more common. We will look at improving the treatment of sea surface BRDF for a future version. (It is worth saying also that this description applies to clear-sky simulations: in the beta version I implemented something similar in the visible

DOM scattering solver, but I now believe this violates some assumptions made regarding the treatment of the surface as Lambertian so in the final version the surface will be treated strictly as Lambertian when DOM is used).

It would be interesting to see an example profile with high reflectance at 1.6µm over Antarctic ice. I don't think this can be due to the BRDF atlas or RTTOV's internal BRDF values. If the atlas is used (requires surface type set to land) and has data for the given location, the BRDFs at 1.6µm would be roughly 0.1-0.2. If calcrefl is true then the BRDF used is 0.3/pi (surftype=land) or 0.8/pi (surftype=sea-ice). None of these values should result in TOA reflectances above 1. Usually such high reflectances can only occur in cases of strong near-specular reflection at the highest satellite and solar zenith angles, particularly with the sun glint model over sea.

Section 3 - Test suite results

I will add a note to the documentation to say that not all the tests defined in the tests.0/ directory are intended to be run by users. A small number of these are for historical coefficients (which may or may not be regenerated) or for specific developer tests (and occasionally some old tests get left behind). There is nothing unexpected in the test log provided.

Section 4 - Documentation

I have made updates for all typos and comments: I agree with almost everything you say. Regarding some specific questions you asked and the few points I disagree with:

- Sec 2, P5: "Not all parameters have to be supplied as RTTOV can assume default values": I have removed this sentence. I think it referred to optional trace gases in which case the reference profiles from the training profile set are used if no data are provided. Pretty much all profile variables are initialised to zero because we have just one subroutine for initialising the profile structure. This is used by the AD/K models as well as the direct model and the AD/K require everything to be zero at the start (unless the user has some specific reason to initialise variables otherwise).
- Gas units in Table 1: I have added a note to specify the units. In fact these are ppmv wrt **dry** air because RTTOV is trained using gas profiles in these units and this is the context in which the limits are applied.
- I have added a comment and link to the page on the RTTOV website which gives the channel spectral response functions and passbands as this shows the channel order in the coefficient files and provides channel wavelengths (visible/IR) or frequencies (MW) as well as wavenumbers.
- Passing multiple profiles: RTTOV imposes no fixed limit, it is down to the available memory. I have added a comment to this effect.
- IREMIS model: yes, all visible/IR coefficient files (except SSU) contain IREMIS coefficients. I've updated the text to make this clearer.
- The background (reference) gas profiles used by RTTOV when optional gas inputs are omitted are contained in the coefficient files: I have added a description of where to find them in the user guide. I will also put them on the website when we update this for the v12 release.
- Profile interpolation: the interpolator works by first calculating a set of weights on the input levels for each interpolated output level determining how much each input level contributes

to each output level. This calculation is based on the input/output pressure levels alone and is the more expensive part of the interpolation calculation. Once the weights are calculated, the temperature and gas profiles are all interpolated for every profile (this is relatively fast). If all input profiles are on the same pressure levels, the calculation of the weights is only done once. Otherwise it is done for every profile. The benefits due to this increase as more profiles are passed into RTTOV per call. I have added a sentence in the user guide to indicate that the interpolation is faster if all profiles use the same pressure levels.

- FASTEM versions: generally we would recommend FASTEM-6 except for ICI simulations where the new TESSEM2 model is recommended. ECMWF have found FASTEM-6 to perform best in their model. However we (the Met Office) have found earlier versions (in particular v3) to be more beneficial in operations. We retain all versions as they are not burdensome to maintain, users often like backward compatibility, and in practice there is no version which is unequivocally the best. I have added a note to say FASTEM-6 is generally recommended, but users should consider experimenting to determine the best model for their application. Our development plans include creating a new physical MW emissivity model which will ultimately replace FASTEM.
- Sec 7.9, P47: "For "solar" channels (those with wavelength <3um)…": yes, this should be "solar only" channels.
- Sec 8.1, P50: I agree this is repeating information, but it is summarised here for completeness. The idea of section 8 is to describe each type of simulation so it would seem remiss to exclude the most basic IR/MW simulations. I'm inclined to keep it in.
- Sec 8.2, P51: the sun-Earth distance calculation used by RTTOV is a common one (the primary reference appears to be Spencer 1972: Fourier series representation of the position of the Sun). I'm not aware of an upper time limit of the applicability of this formula, but I would imagine it is good for upwards of a century from now if not significantly longer since this particular parameter of the Earth-sun geometry is relatively stable/predictable. Note that the only reason for having this effective lower bound is to define a cut-off date so that no correction to the TOA solar irradiance is applied for profile dates prior to this: the lower bound is an arbitrary date selected before the first satellite was launched.
- IWC limits: this is complicated by the fact that for a given IWC value in g/m^3 the equivalent IWC in kg/kg can vary quite significantly with the input profile (or indeed *within* a given input profile as it depends on pressure, temperature and water vapour content) so it is difficult to express limits concisely in kg/kg.
- Ice cloud referred to as "CIRR": good point. This comes from the abbreviations for cloud types in the OPAC database (the water cloud properties come from OPAC). I have added a clarification in the table.

Section 5 - Minor issues

I have modified the compile script so that it requires y or n in answer to the questions and prompts the user if they input something else.

Section 6 - Conclusions

Regarding the visible channel clear-sky simulations it should be noted that, aside from the sea surface BRDF calculations, the differences between v11 and v12 are extremely small and the BRDF atlas has not changed so v12 should be no worse than v11. As noted above we will look at improving the sea surface BRDF model for a future version. It seems the modifications made to the sea surface BRDFs for v12 may have resulted in improvements in the ORAC algorithm and my own comparisons to observations (which will be shown in the Science and Validation Report) showed an overall decrease in bias against observations for SEVIRI which suggests they are a positive change.

Additional features

Twilight simulations: this is challenging due to the way RTTOV's optical depth parameterisation works. Increasing the range of angles over which it is trained usually reduces the accuracy of the predicted optical depths. Nevertheless there may be some scope to address this for clear-sky simulations. However it is not possible with the scattering simulations using the DOM solver as it is currently implemented because it is a 1D solver requiring a strictly plane-parallel atmosphere so the solar zenith angle must be strictly less than 90 degrees, and as it approaches 90 degrees the atmospheric path length is unbounded. I have made a note of this as an idea for our long term plans, but it probably requires a different approach to solving the radiative transfer equation to those currently employed by RTTOV.

Water vapour inputs as relative humidity: this should be relatively easy. I have put this on the plans for the next minor update to v12.

Land/sea mask for atlases: for the BRDF and IR emissivity atlases, if you set the profile surface type to land then the atlas returns a BRDF/emissivity value if it has one and otherwise returns a negative value. In a sense this represents a land/sea mask for the atlas, although in practice it could be the case that there are missing data in some localised regions over land, for example due to persistent cloud cover. It would be possible to create an "rttov_emis_landsea(atlas, lat, lon)" subroutine (and similar for BRDF) which, given a lat/lon position and an atlas data structure, will tell you whether the given atlas has data at that location. However in their current form there is no way to be sure of the surface type where there is missing data.

GPU version: a few years ago RTTOV v7 was rewritten using CUDA as a proof of concept. This was successful and did offer significant performance benefits. The downside is that GPU coding is (as you may well be aware) technically rather complicated as it requires very careful management of data transfers to and from the GPU as this is the primary bottleneck. In addition, RTTOV has grown significantly more complicated since v7 (primarily in respect of the scattering and PC options) which would make a GPU implementation a very large piece of work. And then there is also the issue of porting to C as you mention. It would require a significant development effort which would inevitably mean less development of other scientific and technical aspects of RTTOV. For these reasons a GPU implementation of RTTOV is not on our current development plans. However if supercomputing moves in the direction of GPUs this is something we will have to consider again.

--END--

Report of Associate Scientist mission

12 October 2014

RTTOV package : β – Testing of RTTOV v12

Robin Faulwetter

Deutscher Wetterdienst (DWD), Offenbach, Germany

1. **Introduction**

RTTOV v12 code developed within the NWPSAF was received at DWD on 15 August 2016 for beta testing of the package prior to its official release. This report documents the tests that were done at DWD along with the main findings and comments. Some results and remarks were additionally, as requested, already communicated to the contact person at the MetOffice, UK (James Hocking) during the testing period.

The testing of v12 at DWD was done, as previously agreed, focusing on our currently operational implementation of RTTOV. Therefore, most tests were done in comparison to the operationally used RTTOV-10 in the global model context of the ICON-EnVAR system for clear-sky IR and MW simulations using the direct radiative transfer (RT) and k-code components of the RTTOV package. Cloudy IR simulations were performed only for SEVIRI in the implementation context of our regional model COSMO-DE. The RTTOV-SCATT module for MW or the PC-RTTOV component of the code were not tested for this report within a model implementation, but the test_rttovscatt.sh script was run on various architectures. The surface modules for sea emissivity (FASTEM) are used as part of the clear-sky calculations, while the land surface emissivity modules and atlases are being currently implemented and tested as part of our ongoing in house development. Any findings on the atlases and their use will be reported directly to the NWPSAF/RTTOV team independent of this report.
The report first gives an overview of the IT structure and compilation results (Section 2). Section 3 reports on the standard RTTOV tests provided as part of the package. Section 4 and 5 describe results from the implementation in the operational ICON-EnVAR system and COSMO-DE, respectively. Section 6 summarizes comments on the technical and scientific documentation provided with the RTTOV v12 code.

2. Overview of used IT testing environment and compilation tests

a) Testing environment: We tested RTTOV-12 on a range of available IT architectures and employed the different available compilers which are also used for our normal development tasks and routine operations. Tests were done on LINUX workstations and LINUX servers and the Cray XC30/XC40 using the compilers gfortran, ifort, crayftn.
b) The following table summarizes the systems and compiler combinations and the results of the compilation tests. Compilation was successful in all combinations, but some issues were found and are explained in the indicated comments (following the table):

Architecture	**Compiler**	**Version**	**Options**	**HDF5 version**	**f2py**	**Result**	**Comment**
Workstation/LINUX	gfortran	4.8.1	RTTOV gfortran default			Ok	
Workstation/LINUX	gfortran	4.8.1	RTTOV gfortran default	1.8.14		Ok	
Workstation/LINUX	gfortran	4.8.1	RTTOV gfortran default	1.8.14	yes	Ok	

LINUX server	gfortran	4.7.2	RTTOV gfortran default	1.8.10	yes	Ok	
LINUX cluster	gfortran	4.3.4	RTTOV gfortran default			Ok	a
LINUX cluster	ifort	14.0.0	RTTOV ifort default			Ok	a
LINUX cluster	ifort	14.0.0	RTTOV ifort default	1.8.13		Ok	a
XC30/XC40 Cray	crayftn	8.4.1	RTTOV cray-ecmwf default			Ok	
XC30/XC40 Cray	crayftn	8.4.1	RTTOV cray-ecmwf default	1.8.13		Ok	
XC30/XC40 Cray	Ifort	14.0.0	cray-intel-dwd	1.8.13		Ok	b
XC30/XC40 Cray	gfortran	4.9.2	cray-gnu-debug	1.8.13		Ok	c

a: Although rttov_compile.sh detects f2py, the compilation fails with the following error message:

```
        eror: file '/usr/lib64/python2.6/site-
packages/numpy/f2py/src/fortranobject.c' does not exist
        make[1]: *** [../../../gfortran/lib/rttov_wrapper_f2py.so] Error 1
        make[1]: Leaving directory
`/panfs/e/vol7/rfaulwet/rttov/rttov12/trunk/src/wrapper'
        make: *** [wrapper/bin] Error 2
```

This problem was reported to James Hocking by email (15/08/2016).

b: -fPIC in RTTOV default does not work for static linking.
Suggestion: We suggest to either add the cray-intel-dwd arch file into RTTOV or to add a hint on this issue in the cray-mo-ifort arch file.

c:
Suggestion: We suggest to add the cray-gnu-debug arch file to RTTOV.

Further minor problems, suggestions and remarks:

1. A first attempt to download the coefficient files did not succeed. This problem was reported to James Hocking (15/08/2016), who fixed the problem.
2. The download script `rttov_coef_download.sh` does not notify the user about all problems with the downloading with the aid of wget (example: download from a machine with incorrect proxy configuration).

3. The compilation creates `src/Makefile.` This prevents to do multiple compilations at the same time.
   Suggestion: We suggest, that the name of the Makefile should depend on the selected architecture, e.g. `src/Makefile-cray-ecmwf`, such that multiple compilations might be done at the same time.
4. We like the renaming of types in the new version, e.g. profile_type -> rttov_profile. This decreases the risk of conflicts with user software.
5. In many subroutines the ordering of the arguments is not in agreement with the ordering of the definitions of these arguments in the variables definitions section of the code. This reduces the readability of the code.
   Suggestion: We suggest to order the definitions of arguments according to the ordering in the argument list of the subroutines.
6. Some *.F90 source code files have wrong permissions (the executable bit is set):

```
-rwxr-xr-x 1 * * 9952 Aug 12 12:55 ./main/rttov_sublayer_k.F90
-rwxr-xr-x 1 * * 9582 Aug 12 12:55 ./main/rttov_apply_reg_limits_ad.F90
-rwxr-xr-x 1 * * 9585 Aug 12 12:55 ./main/rttov_apply_reg_limits_tl.F90
-rwxr-xr-x 1 * * 30503 Aug 12 12:55 ./main/rttov_layeravg_ad.F90
-rwxr-xr-x 1 * * 24038 Aug 17 10:10 ./main/rttov_alloc_trans_scatt_ir.F90
-rwxr-xr-x 1 * * 9748 Aug 12 12:55 ./main/rttov_apply_reg_limits_k.F90
-rwxr-xr-x 1 * * 10129 Aug 12 12:55 ./main/rttov_sublayer_ad.F90
-rwxr-xr-x 1 * * 38868 Aug 12 12:55 ./main/rttov_user_profile_checkinput.F90
-rwxr-xr-x 1 * * 8709 Aug 12 12:55 ./main/rttov_sublayer_tl.F90
-rwxr-xr-x 1 * * 30064 Aug 12 12:55 ./main/rttov_layeravg_k.F90
-rwxr-xr-x 1 * * 30064 Aug 12 12:55 ./main/rttov_layeravg_tl.F90
```

3. Overview list of completed tests with RTTOV v12 test suite

This section lists an overview of all the completed tests using the RTTOV-12 test suite as supplied with the beta-version of the code. As above for the compilation (see Section 2), our range of available computer systems and compilers was used and is listed in the table below. All tests could be completed obtaining correct results. However, some practical handling issues were encountered during execution. Details and some suggestions for improvement can be found following the table under the letters as indicated in the comments column.

Code part	System	Compiler (build/arch/*)	Options	Result	Comment
test_core.sh	Linux cluster	Intel		OK	
test_core.sh	Linux cluster	Intel	hdf5	OK	
test_core.sh	Linux cluster	gfortran		OK	
test_core.sh	Linux workstation	gfortran		OK	
test_core.sh	Linux	gfortran	hdf5 + f2py	OK	

	workstation				
test_core.sh	XC30	Cray cray-ecmwf	hdf5	OK	a, b
test_core.sh	XC30	Intel cray-intel-dwd	hdf5	OK	a, b
test_core.sh	XC30	gfortran cray-gnu-debug	hdf5	OK	a, b
test_core.sh	XC30	gfortran , in DWD compilation setup (different Makefiles)	hdf5	OK	a, b
test_core.sh	XC30	Intel , in DWD compilation setup (different Makefiles)	hdf5	OK	a, b
test_core.sh	XC30	cray , in DWD compilation setup (different Makefiles)	hdf5	OK	a, b
test_coef_io.sh	Linux cluster	Intel	hdf5	OK	c
test_coef_io.sh	Linux cluster	Intel		OK	c
test_coef_io.sh	Linux cluster	gfortran		OK	c
test_coef_io.sh	Linux workstation	gfortran	hdf5 + f2py	OK	c
test_coef_io.sh	XC30	cray cray-ecmwf	hdf5	OK	a, c
test_coef_io.sh	XC30	Intel cray-intel-dwd	hdf5	OK	a, c
test_coef_io.sh	XC30	gfortran cray-gnu-debug	hdf5	OK	a, c
test_coef_io.sh	XC30	gfortran , in DWD compilation setup (different Makefiles)	hdf5	OK	a, c
test_coef_io.sh	XC30	Intel , in DWD compilation setup (different Makefiles)	hdf5	OK	a, c
test_coef_io.sh	XC30	cray , in DWD compilation setup (different Makefiles)	hdf5	OK	a, c
test_coef_io_hdf.sh	Linux cluster	Intel	hdf5	OK	
test_coef_io_hdf.sh	Linux workstation	gfortran	hdf5 + f2py	OK	
test_coef_io_hdf.sh	XC30	cray cray-ecmwf	hdf5	OK	a
test_coef_io_hdf.sh	XC30	Intel cray-intel-dwd	hdf5	OK	a
test_coef_io_hdf.sh	XC30	gfortran cray-gnu-debug	hdf5	OK	a
test_coef_io_hdf.sh	XC30	gfortran	hdf5	OK	a

		within DWD compilation setup (different Makefiles)			
test_coef_io_hdf.sh	XC30	Intel , within DWD compilation setup (different Makefiles)	hdf5	OK	a
test_coef_io_hdf.sh	XC30	Cray , within DWD compilation setup (different Makefiles)	hdf5	OK	a
test_rttovscatt.sh	Linux cluster	Intel		OK	
test_rttovscatt.sh	Linux cluster	Intel	hdf5	OK	
test_rttovscatt.sh	Linux cluster	gfortran		OK	
test_rttovscatt.sh	XC30	Cray cray-ecmwf		OK	a
test_rttovscatt.sh	XC30	Cray cray-ecmwf	hdf5	OK	a
test_rttovscatt.sh	XC30	Intel cray-intel-dwd	hdf5	OK	a
test_rttovscatt.sh	XC30	gfortran cray-gnu-debug	hdf5	OK	a
run_example_*.sh	Linux cluster	Intel		OK	d
run_example_*.sh	Linux cluster	Intel	hdf5	OK	d
run_example_*.sh	Linux cluster	gfortran		OK	d
run_example_*.sh	XC30	Cray cray-ecmwf		OK	a, d
run_example_*.sh	XC30	Cray cray-ecmwf	hdf5	OK	a, d
run_example_*.sh	XC30	Intel cray-intel-dwd	hdf5	OK	a, d
run_example_*.sh	XC30	gfortran cray-gnu-debug	hdf5	OK	a, d
test_*_atlas.sh	Linux cluster	Intel		OK	d
test_*_atlas.sh	Linux cluster	Intel	hdf5	OK	f
test_*_atlas.sh	Linux cluster	gfortran		OK	e
test_*_atlas.sh	XC30	Cray cray-ecmwf		OK	a, e
test_*_atlas.sh	XC30	Cray cray-ecmwf	hdf5	OK	a, f
test_*_atlas.sh	XC30	Intel cray-intel-dwd	hdf5	OK	a, f
test_*_atlas.sh	XC30	gfortran cray-gnu-debug	hdf5	OK	a, f
test_*_atlas.sh	XC30	gfortran , in DWD compilation setup (different Makefiles)	hdf5	OK	a, f
test_*_atlas.sh	XC30	Intel , in DWD	hdf5	OK	a, f

		compilation setup (different Makefiles)			
test_*_atlas.sh	XC30	cray , in DWD compilation setup (different Makefiles)	hdf5	OK	a, f

Comments:

a: Unfortunately it is not straightforward to run the test scripts on a CRAY supercomputer. In order to run a program on a CRAY machine, it is necessary to start it with the aid of "aprun", e.g. `aprun test_core.sh`. However, this crashes with the following error message: `Use of uninitialized value $user in concatenation (.) or string at ./rttov_test.pl line 1477.`

Suggestion: We would like to suggest, that either this problem is fixed or that rttov_test.pl is enabled to run rttov_test.exe and rttov_conv_coef.exe via the "aprun" command (or similar commands). In other words: there should be an option to specify a launcher program that runs the rttov test binaries.

b: On the XC30 supercomputer the test scripts called by test_core.sh did not work correctly. The rttov_test.pl script did not get the full input from the here-document. We changed the scripts such that rttov_test.pl gets the input from a file. With the unmodified test scripts only the first entry of TEST_LIST=... was read by rttov_test.pl. We did not fully understand the problem. Presumably, the problem is caused by some minor software/hardware misconfiguration in our specific system, and there is no need to improve the scripts.

Suggestion: However, we suggest to implement a check in test_core.sh whether all tests were really run and completed. When we used the unmodified scripts, the output of the script looked fine, despite having executed only the first test according to the entry of TEST_LIST=... (which executed without error). There should be a warning or an error message if not all tests were run by the test script.

c: In order to run test_coef_io.sh it was necessary to convert some of the rtcoef*.H5 files to the ASCII version. Unfortunately, the usage help output of the new rttov_conv_coef.exe is not very helpful. It documents only the –coef-in option:

```
PROGRAM: ../../intel_hdf5/bin/rttov_conv_coef.exe
ERROR:   Option `--coef-in' is mandatory
         --coef-in : input coefficient file name
```

All other arguments, which are required to work with this program are not documented in the usage help output.

Suggestion: We strongly recommend to improve the usage help output like in older versions:

```
 Usage: --format-in  FORMATTED|UNFORMATTED
        --format-out FORMATTED|UNFORMATTED
        --channels 1 2 3 4 5 ...
        --coef-in  ... --scaer-in  ... --sccld-in  ... --pccoef-in  ...
        --coef-out ... --scaer-out ... --sccld-out ... --pccoef-out ...
      …
```

For the conversion of principal component coefficient files (from *.H5 to ASCII) it appears to be necessary to read the coefficient files for the raw radiances, at least rttov_conv_coef.exe expects the –coef-in option in addition to the –pccoef-in option. We do not understand why rttov_conv_coef.exe always expects the –coef-in option.

Suggestion: The –coef-in option should not be mandatory if it is not required.

d: Note: The star "*" in the column 'code part' stands for fwd cld_file_fwd , cld_param_fwd , aer_file_fwd , aer_param_fwd , rttovscatt_fwd , and pc_fwd k

e: Note: The star "*" in the column 'code part' stands for telsem2

f: Note: The star "*" in the column 'code part' stands for uwiremis , camel , telsem2 , cnrm_mw , brdf

4. RTTOV v12 testing in operational ICON VarENKF

4.1 Technical remarks

It was quite straightforward to implement RTTOV v12 into out operational code, since the changes in the user interfaces since RTTOV v10 are relatively minor.

- In our operational global assimilation code we use the following RTTOV routines:
  - rttov_direct
  - rttov_k
  - rttov_alloc_rad
  - rttov_alloc_prof
  - rttov_errorhandling
  - rttov_errorreport
  - rttov_alloc_transmission
  - rttov_coeffname
  - rttov_dealloc_coefs
  - rttov_init_transmission
  - rttov_nullify_coef
  - rttov_nullify_coef_scatt_ir
  - rttov_nullify_coef_pccomp
  - rttov_nullify_optpar_ir
  - rttov_read_coefs
  - rttov_init_prof

- For this report we implemented and tested also the **rttov_parallel_direct and rttov_parallel_k** routines. We ran the assimilation code for one particular date using 4 OMP threads, compared the results with a similar run, that did not use OMP and the rttov_parallel_* routines. We did not find any significant difference. The folllowing results were all produced without OMP and the rttov_parallel_* routines.

- We also tested the different values for the **gas_units option** (which is only relevant for humidity in our current system), and did not find any significant difference in the results.

- **Modification and speed-up of coefficient file reading:**
  For previous RTTOV versions we found, that it is extremely inefficient to read the RTTOV coefficient files on each processor of a highly parallelized program. Thus, we read the required coefficient files on one particular processor and broadcast the rttov_coefs structures to the other processors. To write/modify the MPI routines for broadcasting the rttov_coefs structures for a new RTTOV version is usually a lot of work.
  Suggestion: We think, that a MPI routine to broadcast the rttov_coefs structure should be a part of the official RTTOV distribution, and that many users could benefit from such a routine. If desired we could streamline our routine and make it available for the NWPSAF (possibly for CDOP-3, details to be discussed).

- For writing broadcasting routines for the **structures contained in rttov_coefs** it would be very helpful, if the structures were self-describing. This is currently not the case, e.g.:
  `rttov_coefs%optp%optpicl%fmv_icl_deff` array bounds should be desribed by `rttov_coefs%optp%optpicl%fmv_icl_ndeff` and not by `rttov_coefs%coef_scatt_ir%fmv_icl_ndeff`
  Currently, `rttov_coefs%optp%optpicl%fmv_icl_ndeff=0`
  Suggestion: Adapt the structures accordingly.

- Instructions like `#include "rttov_errorreport.interface"` or similar are heavily used in the RTTOV code. We assume that this design was chosen in order to avoid unnecessary compilation cascades, when RTTOV is recompiled. This makes sense from a developer's perspective. However, from the perspective of a user, this design is not optimal.
  Suggestion: It would be more convenient, elegant and adequate for modern Fortran to **make use of Fortran modules.** In doing so, all the *.interface files would become obsolete. Furthermore, a usual user compiles RTTOV only once, such that the compilation cascade issue is likely not that relevant.

- In our operational setup the coefficient files are held in a directory which is not the current work directory. Since the **rttov_read_coefs (and getlun)** are searching in the current work directory only, we can not use these routines to detect the form and suffix of the coefficient files.
  Suggestion: It would be useful to add a "path" option to rttov_read_coefs and getlun, which specifies in which directory the coefficient file is to be searched.

- In our operational global assimilation we do not analyze humidity above a given pressure level, and therefore we set the humidity values above that level to the lower hard limit for this level as input to RTTOV. On the other hand we would like to have (at least qualitatively) reasonable humidity Jacobians above this level. With RTTOV-10 we relied on the apply_reg_limits option to fill the profile with reasonable humidity values and we got humidity Jacobians that were derived from the adapted profile.

RTTOV-12 yields zero Jacobians, where the profile was adapted, which is mathematically consistent. This is clearly an improvement.

Suggestion: However, the abovementioned usage of RTTOV (have the profile adapted and get Jacobians for the adapted profile) is not possible any more. In order to allow this, we suggest to add an option "prof_out" to the **rttov_user_profile_checkinput** routine, which should return the adapted profile. In this way the user could first adapt the profile and then calculate Jacobians for the adapted profile.

4.2 Setup of experiments

The implementation was done within the operational global ICON-EnVar system which is running currently at 13km resolution for the deterministic forecast. The analysis is provided at 13km by a 3Dvar with a B-matrix combining 30% climatology and 70% from a 40 member LETKF ensemble at 40km.
For the tests, a lower resolution version at 40km was used for efficiency reasons. We tested RTTOV-12 for a one month period in January 2016 for all operationally assimilated or monitored instruments plus all instruments that are available for experimental use in our system. These are listed in the following table:

Instrument	**Satellites**	**Over land**	**Status**
HIRS	NOAA-19, Metop-A, Metop-B	no	operational
AMSU-A	NOAA-15, NOAA-18, NOAA-19, Metop-A	yes	operational
SSMIS	DMSP-17	no	experimental
MHS	NOAA-15, NOAA-18, NOAA-19, Metop-A	no	preoperational
IASI	Metop-A, Metop-B	no	operational
ATMS	NPP	yes	operational
MVIRI (CSR data)	Meteosat-7	no	experimental
SEVIRI (CSR data)	Meteosat-10	no	experimental
CRIS	NPP	no	experimental
SAPHIR	Megha-Tropiques	no	experimental
AMSR2	GCOM-W1	no	experimental
GMI	GPM-core	no	experimental
MWHS2	FY-3C	no	experimental

We ran two types of experiments:

1. So-called **"cycled experiments":**
A pre-operational version of the global assimilation system was run with lower resolution (40 km instead of 13 km), and the ensemble part of the B-matrix is taken from the operational assimilation stream. We use a pre-operational version of the system as the basis of these experiments, as it contains several improvements in the assimilation of radiances in comparison to the currently operation system (assimilation of MHS and IASI water vapour sensitive channels, less thinning of radiances (~160 km), improved IASI bias correction).

2. So-called **"fixed FG experiments":**
The assimilation system is run at 40km resolution, taking the first guess fields from an independent experiment. In doing so the effect of a modification in the experiment (e.g. RTTOV-10 -> RTTOV-12) does not affect the first guess, i.e. the same first guess is used in the forward calculations so that any differences can be directly attributed to changes from RTTOV-10 to RTTOV-12. Furthermore we modified the operational observation thinning such that it is not affected by the first guess brightness temperature values. This is done in order to ensure that the observation selection is not affected by potential differences in the RTTOV versions and identical data point samples enter the comparisons. The First Guess of these experiments is taken from that pre-operational experiment setup used in the "cycled experiments".

For both types of experiments we ran different setups as to coefficient files, IR emissivity, and use_q2m option used:

- one experiment with RTTOV-10 using RTTOV-11 54Levels coefficient files (rttov7pred54L),
- one experiment with RTTOV-12 using RTTOV-11 54Levels coefficient files (with ISEM)
- one experiment with RTTOV-12 using RTTOV-12 54Levels coefficient files (with IREMIS).

- In order to have as little systematic differences as possible, the use_q2m option was switched off in all these experiments (as is in our current RTTOV-10 implementation).
- Additionally, we ran one cycled RTTOV-12 experiment with the use_q2m option switched on.

For MW emissivity all experiments ran with FASTEM version 5.
The setup of the experiments is summarized in the following table.

Exp.	Type	RTTOV version	Coeff. File version	IR Surface emissivity	use_q2m	Instruments	Start	End
1	Fixed FG	10	11	ISEM	false	op. + preop. + exp.	2016/01/01	2016/01/31
2	Fixed FG	12	11	ISEM	false	op. + preop. + exp.	2016/01/01	2016/01/31

3	Fixed FG	12	12	IREMIS	false	op. + preop. + exp.	2016/01/01	2016/01/31
4	Cycled	10	11	ISEM	false	op. + preop.	2016/01/01	2016/01/31
5	Cycled	12	11	ISEM	false	op. + preop.	2016/01/01	2016/01/31
6	Cycled	12	12	IREMIS	false	op. + preop.	2016/01/01	2016/01/31
6	Cycled	12	12	IREMIS	true	op. + preop.	2016/01/01	2016/01/31

4.3 Differences between RTTOV-12 and RTTOV-10 clear-sky forward calculations (based on results of "fixed FG experiments")

The purpose of the "fixed FG" experiments is to check for a long period and a huge number of profiles and instruments whether there are

a) systematic differences between RTTOV-10 and RTTOV-12
b) certain profile/instrument combinations with large differences between RTTOV-10 and RTTOV-12.

Results of the forward calculations (FG brightness temperatures) were examined for all channels of the listed instruments in terms of the mean difference, the RMS, the mean absolute difference (averaged over the whole period) and the maximum absolute difference within the period between the RTTOV-12 and RTTOV-10 experiments. We also inspected geographic plots of the maximum differences within the period for channels with larger differences. The plots are available in Annex A of this report.

Findings: For all the MW sensors the mean differences are very small and even maximum differences are only a few 1/100 K, in both tests using either the v11 or the v12 coefficients and can be explained by rounding errors or optimizations in RTTOV-12.
For the IR sensors, larger differences occur. If the same coefficient files (v11) are used (Experiments 1 and 2, see top plots in Annex A), differences stay also negligeable below 1/100 K. When both v12 coefficient files and the IREMIS emissivity model are used (Experiment 3 compared to Experiment 1), mean differences for HIRS and IASI, CrIS reach up about 0.2 K, with maximum differences of up to 1K for channels sensitive to the surface.
For the geostationary instruments, e.g. SEVIRI, similar differences as for the other IR instruments occur. The largest absolute differences are found for large zenith angles at the edge of the disk, which are most likely linked as well to the use of IREMIS. The reason for the large deviation visible in a single over South America is being looked into.

4.4 Speed, memory use and convergence of RTTOV-12 (based on evaluations of the "cycled experiments")

The forward calculations of RTTOV-12 execute much faster (~ 50%) in comparison to our current RTTOV-10 implementation. This is likely a consequence of our particular RTTOV-10 implementation as we invested extra effort to highly optimize RTTOV-10 for our previous supercomputer (NEC SX-9) when it was installed. The NEC SX-9 with its vector architecture required re-organisation of core code parts, which are likely very much sub-optimal for our current scalar type supercomputer (CRAY XC40). Not much further work was invested for optimizing our RTTOV-10 implementation again for our current CRAY supercomputer. Therefore, very likely a large part of the speed difference is caused by our specific RTTOV-10 implementation version. There is no significant change in speed for the calculation of Jacobians (rttov_k).

In order to check whether RTTOV-12 requires more memory than RTTOV-10 and in order to detect potential memory leaks, we monitored the memory used by the RTTOV routines. We did not find any memory leaks or significant difference in memory usage between RTTOV-12 and RTTOV-10.

We observed a slightly better convergence of our 3DVar minimization with RTTOV-12 in comparison to RTTOV-10. In the 3DVar minimization we run several outer loops with corresponding inner loops. The stop criteria in both inner and outer loops depend on the convergence obtained with certain maximally allowed iteration numbers, but full convergence is often reached. With RTTOV-10 we initially had issues with non-sufficient convergence which were tracked back to inconsistent results of rttov_direct and rttov_k that were reported back to the NWPSAF at the time (and fixed).
With RTTOV-10, the minimization currently requires on average 20.5 iteration steps, while RTTOV-12 takes 17.8 iteration steps on average. Approximately 50% of this improvement can be attributed to the use of q2m in RTTOV-12. Given the faster convergence observed with RTTOV-12, we conclude that rttov_direct and rttov_k yield slightly more consistent results for RTTOV-12 which is a very positive outcome.

4.5 Results of "cycled experiments"

We produced a large number of plots of obs-fg statistics for all observation systems for the cycled experiments. In almost all cases no significant changes are observed by the upgrade to RTTOV-12.
Only for IASI water vapour sensitive channels a small, but insignificant, improvement was found that might be due to the use of q2m and the slightly improved convergence with RTTOV12.

Evaluation of the full experiment results in terms of analysis differences and forecasts is still ongoing, but these initial evaluations suggest that we can introduce RTTOV-12 for our clear-sky assimilation without any issues. We are looking forward to exploit the improved capabilities for the cloudy calculations and the land surface emissivity/atlas modules.

5. RTTOV-12 in operational COSMO-DE

The use of satellite data in our high-resolution operational regional model COSMO-DE with a 2.8 km grid is still in experimental mode and work is ongoing for both active assimilation of clear sky and also cloudy IR radiances. Therefore, RTTOV-12 was implemented for both clear-sky and cloudy forward IR radiative transfer for SEVIRI. For cloudy calculations, a difference is the use of the ice cloud parameterization (Baran 2014) in RTTOV-12compared to RTTOV-10.

Tests were run using RTTOV-10 and RTTOV-12 with 54Levels coefficient files (rttov7pred54L), starting from the same first guess fields in order to examine the difference between RTTOV-10 and RTTOV-12. The setup of experiments corresponds to those described in the global framework under Experiment 1 and Experiment 3. Calculations were done for a period of four days in May 2016 and resulting plots are also included in Annex A.

All technical remarks on encountered issues in the Section 4 apply to the implementation in COSMO, too.

Evaluating the computations, findings are similar for the clear sky radiances to the global context. Generally, the clear-sky differences are very small as expected. RMS differences are generally smaller than in the global model (compare to middle plots of the global results) as the range of used atmospheric situations is much more limited and also the maximally occurring zenith angle is smaller. But some outliers (up to nearly 3K in channel 3, 7.3 µm) do occur. The evaluation has not yet been completed and the reason for these is not fully understood yet. We suppose that they may be linked to the use of IREMIS emissivities in RTTOV-12, but we were not able to investigate the differences in detail in the remaining time. We will do that as soon as possible and communicate the results to the NWPSAF.
Likewise a more thorough evaluation of differences for the cloudy simulations is ongoing.

6. RTTOV-12 GUI

For RTTOV-10 we did not succeed to install the GUI on our system with an acceptable amount of work. Therefore, we appreciated now the hint to install the anaconda python distribution, which was the crucial element to make the RTTOV-12 GUI installation work for our system.

As 'RTTOV-GUI beginners' we found that the general use of it is comfortable and that it is an excellent and appreciated tool for investigations and learning. We did not encounter any implausible results in our 'play around sessions'.
However, we have the following *suggestions:*

- It would be nice to have some basic information or simple naming of the provided profiles. Currently they are only identified by profile numbers and, once chosen, there is the option to view the profile structure in the profile editor window. Some basic indication like e.g. 'polar', 'mid-latitude winter', 'tropical' would be useful in a self-learning context for newcomers to choose profiles.

- Some profiles have a blackbody cloud defined. However, this was not obvious from just choosing a profile number and in the beginning we were really confused by the spikes in HIRS Jacobians with e.g. the "standard54lev_allgas" profile number 3, since no cloud was marked in the profile editor window. The blackbody cloud (ctp and cfraction) property of the profile(s) is visible and accessible in the "surface editor window" (and we can see why it was placed there) but this is a bit counter-intuitive for beginners. It would be useful to at least somehow mark the presence of a blackbody cloud in the profile plots.
- It would be interesting to be able to visualize the Jacobians for the surface properties. Currently only the T_{skin} Jacobian is visualized. The results could be displayed in a manner similar to the "byRun" view for the brightness temperatures for the rttov_direct calculations.
- For the 1Dvar applications it may be interesting to add an option to choose particular channels to be used in the retrieval.

7. **Comments on the documentation provided with RTTOV v12**

The available documentation (User Guide, test suite guide, GUI guide) has been screened in general and read in detail for several, but not all, sections. Generally, it is well written and covers all relevant aspects from technical installation to usage, call interfaces and important variable structures. In the following, some spotted mistakes and some purely editorial suggestions:

- **RTTOV v12 User Guide:**
  - Subroutine names and variables are highlighted in the text, however, the way it is done varies between document chapters, sometimes it is bold print, sometimes a different font. The bold print may be clearer to read and could be used throughout all sections.
  - Within a section, the different aspects/items to pay attention to are generally separated in paragraphs. Especially for long sections, it may help readability if each paragraph is preceded by a keyword (sort of small title). To illustrate this suggestion, e.g. for section 8.8:
    Principal component version: ….
    Compatible regression coefficients: …
    Trace gas specification for PC-RTTOV: …..
    Surface/emissivity settings: ….
  - **Page 38:** `profiles(i)% cfrac(:,:) -> profiles(i)% cfrac(:)`

- **Test suite guide**
  - **Page 3:** `rttov_coef_io.sh` and `rttov_coef_io_hdf.sh` do not exist, `test_coef_io.sh` and `test_coef_io_hdf.sh` are meant.
  - **Page 16:**
    We provide the following user test scripts:
    `test_fwd.sh`
    `test_rttov12.sh`

`test_rttov12_hires.sh`
`test_solar.sh`
`test_pc.sh`
`test_multi_instrument.sh`
`test_coef_io.sh`
`test_coef_io_hdf.sh`
`test_cpu.sh`

The list of tests above may be run using a single script:

```
$ ./test_core.sh ...
```

The last three tests in the above list are missing in `test_core.sh`. This was reported already in an email to James Hocking (16/08/2016).

- **Page 19:** gudie -> guide

- **Documentation within code and coefficient files**
  - main/rttov_types.F90 and in pccoef_*.H5: reconstrucetd -> reconstructed

8. Conclusion

During the RTTOV-12 beta testing we did not find any major issues within the tested modules and we are overall very happy with the provided code and version. However, some technical issues were encountered and suggestions for improvement are made (see Sections 2-7).
As indicated above, DWD would be happy to provide a MPI routine designed to speed up the reading of the coefficient files on heavily parallelized systems, which broadcasts the rttov_coefs structure from one reading node to the other nodes as this is expected to also benefit other users.

Annex A:

Plots of Section 4:

The following plots are regrouped to show results of one instrument per page. The top two plots present results of the forward calculations (in FG brightness temperatures) for all channels of one instrument in terms of the mean difference, the RMS, the mean absolute difference (averaged over the whole period) and the maximum absolute difference (on logarithmic scale) within the period between the RTTOV-12 and RTTOV-10 experiments. The top plots show the difference of Experiment 2 minus Experiment 1, the middle plot the difference between Experiment 3 minus Experiment 1.

Some geographic plots of the maximum differences within the period are added for selected channels (bottom plots). These geographic plots always refer to the experiments with RTTOV11 coefficient files for RTTOV10 and RTTOV12 (i.e. Experiment 2 minus Experiment 1).

For more details on the underlying experiment setup, please refer to Section 4.2.

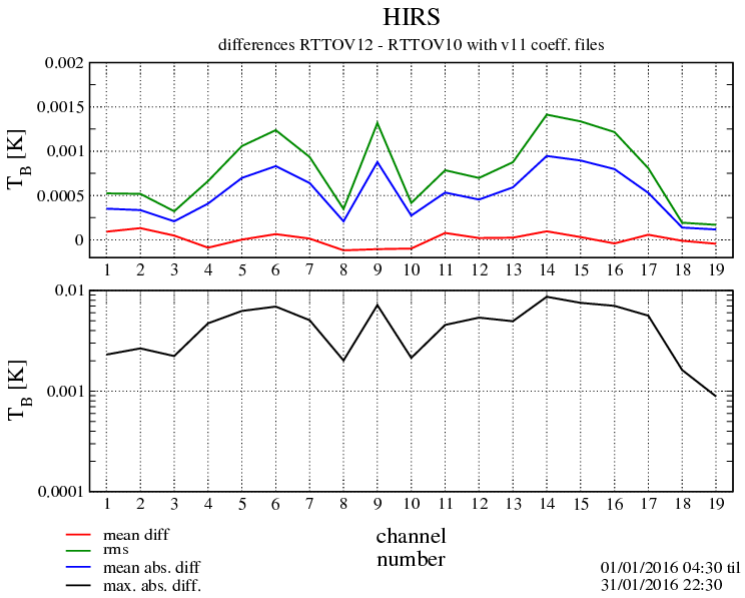
HIRS
differences RTTOV12 - RTTOV10 with v11 coeff. files
T_B [K]
channel number
mean diff
rms
mean abs. diff
max. abs. diff.
01/01/2016 04:30 til
31/01/2016 22:30

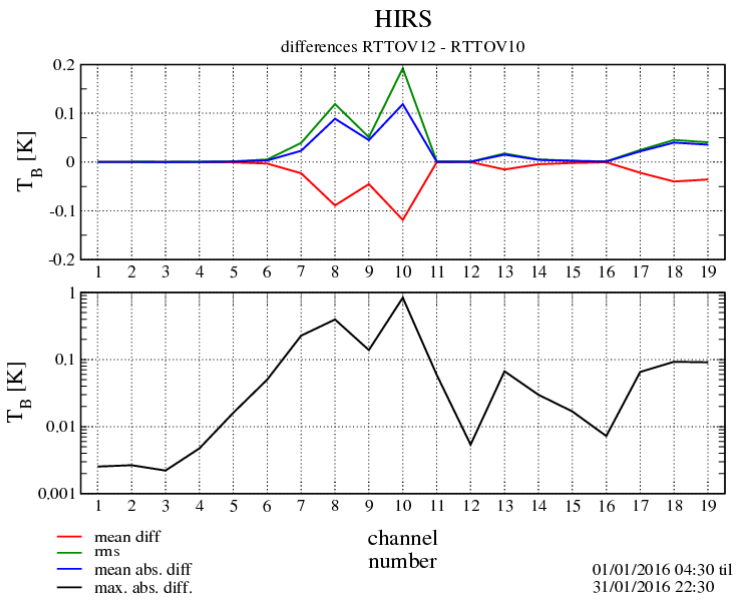
HIRS
differences RTTOV12 - RTTOV10
T_B [K]
channel number
mean diff
rms
mean abs. diff
max. abs. diff.
01/01/2016 04:30 til
31/01/2016 22:30

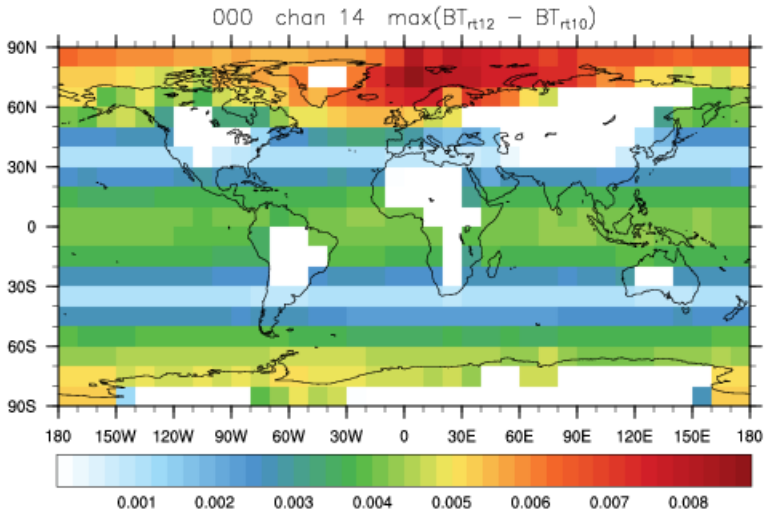
000 chan 14 max(BT_rt12 − BT_rt10)
90N
60N
30N
0
30S
60S
90S
180 150W 120W 90W 60W 30W 0 30E 60E 90E 120E 150E 180
0.001 0.002 0.003 0.004 0.005 0.006 0.007 0.008

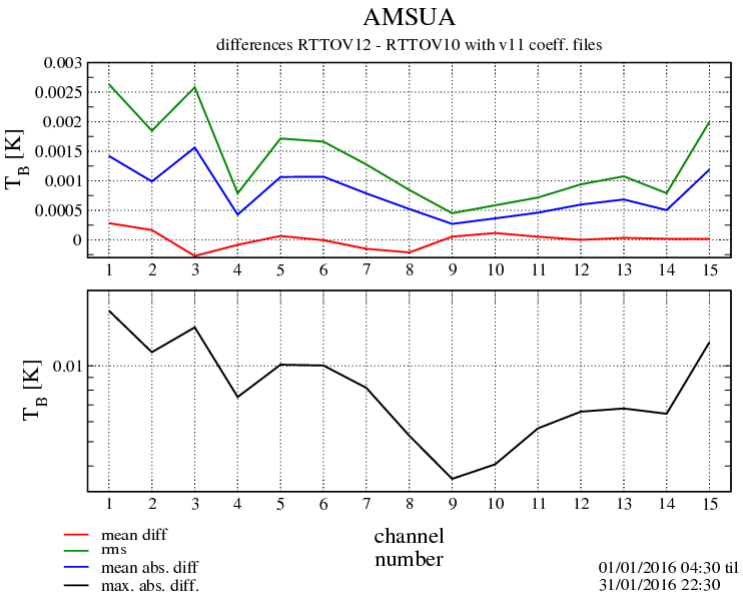
AMSUA
differences RTTOV12 - RTTOV10 with v11 coeff. files
T_B [K]
channel number
mean diff
rms
mean abs. diff
max. abs. diff.
01/01/2016 04:30 til
31/01/2016 22:30

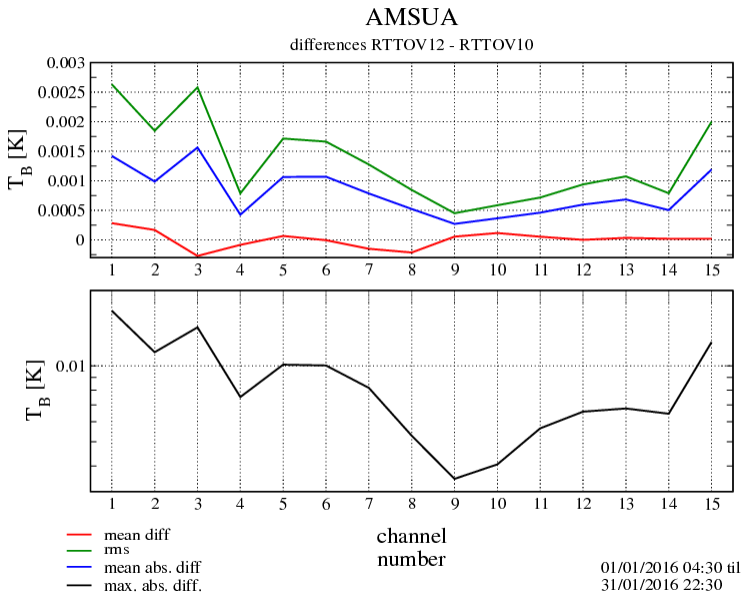
AMSUA
differences RTTOV12 - RTTOV10
T_B [K]
channel number
mean diff
rms
mean abs. diff
max. abs. diff.
01/01/2016 04:30 til
31/01/2016 22:30

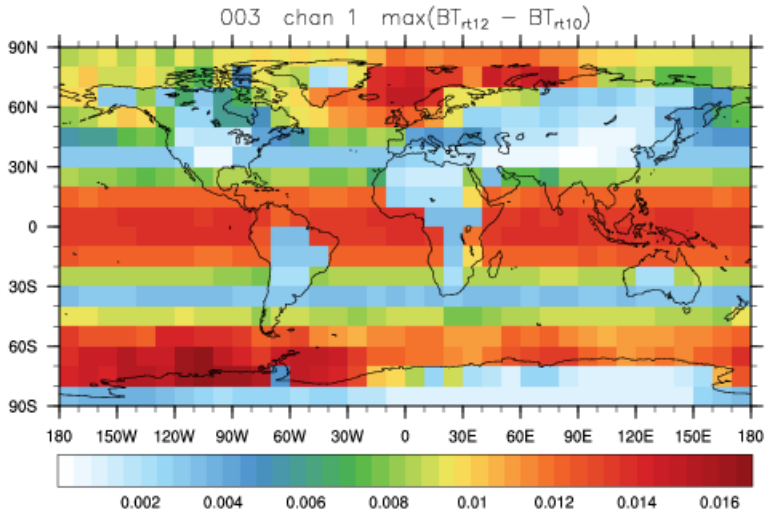
003 chan 1 max(BT_rt12 − BT_rt10)
90N
60N
30N
0
30S
60S
90S
180 150W 120W 90W 60W 30W 0 30E 60E 90E 120E 150E 180
0.002 0.004 0.006 0.008 0.01 0.012 0.014 0.016

SSMIS

differences RTTOV12 - RTTOV10 with RTTOV11 coeff. files

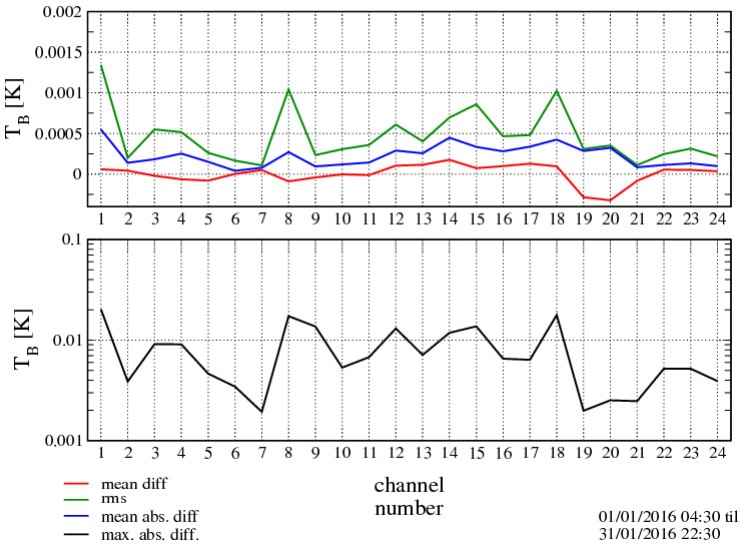

01/01/2016 04:30 til
31/01/2016 22:30

SSMIS

differences RTTOV12 - RTTOV10

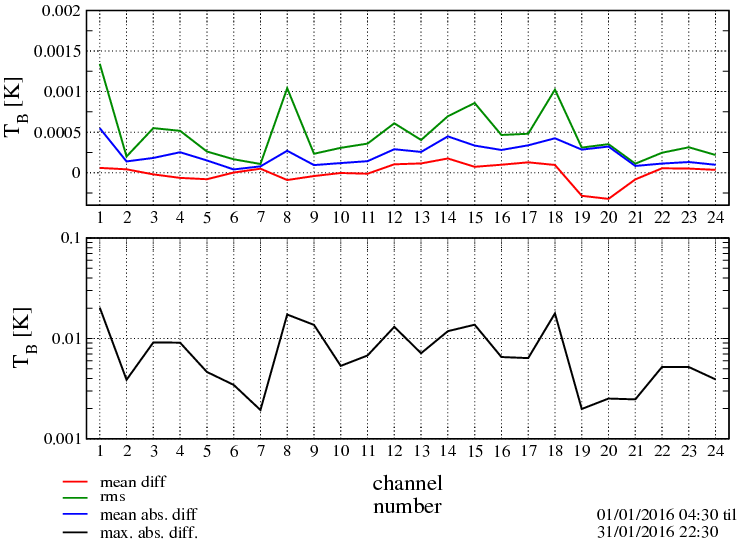

01/01/2016 04:30 til
31/01/2016 22:30

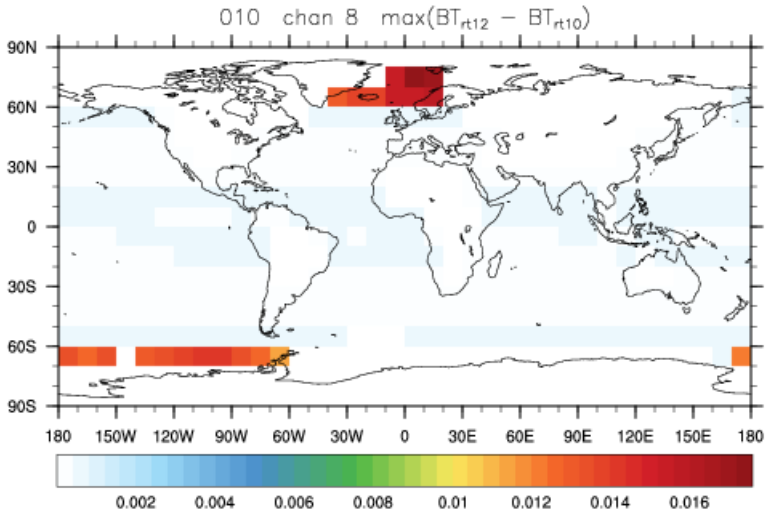

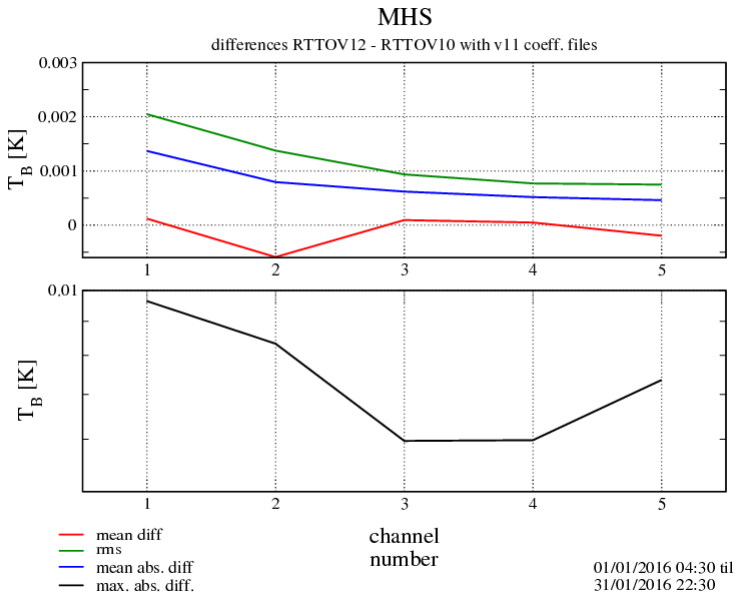
MHS
differences RTTOV12 - RTTOV10 with v11 coeff. files
T_B [K]
channel number
mean diff
rms
mean abs. diff
max. abs. diff.
01/01/2016 04:30 til
31/01/2016 22:30

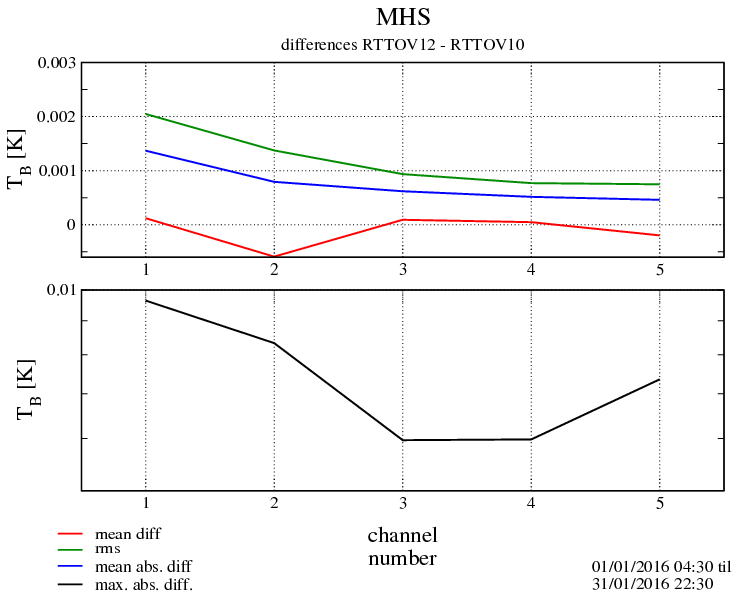
MHS
differences RTTOV12 - RTTOV10
T_B [K]
channel number
mean diff
rms
mean abs. diff
max. abs. diff.
01/01/2016 04:30 til
31/01/2016 22:30

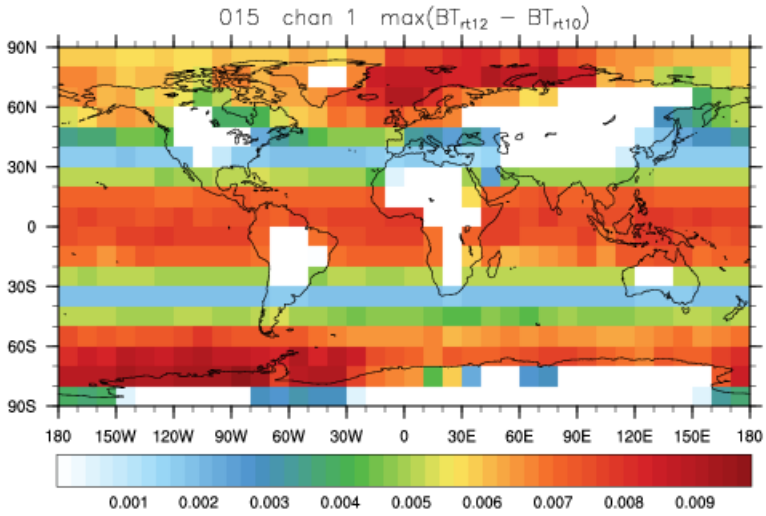
015 chan 1 max(BT_rt12 − BT_rt10)
90N
60N
30N
0
30S
60S
90S
180 150W 120W 90W 60W 30W 0 30E 60E 90E 120E 150E 180
0.001 0.002 0.003 0.004 0.005 0.006 0.007 0.008 0.009

X

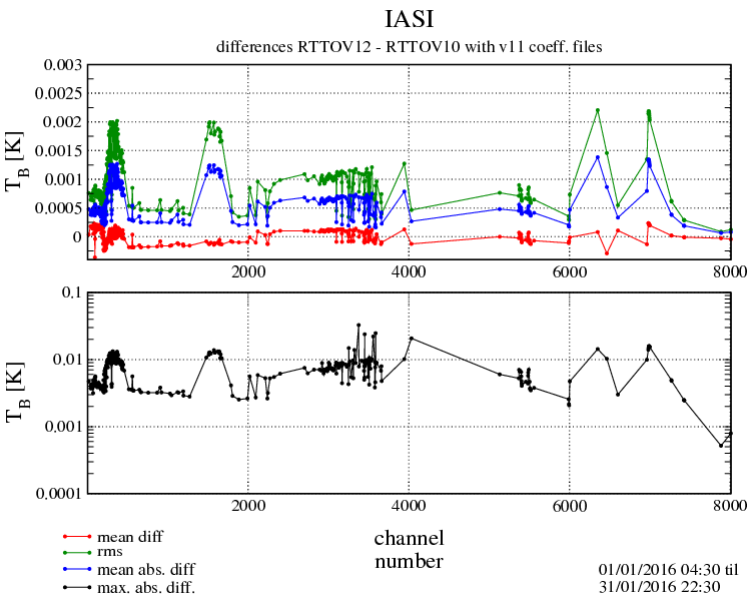
IASI
differences RTTOV12 - RTTOV10 with v11 coeff. files
T_B [K]
0.003
0.0025
0.002
0.0015
0.001
0.0005
0
2000
4000
6000
8000
0.1
0.01
0.001
0.0001
mean diff
rms
mean abs. diff
max. abs. diff.
channel number
01/01/2016 04:30 til
31/01/2016 22:30

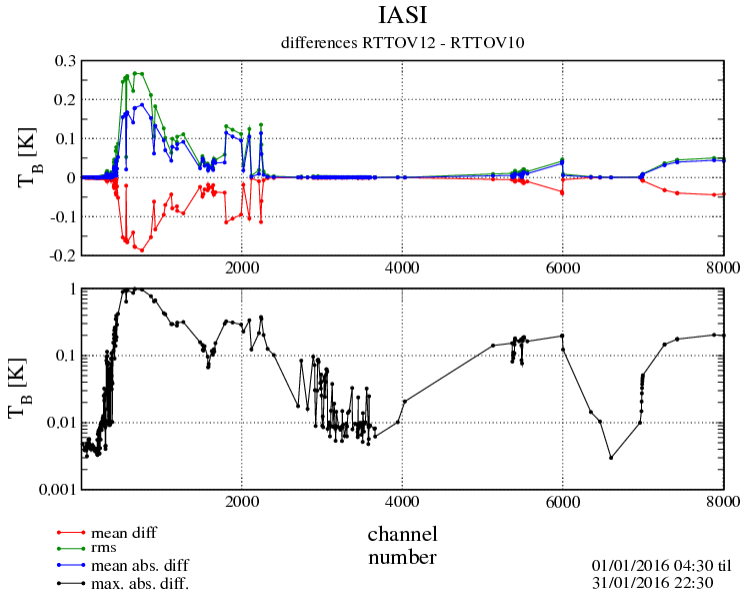
IASI
differences RTTOV12 - RTTOV10
T_B [K]
0.3
0.2
0.1
0
-0.1
-0.2
2000
4000
6000
8000
1
0.1
0.01
0.001
mean diff
rms
mean abs. diff
max. abs. diff.
channel number
01/01/2016 04:30 til
31/01/2016 22:30

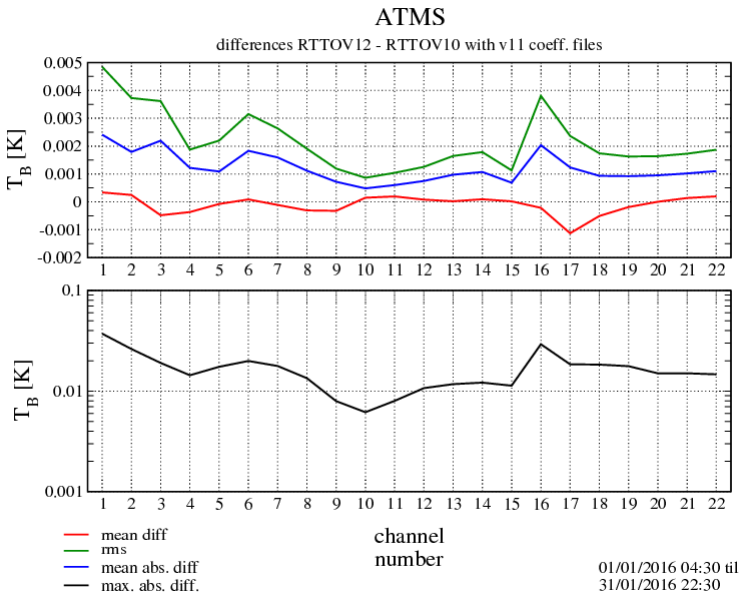
ATMS
differences RTTOV12 - RTTOV10 with v11 coeff. files
T_B [K]
channel number
mean diff
rms
mean abs. diff
max. abs. diff.
01/01/2016 04:30 til
31/01/2016 22:30

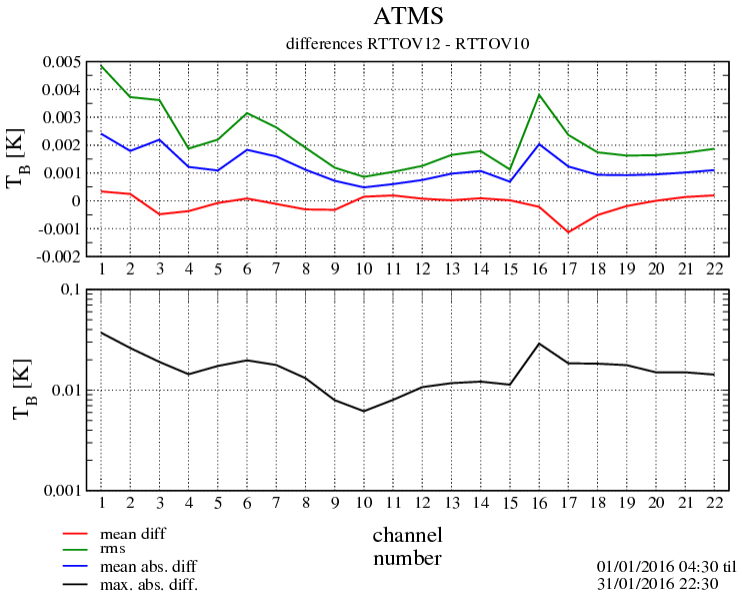
ATMS
differences RTTOV12 - RTTOV10
T_B [K]
channel number
mean diff
rms
mean abs. diff
max. abs. diff.
01/01/2016 04:30 til
31/01/2016 22:30

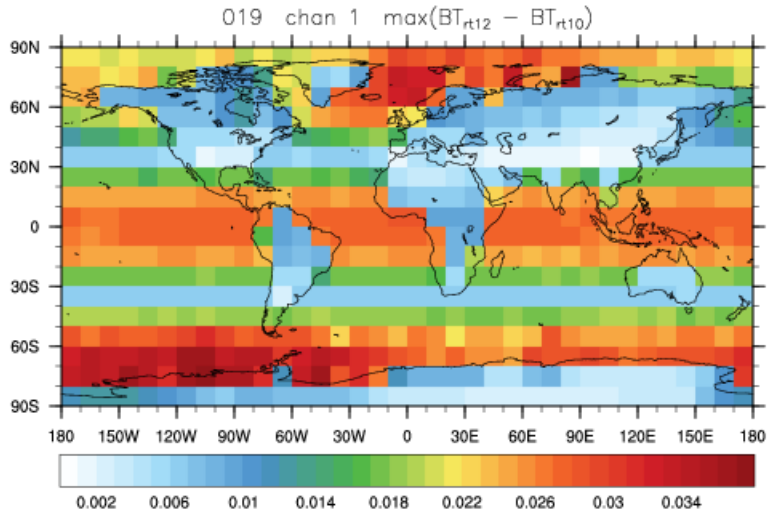
019 chan 1 max(BT_rt12 − BT_rt10)
90N
60N
30N
0
30S
60S
90S
180 150W 120W 90W 60W 30W 0 30E 60E 90E 120E 150E 180
0.002 0.006 0.01 0.014 0.018 0.022 0.026 0.03 0.034

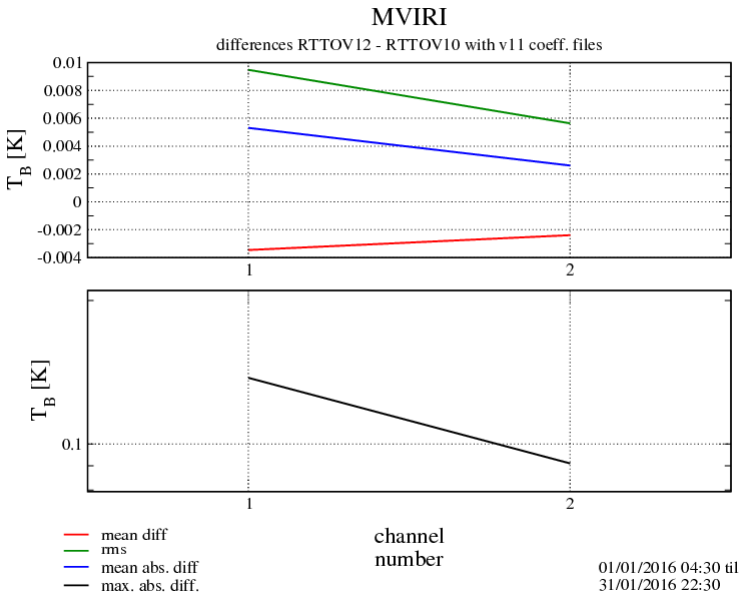
MVIRI
differences RTTOV12 - RTTOV10 with v11 coeff. files
0.01
0.008
0.006
0.004
0.002
0
-0.002
-0.004
T_B [K]
1
2
0.1
mean diff
rms
mean abs. diff
max. abs. diff.
channel
number
01/01/2016 04:30 til
31/01/2016 22:30

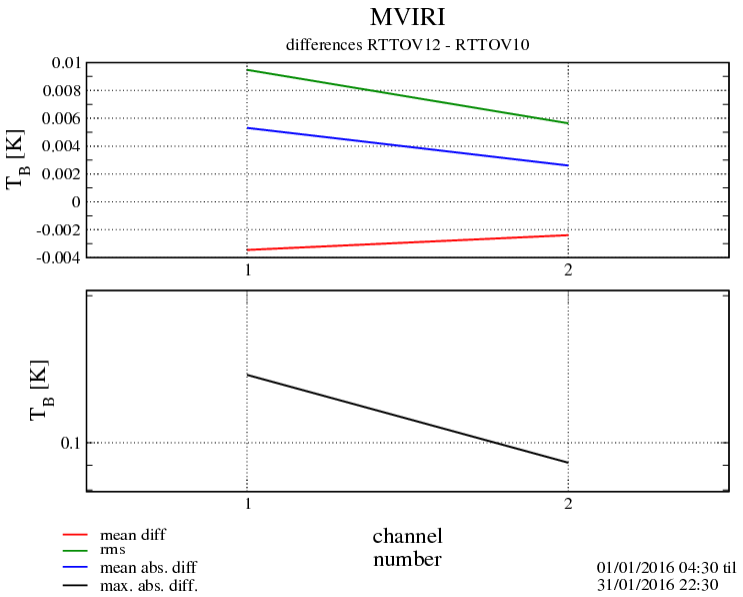
MVIRI
differences RTTOV12 - RTTOV10
0.01
0.008
0.006
0.004
0.002
0
-0.002
-0.004
T_B [K]
1
2
0.1
mean diff
rms
mean abs. diff
max. abs. diff.
channel
number
01/01/2016 04:30 til
31/01/2016 22:30

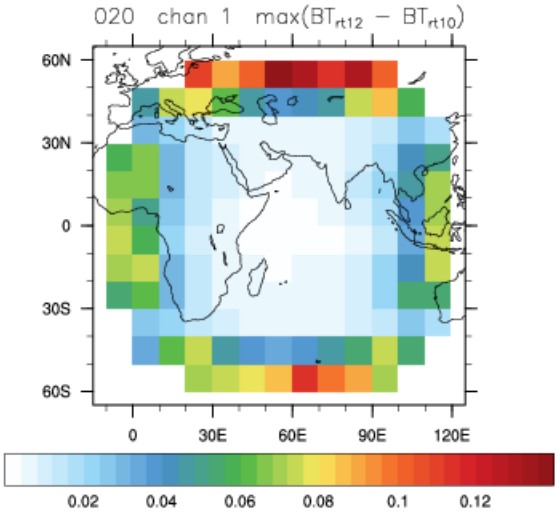
020 chan 1 max(BT_rt12 − BT_rt10)
60N
30N
0
30S
60S
0
30E
60E
90E
120E
0.02
0.04
0.06
0.08
0.1
0.12

SEVIRI

differences RTTOV12 - RTTOV10 with v11 coeff. files

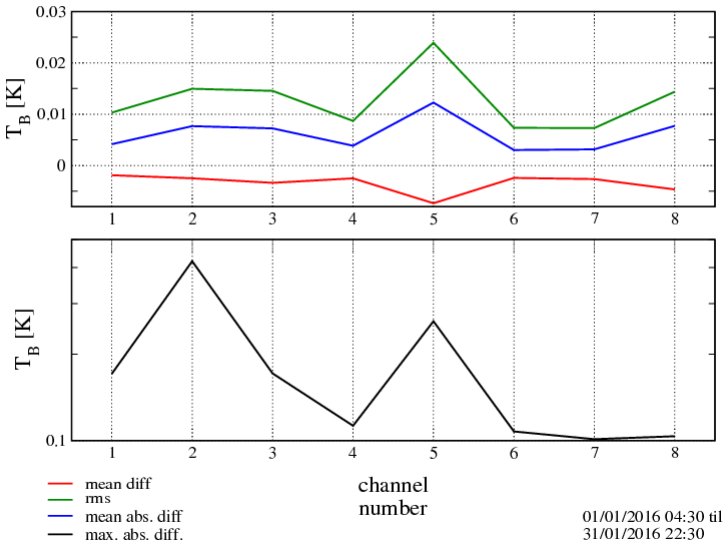

01/01/2016 04:30 til
31/01/2016 22:30

SEVIRI

differences RTTOV12 - RTTOV10

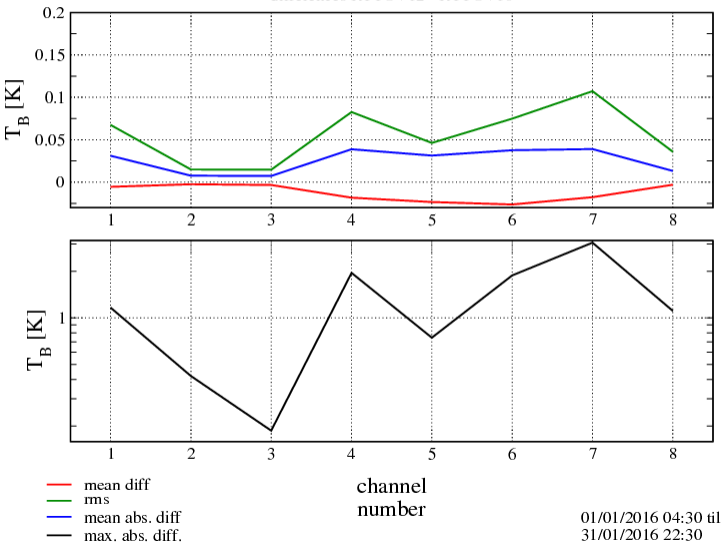

01/01/2016 04:30 til
31/01/2016 22:30

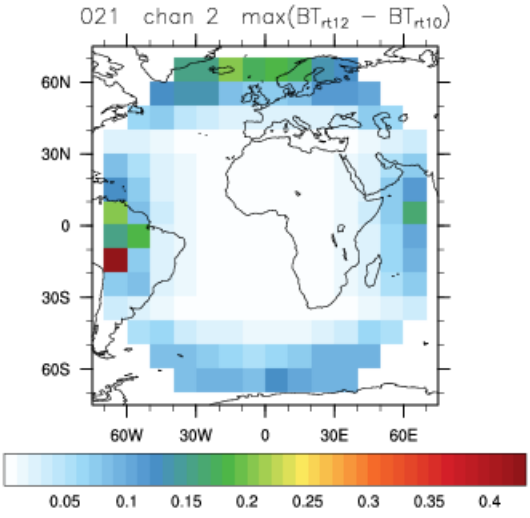

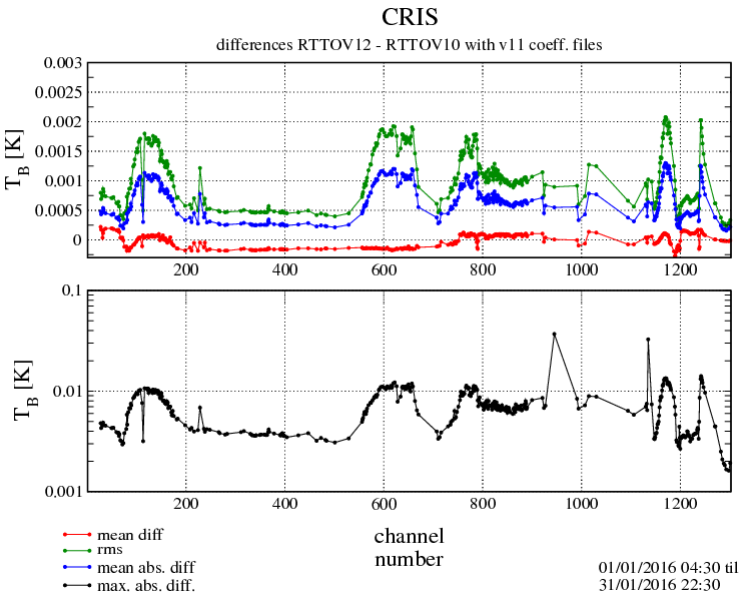
CRIS
differences RTTOV12 - RTTOV10 with v11 coeff. files
T_B [K]
0.003
0.0025
0.002
0.0015
0.001
0.0005
0
200
400
600
800
1000
1200
0.1
0.01
0.001
channel
number
mean diff
rms
mean abs. diff
max. abs. diff.
01/01/2016 04:30 til
31/01/2016 22:30

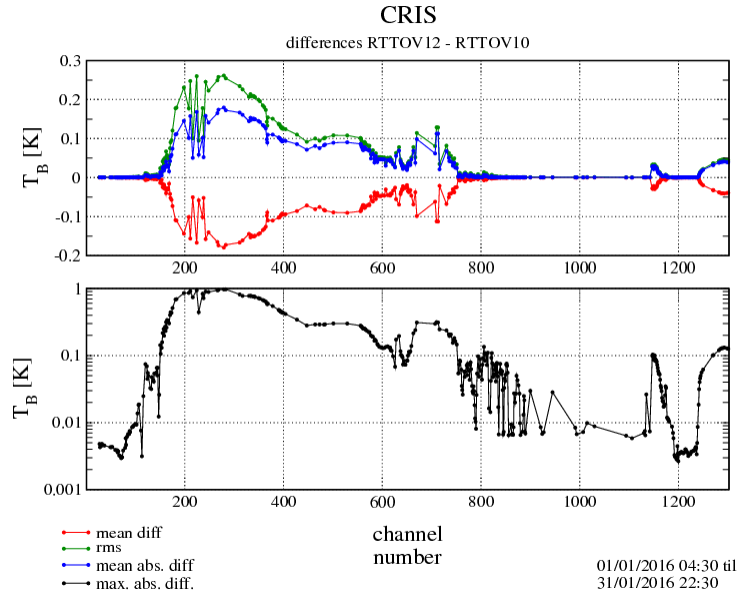
CRIS
differences RTTOV12 - RTTOV10
T_B [K]
0.3
0.2
0.1
0
-0.1
-0.2
200
400
600
800
1000
1200
1
0.1
0.01
0.001
channel
number
mean diff
rms
mean abs. diff
max. abs. diff.
01/01/2016 04:30 til
31/01/2016 22:30

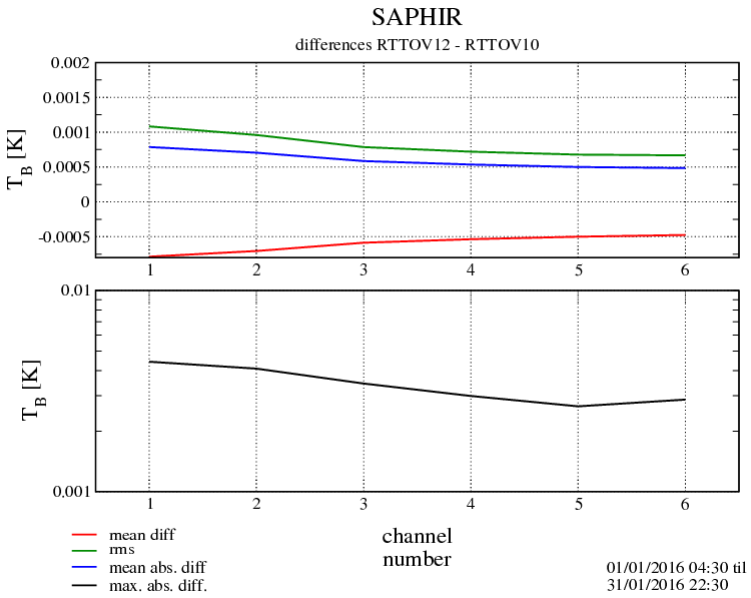
SAPHIR
differences RTTOV12 - RTTOV10
T_B [K]
0.002
0.0015
0.001
0.0005
0
-0.0005
1
2
3
4
5
6
0.01
0.001
mean diff
rms
mean abs. diff
max. abs. diff.
channel
number
01/01/2016 04:30 til
31/01/2016 22:30

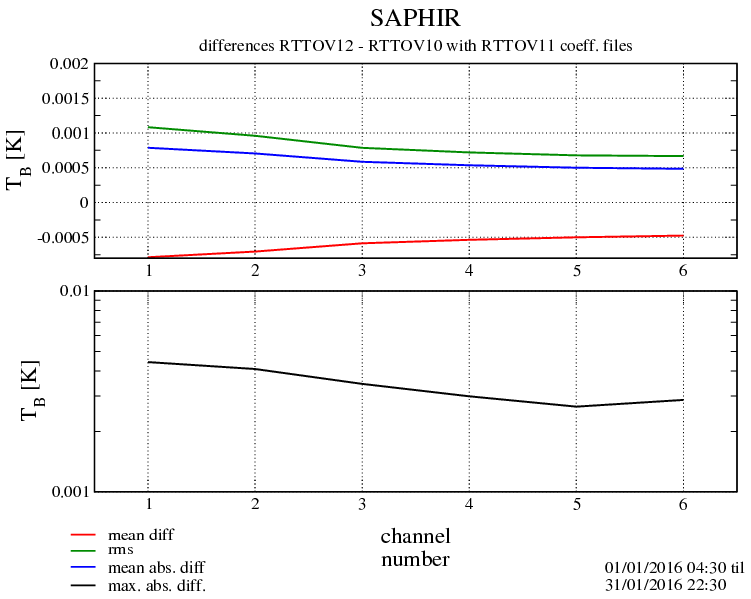
SAPHIR
differences RTTOV12 - RTTOV10 with RTTOV11 coeff. files
T_B [K]
0.002
0.0015
0.001
0.0005
0
-0.0005
1
2
3
4
5
6
0.01
0.001
mean diff
rms
mean abs. diff
max. abs. diff.
channel
number
01/01/2016 04:30 til
31/01/2016 22:30

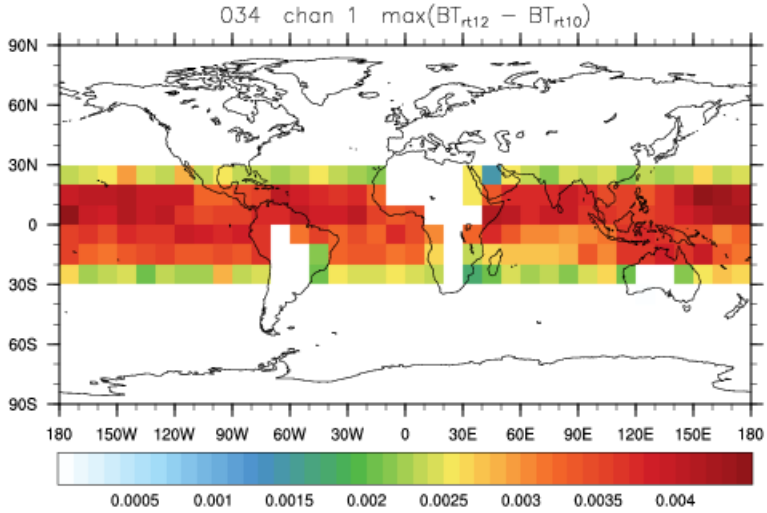
034 chan 1 max(BT_rt12 − BT_rt10)
90N
60N
30N
0
30S
60S
90S
180
150W
120W
90W
60W
30W
0
30E
60E
90E
120E
150E
180
0.0005
0.001
0.0015
0.002
0.0025
0.003
0.0035
0.004

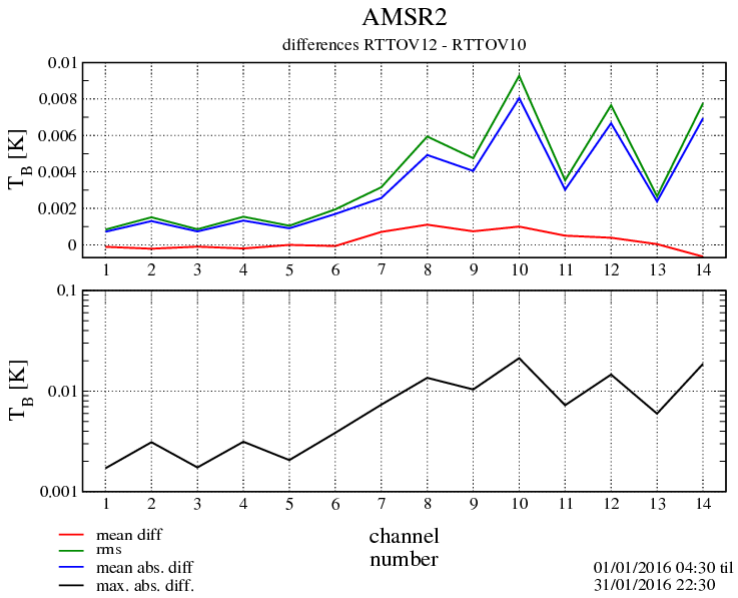
AMSR2
differences RTTOV12 - RTTOV10
T_B [K]
channel number
mean diff
rms
mean abs. diff
max. abs. diff.
01/01/2016 04:30 til
31/01/2016 22:30

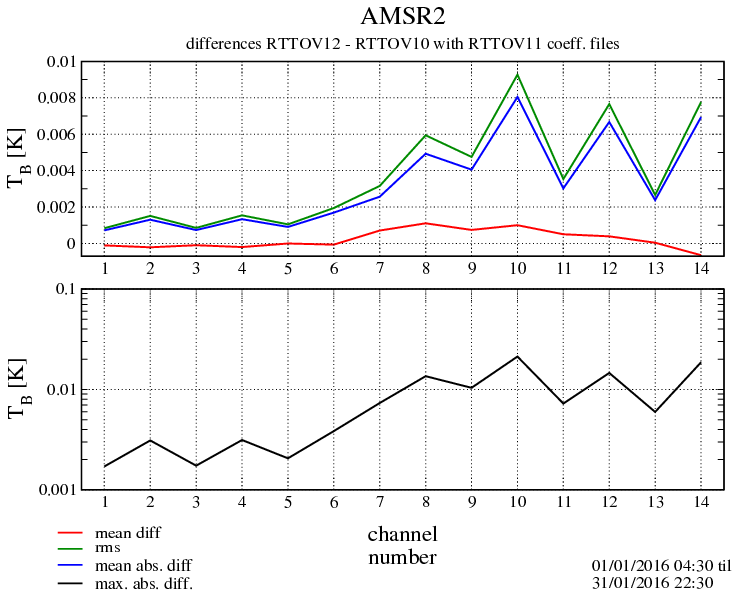
AMSR2
differences RTTOV12 - RTTOV10 with RTTOV11 coeff. files
T_B [K]
channel number
mean diff
rms
mean abs. diff
max. abs. diff.
01/01/2016 04:30 til
31/01/2016 22:30

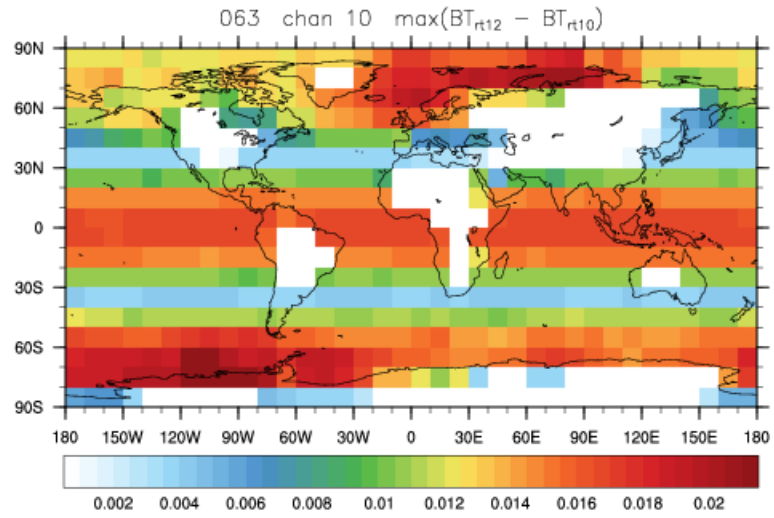
063 chan 10 max(BT_rt12 − BT_rt10)
90N
60N
30N
0
30S
60S
90S
180 150W 120W 90W 60W 30W 0 30E 60E 90E 120E 150E 180
0.002 0.004 0.006 0.008 0.01 0.012 0.014 0.016 0.018 0.02

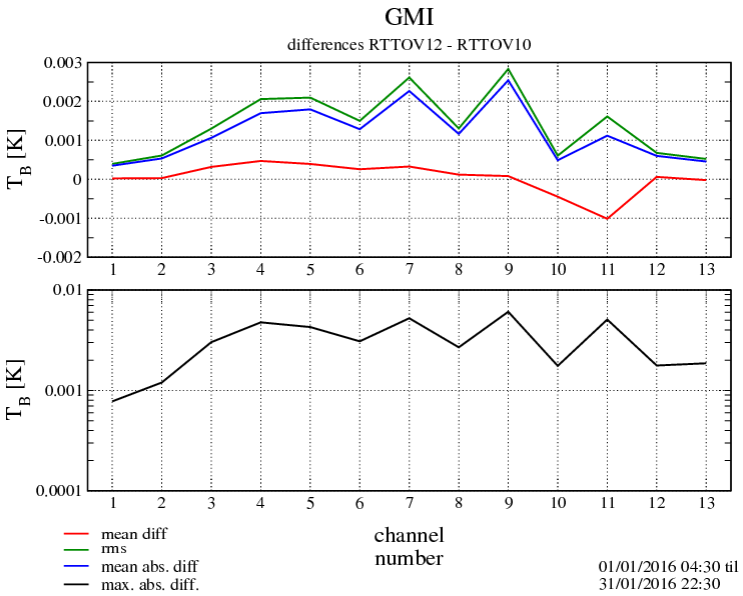
GMI
differences RTTOV12 - RTTOV10
T_B [K]
0.003
0.002
0.001
0
-0.001
-0.002
1 2 3 4 5 6 7 8 9 10 11 12 13
T_B [K]
0.01
0.001
0.0001
1 2 3 4 5 6 7 8 9 10 11 12 13
mean diff
rms
mean abs. diff
max. abs. diff.
channel number
01/01/2016 04:30 til
31/01/2016 22:30

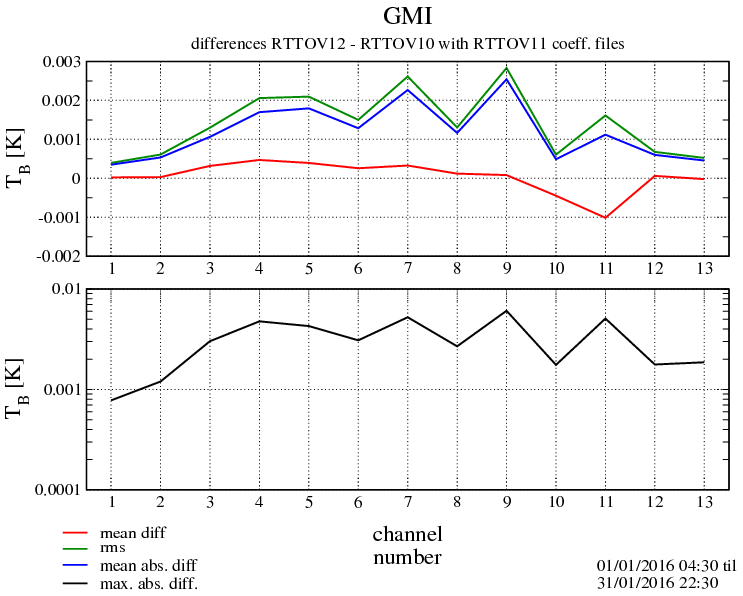
GMI
differences RTTOV12 - RTTOV10 with RTTOV11 coeff. files
T_B [K]
0.003
0.002
0.001
0
-0.001
-0.002
1 2 3 4 5 6 7 8 9 10 11 12 13
T_B [K]
0.01
0.001
0.0001
1 2 3 4 5 6 7 8 9 10 11 12 13
mean diff
rms
mean abs. diff
max. abs. diff.
channel number
01/01/2016 04:30 til
31/01/2016 22:30

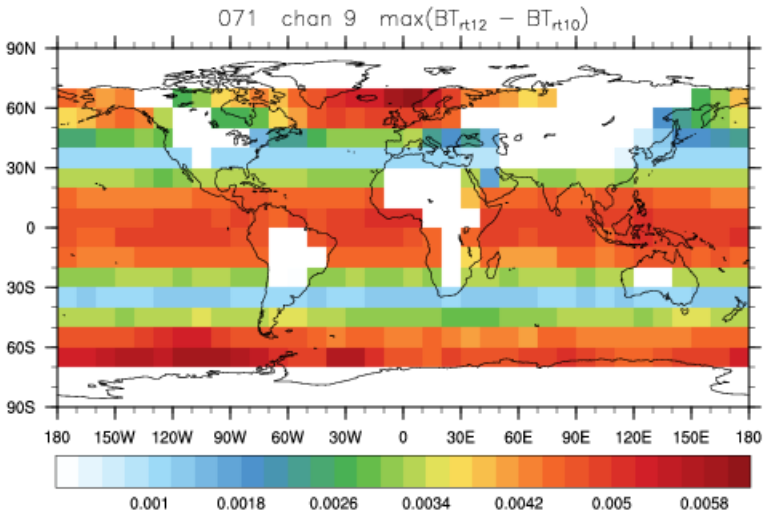
071 chan 9 max(BT_rt12 − BT_rt10)
90N
60N
30N
0
30S
60S
90S
180 150W 120W 90W 60W 30W 0 30E 60E 90E 120E 150E 180
0.001 0.0018 0.0026 0.0034 0.0042 0.005 0.0058

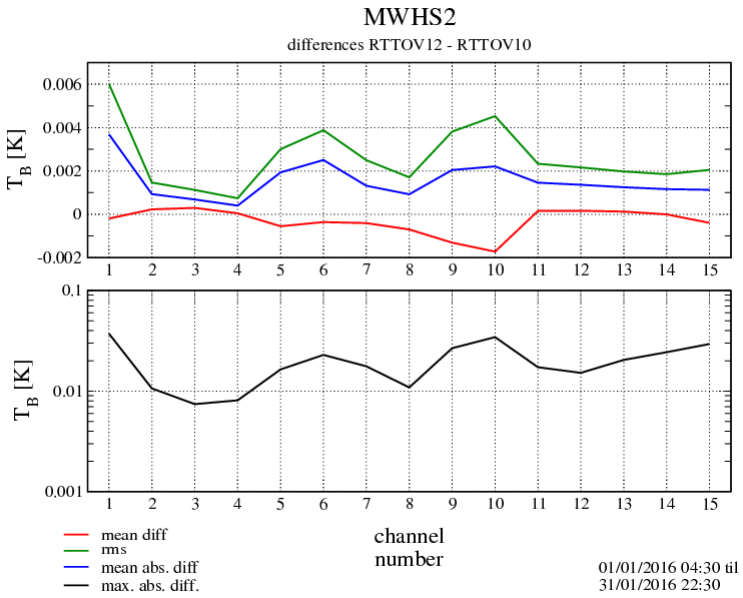
MWHS2
differences RTTOV12 - RTTOV10
T_B [K]
channel number
mean diff
rms
mean abs. diff
max. abs. diff.
01/01/2016 04:30 til
31/01/2016 22:30

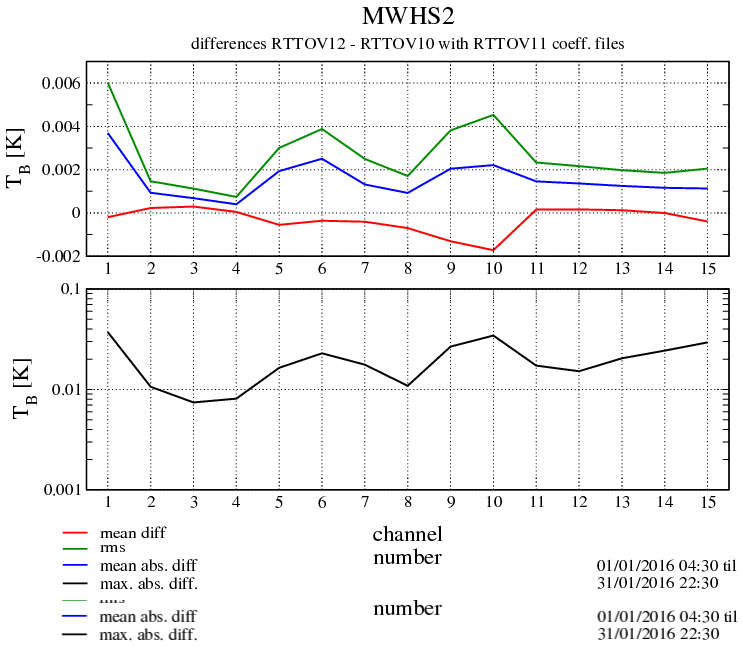
MWHS2
differences RTTOV12 - RTTOV10 with RTTOV11 coeff. files
T_B [K]
channel number
mean diff
rms
mean abs. diff
max. abs. diff.
01/01/2016 04:30 til
31/01/2016 22:30

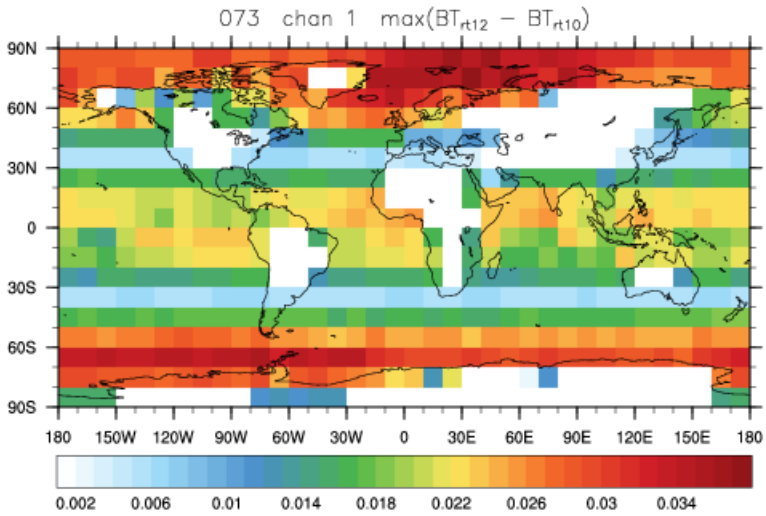
073 chan 1 max(BT_rt12 − BT_rt10)
90N
60N
30N
0
30S
60S
90S
180 150W 120W 90W 60W 30W 0 30E 60E 90E 120E 150E 180
0.002 0.006 0.01 0.014 0.018 0.022 0.026 0.03 0.034

Plots of Section 5: Comparisons for SEVIRI clear and cloudy RT within the context of COSMO-DE

The plots present results of the forward calculations (in FG brightness temperatures) for all channels of one instrument in terms of the mean difference, the RMS, the mean absolute difference (averaged over the whole period) and the maximum absolute difference (logarithmic scale up to 3K) within the period between the RTTOV-12 and RTTOV-10 experiments for the difference between the Experiment using RTTOV-12 with IREMIS and RTTOV-10 using ISEM (same setup as Experiment 3 minus Experiment 1 in the global context).

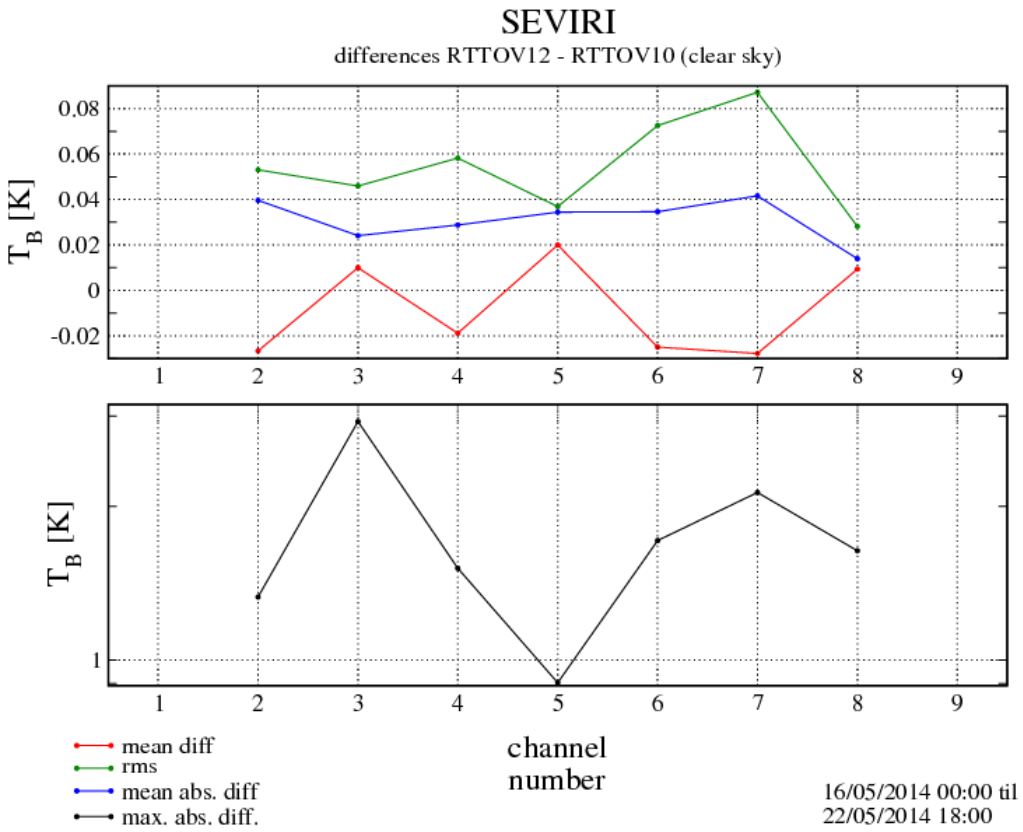

The scatterplots on the following page show the difference of FG brightness temperatures between RTTOV-12 and RTTOV-10 in dependence of the RTTOV-10 FG values. Left panels show results for all-sky (clear and cloudy calculations), right panels the clear sky results. Each row shows results for one channel as labelled.

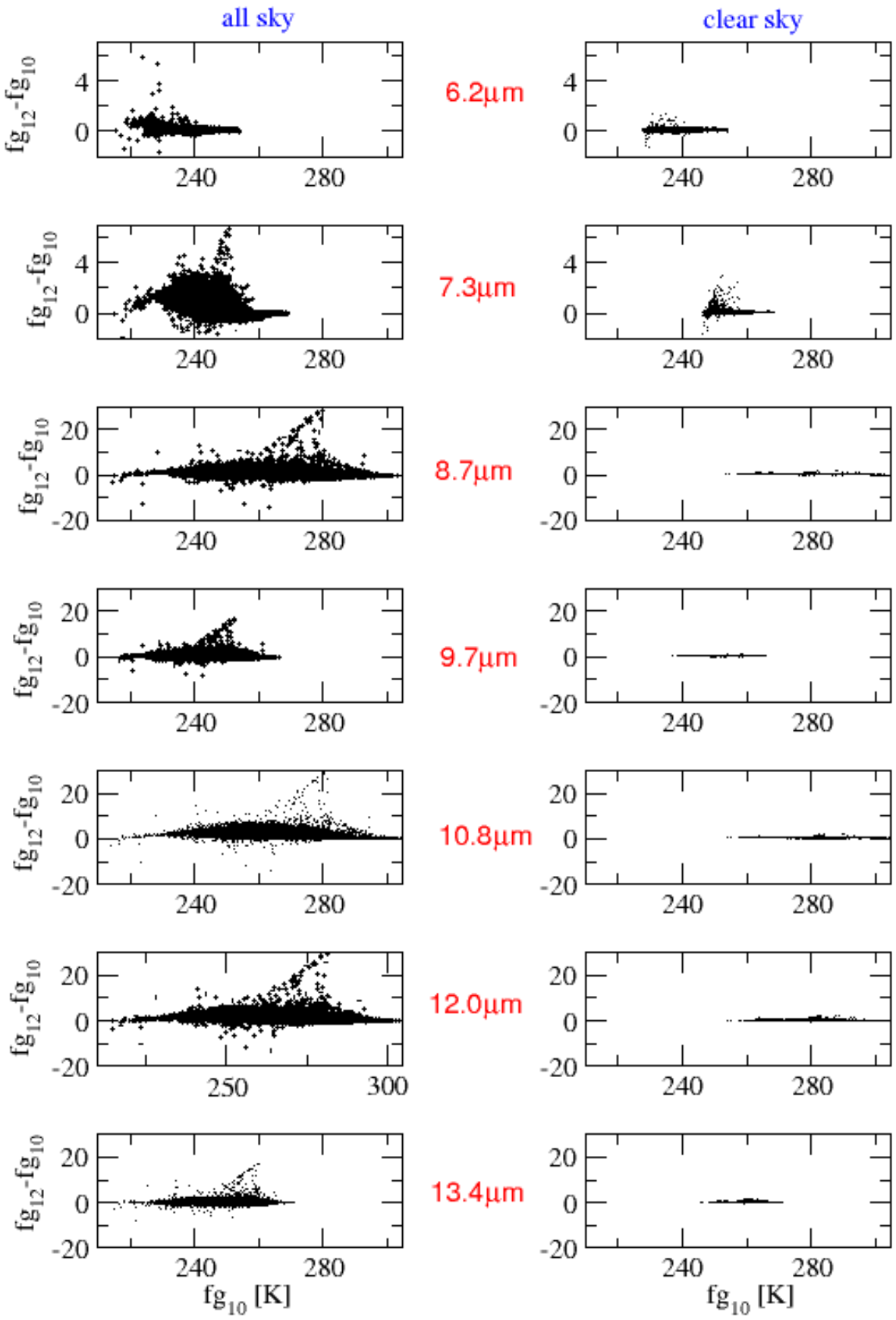
all sky
clear sky
6.2μm
7.3μm
8.7μm
9.7μm
10.8μm
12.0μm
13.4μm
fg12-fg10
fg10 [K]

Responses to DWD beta test report

Section 1

N/A

Section 2

Compilation results:

a) The script to detect f2py does only a very basic check (success or not of f2py -h) – I have improved the script so that it tries a simple f2py compilation to test for a successful installation.

b) I have removed "-fPIC" from the cray-mo-ifort flags. It is only required for compilation with f2py (for the GUI and the Python wrapper) which is not likely to be required on a supercomputer platform.

c) I have added the DWD-specific compiler flags you sent.

Further minor problems, suggestions and remarks:

1. This was a permissions problem on the server.
2. The coef download script now reports non-zero error codes from wget instead of failing silently. There is also a flag a the top of the file which can be set to turn on verbose wget output.
3. As long as the compilation options have not changed (with/without HDF5 and with/without f2py) there is actually no need for the Makefiles to be regenerated for multiple compilations. The script does it anyway to make it simpler for users (one less question to ask). If any compilation option did change the Makefiles need to be updated anyway so you cannot do multiple simultaneous compilations. Similarly if you need to link to different HDF5 libraries (e.g. built with different compilers) then you cannot do multiple compilations simultaneously because the build process picks up the HDF5 lib from Makefile.local. I would prefer to leave the compilation shell script as it is to keep it as simple as possible. If you compile manually (running Makefile.PL once as required and then calling make with appropriate arguments – described in section 5.2 of the user guide) you can run multiple compilations simultaneously so long as they are mutually compatible (as described above). In fact it is also possible to specify different Makefile.local files by passing MAKEFILE_LOCAL=my_Makefile_local to make which allows you to simultaneously compile with different compilers linking to different HDF5 libraries (this isn't documented as it is an advanced feature and most users only need to compile once).
4. Good ☺
5. There are a few cases where this is required, most notably in the wrapper code where we want the array dimension arguments last, but Fortran requires those arguments to be defined first if they are used as size specifications for other arguments. Aside from those limited cases I agree. I propose that we (the developers) keep this in mind when making future code updates and that we fix this whenever we update subroutines where it occurs (in fact this is something I have been doing in recent months). We have also been adding Doxygen markup which should be a useful for understanding the code: this was not

mentioned in the beta user guide, but I have now added a short description of this in section 6 which lists the user-level data types and subroutines.

6. Permissions on these files have now been changed.

Section 3

a) I've added a SCHED_CMD argument to rttov_test.pl which can be used to insert a scheduler command before each executable is run by the script. This at least enables the test suite to be run with aprun.

b) Given the way the test suite works, enabling the shell script to know whether rttov_test.pl ran all the tests in the here document is a bit awkward (the expected number of tests would have to be passed to rttov_test.pl which would then return an error code to be checked by the calling shell script; this would have to be optional as we don't want to have to tell rttov_test.pl the number of tests in all cases). I would consider this lower priority as the tests have been run successfully on the Cray platform so we can think about this after the v12 release.

c) I have made a change so that if no arguments are supplied the full help syntax is printed. If you supply the --help argument the RTTOV executables give the full help messages as well. Regarding why --coef-in is mandatory: the rttov_conv_coef.exe uses the standard RTTOV reading subroutines which always require an optical depth (rtcoef) coefficient file to have been read in before the cloud/aerosol/PC coefficients can be read (some information from the optical depth coefficient file is required in the other read routines, but in any case in general use you always need the optical depth coefficients). It is also assumed that if you are converting, say, a PC-RTTOV coefficient file you would want to convert the associated optical depth file so this is always output too. I don't think it is particularly limiting so I am not inclined to change this behaviour.

Section 4

Section 4.1 technical remarks

OpenMP performance: it is surprising that OpenMP didn't give any improved performance. However as we have discussed it is probably due to the multiple threading causing CPU heating, resulting in the hardware reducing the CPU speed which in turn negates the benefit of the parallelisation.

Coefficient file reading: we would be happy to include such an MPI routine in RTTOV. As you say this could be considered for CDOP-3: as we discussed, we should first look at how each consortium member does this to identify the best method to implement as an example for users. We can discuss this further next year. I also agree about the sub-optimal structure of the cloud and aerosol optical properties: it should be possible to update the internal data structures without affecting the coefficient files or the user interface so we could do this work at the same time as developing the coef broadcast capability.

Removal of interface files, better use of modules: for developers, allowing partial/incremental builds for only those files which have changed is of immense benefit as the rapid edit-compile-test cycle is used a great deal during development. Pascal prefers to keep the interfaces: for users there

are relatively few subroutines which are used so they only need to include a small number of interfaces for RTTOV in their code.

Specifying directory for rttov_read_coefs: this has now been implemented and I also added a similar argument to the Mietable reading subroutine for RTTOV-SCATT.

Allow rttov_user_profile_checkinput to modify the input profile using regression limits: superficially this sounds easy, but it is complicated by the fact that the gas units have to be respected and currently the input profile is converted to ppmv dry (the units of the regression limits) using the internal RTTOV conversion subroutine for comparison with the limits. To modify the profile, the regression limits must be converted to the input gas units and we do not have subroutines written for that (obviously not a problem, but requires a bit more work). More significantly, it should also be noted that rttov_user_profile_checkinput operates on the input pressure levels and the regression limit profiles are interpolated to the input levels. By contrast, within RTTOV the profiles are compared to regression limits after the input profiles have been interpolated to coefficient levels. This means that even if rttov_user_profile_checkinput clips the profiles to the limits there is a potential for the interpolation to cause the profiles interpolated to coefficient levels to fall slightly beyond the limits which would result in zero Jacobians (this is speculation as I haven't tested it, but I would expect this to occur sometimes). It is arguably the user's responsibility to provide coherent profiles to RTTOV. We can discuss this further by email if you have a strong desire to pursue it for v12, but otherwise I do not plan to implement this.

Section 4.3 results

The MW results are what I would expect: the coefficients in the beta package were converted from the most recent official v11 coefficients and as such are identical. There are several code changes which result in small differences to RTTOV v10/v11 of the order of magnitude seen here.

For IR sensors the coefficient generation code was re-run in order to generate the IREMIS coefficients. This results in very small differences in the coefficients compared to v11, but the impact on BTs is of the order of milli-Kelvin at most. As we discussed the greatest contribution to the large differences you saw over South America is related to a change in the calculation of the local path angle for the surface-satellite path. Previously there was an inconsistency in this calculation (two different values of the Earth radius were used at different points in the calculation) which meant that the calculated path angle at the surface was close, but not identical to user-specified zenith angle (it should be identical), and for solar simulations the surface-satellite and surface-sun path angles were close, but not identical when the satellite and solar zenith angles were the same (they should be identical). These inconsistencies have been fixed in RTTOV v12. In general the impact of this is of the order of hundredths of a Kelvin, but at the largest zenith angles it can cause differences of tenths of a Kelvin in some channels as you have observed.

For the RTTOV v12 - RTTOV v11 case (experiment 3 minus experiment 1) the larger differences for all IR instruments are explained by the use of IREMIS. In particular for the hi-res sounders the largest differences are seen in the 10-12µm window where the T-skin dependent refractive indices are used by the new emissivity model.

Section 5

I would not expect surface emissivity to impact the water vapour channels so it is not immediately obvious what is causing the larger differences at 6.2 and 7.3um. I don't know if it is practical, but it would be interesting to see an example profile where you see large differences between v10 and v12 so that we can investigate in detail.

[Note: Robin's response to this comment is as follows:

"I agree, that it would be interesting to investigate the differences in detail. Surely, we will do that at some point. However, the RTTOV implementation in our COSMO model has not a big priority, since radiances are not operationally assimilated in COSMO."

Therefore this cannot be investigated in the short-term and in particular not before the planned release date of RTTOV v12.]

Section 6

- I have updated the test suite profiles so that their ID string is descriptive for the AFGL/US76 profiles. This is written to the profile(:)%id string and is displayed at the top of the Surface Editor Window.
- The available profiles are the ones used by the test suite and as such they contain various parameter values designed to exercise the code which is why the ctp/cfraction is set in all the profiles. The GUI has been updated to display the CFRACTION value.
- We can look into Jacobians for other surface variables for a future update.
- The 1DVAR already allows for this: you can modify the channel selection through the Rttov menu ("Select channels").

Section 7

User guide:

- Subroutine/variable name highlighting: I have now been through the user guide updating this so it hopefully now consistent throughout the document.
- Add sub-section headings to improve readability: I have added a number of headings to break up some of the longer sections.
- Typo has been corrected.

Test suite guide:

- Typos have been corrected and the description of test_core.sh has been modified.

Code and coefs:

- Typos have been fixed in the code (this will be reflected in PC coef files when HDF5 versions are next written).

--END--